Emerging roles of Forkhead Box Protein FoxM1 in Cancer: Implications in Tumorigenicity and Drug Therapy

BY

Zebin Wang
B.Sc., Fudan University, 2005

THESIS

Submitted as partial fulfillment of the requirements for the degree of
Doctor of Philosophy in Biochemistry and Molecular Genetics
In the Graduate College of the University of Illinois at Chicago, 2013

Chicago, Illinois

Defense Committee:

Pradip Raychaudhuri, Chair and Advisor
Angela L. Tyner
Srilata Bagchi, Dentistry
Bradley Merrill
Elizaveta Benevolenskaya

This thesis is dedicated to my former adviser, Professor Robert H. Costa (1957-2006)

ACKNOWLEDGMENTS

I would like to acknowledge the support and friendship of numerous people who assisted me during my graduate school. First, I would like to sincerely express my gratitude to Dr. Pradip Raychaudhuri, my thesis advisor, for his guidance and inspiration, whose vision and insight led me through the doctoral program and my dissertation. I am also grateful to Dr. Angela Tyner, Dr.Srilata Bagchi, Dr. Elizaveta Benevolenskaya and Dr. Bradley Merrill for their suggestions and advice. Especially to Dr. Angela Tyner who kindly offered me a lot of guidance and help along my pursuit of scientific achievement. I also thank department of Biochemistry and Molecular Genetics at UIC for providing superior educational experience and stimulating scientific environment.

I would also like to thank all the former and current colleagues of Costa/Raychaudhuri lab, especially to Dr. Hyun Jung Park, Dr. Janai Carr, Dr. Yi-ju Chen, Dr. Dragana Kopanja, Jing Li, Megan Kiefer and Shuo Huang for their genuine friendship and constant support.

Finally, I would like to thank my family and friends for their unconditional love and for the freedom and strength they grant me to pursue my interest. I am blessed to have all of you in my life.

TABLE OF CONTENTS

TABLE OF CONTENTS (continued)

LIST OF FIGURES

LIST OF FIGURES

ABBREVIATIONS

4-OHT	4-hydroxytamoxifen
ARF	Alternative reading frame
AURBK	Aurora kinase B
BMI1	B lymphoma Mo-MLV insertion region 1 homolog
cDNA	Complementary DNA
CDC25B	Cell division cycle 25 homolog B
CENP-A	Centromere protein A
CENP-B	Centromere protein B
CENP-F	Centromere protein F
ChIP	Chromatin Immunoprecipitation
DAB	3, 3′-diaminobenzidine tetrahydrochloride
DAPI	4, 6′-diamidino-2-phenylindole
DEN	Diethylnitrosamine
DMEM	Dulbecco's modified eagle medium
DNA	Deoxyribonucleic acid
EMT	Epithelial to mesenchymal transition
EZH2	Enhancer of zeste homolog 2
FOXM1	Forkhead box M1
FBS	Fetal bovine serum
FITC	Fluorescein isothiocyanate
GFP	Green fluorescent protein

ABBREVIATIONS (continued)

HFH-11	HNF-3 forkhead homolog 11
HCC	Hepatocellular carcinoma
IAP	Inhibitor of apoptosis
INCENP	Inner centromere protein antigens
KGF	Keratinocyte growth factor
MAPK	Mitogen-activated protein kinase
MEF	Mouse embryonic fibroblast
MUT	Mutant
NANOG	Nanog homeobox
NF-M	Neurofilament medium
NSC	Neural stem cell
NPC	Neural progenitor cell
PARP	Poly (ADP-ribose) polymerase
PB	Phenobarbital
PBS	Phosphate buffered saline
PCG	Polycomb Group
PI	Propidium iodide
PLK1	Polo-like kinase 1
PRC	Polycomb repressive complex
qRTPCR	Quantitative real time PCR
RA	Retinoic acid
RNA	Ribonucleic acid

ABBREVIATIONS (continued)

RPMI	Roswell Park Memorial Institute medium
SCID	Severe combined immunodeficiency
SiRNA	Small interfering RNA
SNS	Sympathetic nervous systems
SOX2	SRY (sex determining region Y)-box 2
SUZ12	Suppressor of zeste 12 homolog
TP53	Tumor protein p53
TUNEL	Terminal deoxynucleotidyl transferase dUTP nick end labeling
WT	Wild type

SUMMARY

FoxM1 belongs to the Forkhead Box (Fox) superfamily of transcriptional factors. It is a proliferative specific transcriptional regulator that is expressed during embryogenesis and in the progenitor population of normal tissue. Its expression is diminished in terminally differentiated cells. FoxM1 overexpression is commonly observed in many types of human malignancies. It participates in various cellular events that promote tumorigenesis and metastasis of the cancer cells.

I discovered that FoxM1 is involved in promoting tumorigenicity by maintaining the undifferentiated status of the cancer cell. FoxM1 is overexpressed in neuroblastoma, a childhood malignancy derived from developing neural crust tissue. I found that FoxM1 is essential for the tumorigenicity of neuroblastoma cell in vitro and in vivo. Its presence is required for neuroblastoma to maintain the undifferentiated state and the cells are more resistant to differentiation stimuli. FoxM1 is able to activate the expression of the pluripotency genes SOX2 and Bmi1, which are involved in maintaining the undifferentiated status of the progenitor cells. In addition, in neural stem/progenitor cells, FoxM1 loss results in the reduction in self-renewal accompanied by attenuated expression of SOX2 and Bmi1.

Targeting FoxM1 represents a rational and promising anti-cancer therapeutic strategy. A cell penetrating ARF $_{26\text{-}44}$ peptide which consists of 9 N-terminal D-arginine (D-Arg) residues and amino acid residues 26-44 of the mouse ARF protein was synthesized and proved to be effective in diminishing HCC tumor size in HCC and preventing metastasis in mouse model. I discovered that FoxM1 is critical for the survival

and growth of p53-/- tumor cells both *in vitro* and *in vivo*. By inhibiting FoxM1 activity, ARF peptide effectively reduces the colonization of p53 -/- tumor cells *in vivo* accompanied by the induction of apoptosis. The FoxM1 target genes Survivin and Bmi1 are down regulated in ARF peptide treated cells and in colonized tumors. These observations validate the therapeutic strategy of targeting FoxM1 in tumors with p53 loss of function.

I also established a connection between EZH2 and forkhead box transcription factor FoxM1 during prostate cancer progression. EZH2 expression is positively correlated with FoxM1 in prostate cancer patient samples. The expression of both genes increase gradually as prostate cancer progress to more advanced stages. In prostate cancer cells, the presence of FoxM1 is necessary for the expression of EZH2 and the repression of its target genes DAB2IP and E-cadherin. By modulating EZH2 expression, FoxM1 modulates the invasiveness and migration, which contribute to metastasis.

I. INTRODUCTION

1. Fox family and FoxM1

FoxM1 stands for Forkhead Box M1 which belongs to the Forkhead Box (Fox) superfamily of evolutionarily conserved transcriptional factors consisting 19 subfamilies (FoxA-R). Currently, there are about 50 known *Fox* genes in human genome and 44 in the mouse (1). They were grouped together by the highly conserved DNA binding motif, also known as forkhead or winged-helix domain shared among all family members (2). Despite the structural similarity in DNA binding motif, Fox proteins differ significantly in terms of their expression pattern, regulation and functions. The Fox proteins participate in a wide spectrum of cellular processes including proliferation, differentiation, senescence, apoptosis and longevity(3). Consistently, the deregulation of Fox proteins is detrimental to the cells and is often associated with diseases such as congenital disorders, diabetes and cancer (3).

FoxM1, also known as HFH-11B (in human), Trident (in mouse), WIN (in rat) or MMP2, was cloned independently by two groups from mouse thymus and human colon carcinoma CACO-2 cells (4) (5). The *FoxM1* gene is located at chromosome 12p13.3 consisting of 10 exons spanning about 20kb in length. Two of the exons (exon A1 and exon A2) are alternatively spliced that give rise to three transcripts: *FoxM1a, FoxM1b* and *FoxM1c* (6). *FoxM1b* contains neither of the two exons and *FoxM1c* does not include exon A1. Both of them are transcriptionally active, whereas the longest isoform *FoxM1a*, which includes both exon A1 and A2, remains transcriptionally inactive due to the disruption of DNA binding motif by the presence of exon A2. However, the

expression pattern of the three isoforms in different tissues has not been fully characterized.

2. FoxM1 is a proliferative-specific transcription factor

FoxM1 is regarded as a proliferative-specific transcription factor since its expression tightly correlated with the proliferative capacity of cells. In embryonic tissues, it is found to be broadly expressed in proliferating epithelial and mesenchymal cells in the embryo. However, in the adult, its expression is only limited to tissues with intensive proliferative capacity such as the intestinal crypts, testis, thymus and colon and it is not detectable in terminally differentiated cells that no longer undergo active cell cycle (4, 5).

This proliferative-specific expression feature is observed also when quiescent cells are stimulated to re-enter the cell cycle. In case of liver regeneration, FoxM1 expression is restored in hepatocytes following partial hepatectomy driven by growth factors. Similarly, although low level of FoxM1 is expressed in adult lung, FoxM1 expression is upregulated following tracheal administration of KGF in alveolar type II pneumocytes (5).

This unique feature of FoxM1 is manifested also in tumors due to the highly proliferative nature of cancer cells. FoxM1 overexpression is prevalent in tumor tissues and in established cancer cells lines from a variety of tissue types including prostate, brain, pancreas, and colon. (7-12).

3. FoxM1 in normal development

FoxM1 knockout mice are embryonic lethal suggesting an essential role of FoxM1 in regulating normal development. FoxM1-/- embryos died in utero around embryonic day 18.5 accompanied with defects in developing myocardium and loss of hepatoblasts(13) (14). In *Xenopus*, FoxM1 knockdown in early embryonic development leads to the loss of cells in neural plate and the presence of FoxM1 is essential for the proliferation and differentiation of neuronal precursors (15).

Several conditional FoxM1 knockout strains have been generated to investigate the significance of tissue-specific loss of FoxM1. Cardiomyocytes specific deletion of FoxM1 (Nkx2.5-Cre FoxM1$^{fl/fl}$) leads to disruption of heart morphogenesis in late gestation coupled with a loss of proliferation of cardiomyocytes resulting from altered expression of the cell cycle genes (16). In mouse breast tissue, FoxM1 is expressed at a high level in CD29low and CD61+ luminal progenitors. Mice with conditional deletion of FoxM1 in epithelial cells by WAP-Cre system have defects in developing lobuloalveolar structures during the second pregnancy. A negative regulation of GATA3 by FoxM1 is responsible for the defects observed (17). During brain development, the absence of FoxM1 in the cerebellar granule neuron precursors delays their entry into mitosis without affecting the overall cerebellar morphology (18). In case of thymus, although FoxM1 expression is detectable in CD4+CD8+(DP) thymocytes, the conditional deletion of FoxM1 in these cells has little effect on the subsequent T cell development (19). Most of the phenotypes of FoxM1 conditional loss have been associated with regulation of the cell-cycle genes by FoxM1, whether FoxM1 has a direct role in modulating the differentiation awaits more evidence.

4. Overexpression of FoxM1 in cancer

FoxM1 is aberrantly over-expressed in a wide spectrum of human malignancies. The expression of FoxM1 is thought to be positively associated with the severity of several cancer types including breast and by examining the mRNA expression of patient samples (17, 20). FoxM1 is also abundantly expressed in almost all the tumor cell lines examined so far including prostate carcinoma, glioblastoma, pancreatic cancer(7, 10, 12) .

Based on the current understanding, overexpression of FoxM1 in tumors results from two possible mechanisms: upstream activation of Ras/ERK/MAPK signaling and gene amplification (3). The transcriptional activity of FoxM1 requires phosphorylation at Thr residue 596 by Cdk-cyclin complexes, which are activated by the upstream Ras signaling pathway (21). The Ser-251 residue of FoxM1 is required for the CDK1-dependant phosphorylation and is critical for FoxM1 activity (22). Oncogenic Ras has been shown to stimulate FoxM1 expression by modulating the level of reactive oxygen species (ROS) (23).In malignant peripheral nerve sheath tumors (MPNST), the chromosome region where *FoxM1* gene locates is found to be amplified (24).

5. Multifaceted roles of FoxM1 in cancer

Although, the most well-known function of FoxM1 is to regulate the cell cycle, emerging evidence suggests that FoxM1 plays a multifaceted role in promoting cancer development.

A. FoxM1 and cell cycle

FoxM1 is regarded as a key regulator of the cell cycle. Direct evidence supporting this notion came from the loss-of-function study in culture cells. FoxM1-/- mouse embryonic fibroblasts (MEFs) fail to progress through mitosis and display premature senescence phenotype. Similar effect is also observed in FoxM1 silenced cancer cells, where cells are arrested at G2 with polyploid or aneuploid genotype that in some cases leads to mitotic catastrophe(25-27).

It is clear now that FoxM1 orchestrates proper cell cycle progression by transcriptionally stimulating a number of cell cycle genes at both G1-S and G2-M transition(25, 26, 28). During G1-S transition, FoxM1 contributes to the down-regulation CDK inhibitors p27Kip1, which ensures the activation of the Cdk2-cyclinE complex for progression into S-phase. FoxM1 is able to do so by up-regulating the expression of Skp2, Cks1, the subunits of the SCF ubiquitin ligase complex, which ubiquitinates p27Kip1 and targets it for degradation (25). In addition, FoxM1 also activates KIS which promotes p27Kip1 nuclear export through phosphorylation (29). FoxM1 also activates Cdc25A phosphatase which dephosphorylates inhibitory Cdk2 phosphorylation and activates Cdk2-cyclinE activity during G1-S(25). In G2-M transition, FoxM1 directly activates a cluster of genes involved in entry to mitosis, centrosome duplication, kinetochore assembly, and mitotic spindle checkpoint regulation (25, 26), including PLK1, AURKB, CENP-F, Cdc25B, INCENP, CENP-A and CENP-B. For example, directly activated by FoxM1, PLK1 (polo-like kinase 1) is important for centrosome duplication and the attachment of microtubule spindle to the centrometric kinetochores(25). AURKB (Aurora B kinase) is also a direct transcriptional target of FoxM1 and serves as part of the mitotic

checkpoint complex, the presence of which ensures the proper segregation of the chromosomes (25). CENP-F is required for the sustained activation of the spindle checkpoint(26). While it is expected that a single FoxM1 target gene is unlikely to be responsible for the mitotic defects in FoxM1 deleted cells, the ectopic expression of cyclin B1 partially restores the mitotic index of FoxM1 deficient cells suggesting a central role of cyclin B1 in promoting mitotic entry(26).

The regulation of the cell cycle genes by FoxM1 has a significant impact on the tumor development. Initiation of the tumor development requires the presence of FoxM1. FoxM1 deleted hepatocytes are highly resistant to Diethylnitrosamine (DEN)/Phenobarbital (PB) induced liver formation due to the incapability of the hepatocytes to proliferate (30). In addition, the presence of FoxM1 in respiratory epithelial cells is essential for lung tumorigenesis (31). Moreover, overexpression of FoxM1 accelerates the tumor onset in mouse models of prostate carcinoma and colorectal carcinoma (9, 10).

B. FoxM1 and genomic instability

One of the hallmarks of transformation is the acquired trait of genomic instability of cancer cells in order to accelerate the mutation rate to meet the need for tumorigenesis (32). Although FoxM1 loss of function is known to lead to genomic instability by producing aneuploid and polyploid cells, FoxM1 overexpression in cancer cells also contributes to the genomic instability of cancer cells in several ways. Evidence from keratinocytes demonstrated that overexpression of FoxM1 increases genomic instability in the form of loss of heterozygosity (LOH) and copy number variations (CNV). The

exact mechanism remains unclear(33). In addition, FoxM1 is negatively regulated by p53 after DNA damage to ensure proper G2 arrest. FoxM1 silencing is able to rescue the aberrant mitotic entry of p53 ablated MCF7 cells suggesting that targeting FoxM1 potentially reduces genomic instability(34, 35). The overexpression of FoxM1 also renders the cells resistant to protective apoptotic and senescent stimuli. By up-regulating the expression of Bmi1 through c-Myc, FoxM1 overexpressed cells display reduced senescence response induced by oxidative stress (36). In addition, FoxM1 silencing is able to sensitize cancer cells to DNA damage induced apoptosis (37).

C. FoxM1 and metastasis

It has been proposed that oncogenic transformation is not sufficient for metastatic competence therefore additional properties must be acquired for transformed cells to overcome the barriers against metastasis(38). Numerous studies demonstrated that FoxM1 functions as driver for metastasis by promoting metastatic competent features of the transformed cells during different stages of metastasis.

Metastasis initiation is defined as the process where transformed cells invade into the surrounding tissues and attract supportive stroma to facilitate their dispersion (38). The process involves multiple interrelated changes including the secretion of angiogenic factors to promote vascularization, increased cell motility and invasiveness and the transition from epithelial cells to mesenchymal-like cells. FoxM1 promotes the metastatic initiation by enhancing angiogenesis, motility, invasiveness and mesenchymal-like phenotype of the primary cancer cells. In glioblastoma, FoxM1 directly stimulates the expression of pro-angiogenic molecule vascular endothelial growth factor (*VEGF*) (39).

Similar regulation is observed in other cancers as well (40, 41). Matrix metalloproteinase MMP-9 and MMP-2 are two other transcriptional targets of FoxM1 that function in degrading extracellular matrix proteins (12). In terms of promoting cell motility, Stathmin which regulates the microtubule dynamics is found to be a direct transcriptional target in both breast and liver cancer cell lines, the up-regulation of which by FoxM1 destabilizes the microtubules and enhances cell motility(42, 43). FoxM1 has also been linked to promoting EMT transition of the cancer cells during metastasis. The ARF-/- liver tumor cells with FoxM1 over-expression are more mesenchymal-like with reduced E-Cadherin expression and elevated level of mesenchymal markers vimentin and α-SMA accompanied by the activation of Akt –Snail pathway(42). Consistently, in pancreatic cancer cell lines, FoxM1 over-expression promotes metastatic phenotype and its expression correlates with a number of mesenchymal cell markers including ZEB1, ZEB2, Snail2, Vimentin as well as cancer stem cell markers CD44 and EpCAM through regulating miR-200b and let-7 with unknown mechanism(44). Caveolin-1(Cav-1) is characterized as another direct target gene of FoxM1 implicated in pancreatic cancer EMT transition (45).

Following metastatic initiation, metastatic progression is a process where circulating cancer cells infiltrate distant organs and interact with the microenvironment to proceed towards overt metastasis. Study in mouse metastatic liver cancer model demonstrates that FoxM1 is able to establish the pre-metastatic niches by transcriptionally up-regulating lysyl oxidase genes LOX and LOX2 which function to recruit CD11b+ bone marrow derived cells to facilitate the pre-metastatic niche formation in the lung (42). Whether it is a general effect applicable to a wide spectrum of tumor

types awaits more evidence. Also, it is also unclear whether FoxM1 participates in regulating the metastatic virulence function which controls the organ specific colonization of cancer cells.

D. Drug resistance and protectction from oxidative stress

Recent discoveries have provided strong evidence that connect the over-expression of FoxM1 to acquired drug resistance of cancer cells. In breast cancer patients, FoxM1 over-expression is positively related to the HER2 and serves as an unfavorable prognosis factor (46). The HER2 amplified breast cancer cell lines with ectopic stable over-expression of FoxM1 are more resistant Herceptin compared to the parental cell lines. Herceptin is the monoclonal antibody targeting HER2 and the conferred resistance to Herceptin is associated with the inhibition of p27 caused by FoxM1 over-expression(43). In addition, FoxM1 also confers resistance to microtubule-stabilizing drug paclitaxel by impacting the microtubule dynamics towards a low ratio of polymerized versus soluble form of tubulin. The major effector protein is found to be Stathmin, a microtubule destabilizing protein, which is directly regulated by FoxM1 at the mRNA level (43). In studying the mechanism of cisplatin resistance of the breast cancer cells, it is discovered that FoxM1 expression is elevated in cisplatin-reisistant MCF7 cells compared with sensitive cell lines, together with two of its target genes involved in DNA damage repair pathway: XRCC1 and BRCA2. Therefore, DNA damage repair pathway is thought to contribute to FoxM1 mediated cisplatin resistance (47). The same group also reported that FoxM1 is a target of ERα, and the silencing which is able to facilitate the MCF-7 cells to overcome acquired tamoxifen resistance (48) . In addition, in case of EGFR inhibitor gefitinib (Iressa) treatment in lung cancers,

attenuation of FoxM1 expression restores the sensitivity of Gefitinib resistant lung adenocarcinoma cell line to gefitinib treatment by inhibiting proliferation and inducing apoptosis. Over-expression of FoxM1 in gefitinib-sensitive cells increases resistance(49). There is also clinical evidence supporting that FoxM1 over-expression is significantly associated with chemotherapy in gastric cancer patients treating with docetaxel in addition to 5-fluorouracil (5-FU) plus S-1 plus cisplatin (CDDP)(50) .

Other than mediating drug resistance, FoxM1 also plays an essential role in alleviating the oxidative stress of the cancer cells. FoxM1 expression is first discovered to be stimulated by oxidative stress in adult endothelial cells when exposing the cells to hydrogen peroxide. The activation of FoxM1 is thought to be coupled with the proliferative stimuli by RAS signaling (5). Similar effect is also observed under the oxidative stress stimuli generated by oncogene. While oncogenic H-RasV12 expression is able to stimulate the FoxM1 expression in both transformed immortalized mouse embryonic fibroblasts (MEFs) and primary human fibroblasts, the induction of FoxM1 is reduced if the ROS level is repressed by anti-oxidants (23). Interestingly, after being stimulated by ROS, FoxM1 is able to regulate intracellular ROS level by transcriptionally activating the ROS scavenger genes MnSOD, catalase and PRDX3. By up-regulating these genes, FoxM1 over-expression protects cells from oncogene-induced premature senescence, a mechanism utilized by cancer cell to evade oxidative stress (23). The indirect regulation of FoxM1 on Bmi1through c-Myc is also implicated in alleviating the oxidative stress (36).

6. FoxM1 as therapeutic target

Given the essential role of FoxM1 in promoting tumorigenesis and the fact that is abundantly expressed in cancer cells but not the normal tissues, FoxM1 has been pursued as a popular therapeutic target to treat human malignancies. However, transcriptional factors are traditionally considered as "undruggable" target since it is missing the classical binding pocket allowing for efficient small molecule biding. Therefore, fairly limited therapeutic strategies are available to target FoxM1 directly in cancer cells.

FoxM1 is found to be negatively regulated by p19ARF tumor suppressor and the p19ARF 26-44 residues between 26 and 44 are sufficient to inhibit FoxM1 transcriptional activity by targeting it to the nucleolus of the cell. Based on this study, an ARF peptide containing the ARF 26-44 sequence has been used to target FoxM1(30). The N terminus of the polypeptides is added with nine D-Arginine to enhance the cellular uptake. And a control peptide missing the critical residues to interact with FoxM1 is also synthesized and designated as mutant ARF 37-44 peptide in contrast to the wild type ARF 26-44 peptide(51). Fluorescently tagged wild type ARF 36-44 peptide is found to be co-localized with FoxM1 in the nucleolus of the cell(30, 51). In mouse hepatocellular carcinoma, wild type ARF peptide diminishes proliferation and size of the liver tumor *in vivo* by selectively inducing apoptosis in HCC cells without damaging adjacent normal hepatocyte(51). The induction of apoptosis is associated with the reduction in expression of FoxM1 target gene Survivin, an inhibitor of apoptosis. In addition, wild type ARF peptide treatment also prevents HCC angiogenesis which is related to the increase apoptosis observed in the endothelial cells (51). Furthermore, in experimental metastatic model, HCC metastasis to lung is efficiently blocked by the wild type ARF peptide

treatment compared with mutant and PBS control. The wild type ARF peptide is able to reduce the mRNA expression of two lysyl oxidase genes LOX and LOX2, which contribute to the reduced colonization of the HCC cells to the lung.

The antibiotic thiazole compound Siomycin A has been identified from a high-throughput screening for the small molecules that would inhibit the FoxM1 transcriptional activity. Siomycin A has been shown to induce apoptosis specifically in the transformed cells (52). Another structurally similar antibiotics thiostrepton has been also shown to reduce FoxM1 transcriptional activity (53). Thiazole antibiotics treatment results in loss of FoxM1 expression and induction of apoptotic response of the cancer cells. The exact mechanism by which they act on FoxM1 remains unclear (52, 53). It is reported that Siomycin A and thiostrepton have proteasome inhibitor activity and FoxM1 is a target for general proteasome inhibitors (54).

II. MATERIALS AND METHODS

1. Plasmids and siRNAs

The pCMV-FoxM1b vector was constructed as previously described (21). The Sox2 expression construct was made by amplifying the Sox2 cDNA fragment sequence from pMSCV-Flag-hSox2 (Addgene) (55)and ligate it into the pcDNA3 construct (Invitrogen). pCMV-EZH2 was purchased (Addgene).

The siRNA oligonucleotide sequence specific for human FoxM1 was 5' GGACCACUUUCCCUACUUUUU-3' and for human Sox2 was 5'GGAAUGGACCUUGUAUAGAUU-3'. Oligonucleotides were synthesized by Dharmacon Research (Lafayette, CO). The siRNA oligonucleotide human EZH2 was purchased from IDT. The plasmids and siRNA duplexes were transfected into cells using Lipofectamine 2000 reagent (Invitrogen) in serum-free tissue culture medium following the manufacturer's protocol.

2. Cell culture

The human neuroblastoma cell lines SK-N-BE (2) (ATCC CRL-2271) cells and BE(2)-C (ATCC CRL-2268) cells were cultured in MEM/F12 medium supplemented with 15% fetal bovine The human prostate cancer cell line DU145 (ATCC HTB-81) was cultured in MEM medium supplemented with 10% fetal bovine and LNCaP (ATCC CRL-1740) was cultured in RPMI supplemented with 10% fetal bovine. The benign prostatic hyperplasia epithelial cell line BPH-1 (kindly provided by Simon Hayward [Vanderbilt University, Nashville, TN]) was cultured in RPMI 1640 containing 5% fetal bovine serum. Cells were cultured with 100 U/ml penicillin and 100 μg/ml streptomycin.

3. Establishment of p53 null thymic lymphoma and sarcoma cell lines

Thymic lymphoma tissue was isolated from the thymus of mice and sarcoma was isolated from a tumor encompassing the rear leg of the mouse. Tumors were excised, minced and enzymatically dissociated with 0.25% trypsin or papain (10u/ml). Cells were then washed and replaced with fresh media. Thymic lymphoma cells grew in suspension and sarcoma cells were adherent and they were maintained in DMEM medium supplemented with 10% fetal bovine, L-glutamine and penicillin-streptomycin.

4. Neural stem/progenitor cell isolation, culture and neurosphere frequency assay

Neural stem/progenitor cells were generated from 14.5-day-old embryo cerebral cortical tissue and cultured in serum-free DMEM/F12 medium supplemented with N2 supplement (Invitrogen), 20ng/ml EGF and FGF (Peprotech), 2mM glutamine (Invitrogen), 6mg/ml glucose, 14mM $NaHCO_3$ and 5mM HEPES (Invitrogen). Neurospheres were dissociated by using chemical dissociation kit following the manufacture's protocol (Stemcell Technologies). Dissociated cells were seeded in culture dish with grid (Nunc) at a clonal density. After 6-8 days, the newly generated neurospheres were counted under microscope.

5. Antibodies and immunoblots

Rabbit polyclonal antibody against FoxM1 was described (21). The following antibodies were also used: FoxM1 (Santa Cruz sc-500), Sox2 (Abcam ab15830 and Cell Signaling #3579), Bmi1 (Cell Signaling #2830, #5856 and Millipore clone F6 05-637), cleaved caspase-3(Cell Signaling #9661), β-catenin (BD 610153), NF-M (Zymed 13-

0900), tubulin-βIII (Millipore Mab1637), Nestin (BD Pharmingen 560393), Survivin (Novus Biologicals NB500-201), α-tubulin (Sigma T6074), Cleaved-PARP (Asp214) (Cell Signaling #9544), EZH2 (Cell Signaling: D2C9#5246) and E-Cadherin (Santa Cruz：H-108). Horseradish peroxidase-conjugated secondary antibodies were used to amplify the signal from primary antibody (Bio-rad) and detected by chemiluminescence with SuperSignal West Dura extended duration substrate from Pierce (Rockford, IL). Protein lysates were prepared in NP-40 lysis buffer consisted of 1% NP-40, 5% glycerol, 20nM β-glycerophosphate, 2mM NaF, 5mM EDTA, 5mM EGTA and freshly added protease inhibitor cocktail (Roche).

6. Proliferation, colony formation and soft agar assays

For proliferation assays, cells were trypsinized, counted and seeded in triplicate for each time point at a density of 2×10^3 per well in 48-well plates. The growth of the cell was monitored by measuring the luminescent signal using the CellTiter-Glo kit (Promega) every other day following manufacture's protocol. For colony formation assays, cells were seeded in triplicate at a density of 1×10^3 per well of six-well plates and grown for 14 days before fixing and staining with crystal violet (Sigma-Aldrich). For soft agar assay, cells were plated in six-well plates in 0.35% agarose on a 0.7% agarose bed in triplicate. Colonies were stained with crystal violet and counted after 3 weeks. Pictures were taken under dissecting microscope.

7. Primers and quantitative RT-PCR

Total RNA was extracted using TRIzol reagent (Invitrogen). After DNase I digestion (Promega), 500 ng of RNA was used to generate cDNA using a cDNA synthesis kit (Bio-Rad, Richmond, CA). RT-PCR was performed using the following

mixture: 1 × iQ SYBR Green supermix (Bio-Rad), 100 nM of each primers and 1 μl of cDNA in a 25 μl total volume. Reactions were amplified and analyzed in triplicate using a MyiQ single-color real-time PCR detection system (Bio-Rad). The following primers were used: human FoxM1 5′-GGAGGAAATGCCACACTTAGCG-3′ and 5′TAGGACTTCTTGGGTCTTGGGGTG-3’; human Sox2 5’ TGAATGCCTTCATGGTGTGGTC-3’ and 5’-CCGTCTCCGACAAAAGTTTCC-3’; human Bmi1 5’-TGATGTGTGTGCTTTGTGGAGG-3’ and 5’ GTGGTCTGGTCTTGTGAACTTGG-3’; human cyclophilin 5′ GCAGACAAGGTCCCAAAGACAG-3′ and 5′-CACCCTGACACATAAACCCTGG-3’; mouse Foxm1, 5′-AGCGTTAAGCAGGAACTGGA-3’ and 5’ GGAAGTGGTCCTCAATCCAA-3’; mouse Sox2 5’-AACGGCTCGCCCACCTACAGC-3’ and 5’-CAGGGGCAGTGTGCCGTATTTGG-3’; mouse Bmi1 5’-AGAGGGATGGACTACGAATGC-3’ and 5’-AACAGGAAGAGGTGGAGGGAAC-3’; mouse cyclophilin 5′-GGCAAATGCTGGACCAAACAC-3′ and 5′-TTCCTGGACCCAAAACGCTC-3′. For semi-quantitative RT-PCR experiments, the linear ranges for amplicon of each PCR primers were determined to allow semiquantitative comparisons. The primers used in semiquantitative RT-PCR were : human FoxM1 5′-GGAGGAAATGCCACACTTAGCG-3′ and 5′-TAGGACTTCTTGGGTCTTGGGGTG-3’; human Sox2 5’-TGAATGCCTTCATGGTGTGGTC-3’ and 5’-CCGTCTCCGACAAAAGTTTCC-3’; human Oct4 5’-GGGGTTCTATTTGGGAAGGTATTC-3’ and 5’-GGTTCGCTTTCTCTTTCGGG-3’ ; human Nanog 5’-CCAGTCCCAAAGGCAAACAAC-3’ and 5’-

TGGAGGCTGAGGTATTTCTGTCTC-3’; human Bmi1 5’-TGATGTGTGTGCTTTGTGGAGG-3’ and 5’-GTGGTCTGGTCTTGTGAACTTGG-3’; human Ezh2 5’AGTTGGTGAATGCCCTTGGTC-3’ and 5’-TGCTGTGCCCTTATCTGGAAAC-3’; human Suz12 5’-GCCAACCTGGATTTGCTTTTAGTC’ and ‘TCTTTGCTGTTCTACTTCCCCATC-3’; human cyclophilin 5′-GCAGACAAGGTCCCAAAGACAG-3′ and 5′-CACCCTGACACATAAACCCTGG-3’; human E-cadherin: 5'-ATGCTGATGCCCCCAATACC-3' and 5'-TCCAAGCCCTTTGCTGTTTTC-3' , human EZH2 5’-AGTTGGTGAATGCCCTTGGTC-3’ and 5’-TGCTGTGCCCTTATCTGGAAAC-3’: , human ADRB2: 5’-GTCATCACAGCCATTGCCAAG -3’ and 5’-CACCAGAAGTTGCCAAAAGTCC-3’; human DAB2IP: 5’- TGCCTGGACGATGTGCTCTATG -3’ and 5’-CTTCTTCTTCTTCTTGTCGGTCTCC-3’.

8. Chromatin immunoprecipitation (ChIP)

For chromatin immunoprecipitation, cells were cross linked in situ with 37% formaldehyde to 1% (w/v) for 10 minutes at R.T. and quenched by 125mM glycine for 5 minutes. Cells were washed by PBS collected to 1ml SDS lysis buffer (1%SDS, 10mM EDTA, 50mM Tris pH=8). The extracts were sonicated to 200-1000 bp and insoluble components were removed by centrifuge. The chromatin sample were diluted and pre-cleared with protein A-agarose/salmon sperm DNA or protein G-agarose/salmon sperm DNA beads for 2 h at 4℃. Centrifuge the chromatin samples and transfer the supernatants to fresh microcentrifuge tubes. Relevant antibodies were added to the chromatin samples and rotate overnight at 4℃. Protein A-agarose/salmon sperm DNA or

protein G-agarose/salmon sperm DNA were added beads to the chromatin samples for 2 h at 4℃. Samples were washed following Millipore EZChIP assay protocol(17-295). Resuspend beads and input samples in elution buffer for ChIP supplemented with 1 μL of proteinase K (20 μg/μL), and incubate samples for overnight at 65℃. DNA was purified using PCR purification kit (QIAGEN) and eluted with 50μl ddH_2O. The following primers were used: Sox2 -15k-a (-14964 to -14802) 5'-ACTACTGGTTCCTGATTCCCTCATC-3' and 5'-GCAAGTCCGCAAAAGTTGTCTC-3'; Sox2 -15k-b (-15149 to -15046) 5'-TTCCCAACCCCGTGAGAAAG-3' and 5'-GCAGAAACTGAGGTGACTGACCAG-3'; Sox2 -2.5k (-2668 to -2517) 5'-CCACCCTTATCCACACCAATTCC-3' and 5'-TGATTGTCCAGACGCCACAAAG-3'.

9. Promoter reporters and dual luciferase assay

Cells were plated at 8 × 104 cells per well in a 24-well plate and transfected via Lipofectamine™ 2000 with different combinations of 100 ng of either CMV-FoxM1B expression construct or empty vector and 0.5 μg of luciferase reporter as indicated. In all treatments, 3 ng of CMV-Renilla luciferase was co-transfected as an internal control. Cells were harvested 24 h after transfection, and protein extracts were subjected to Dual luciferase assays (Promega) with firefly luciferase activity normalized to Renilla luciferase activity. Promoter activity was expressed as fold induction of transcription by the FoxM1b expression vector, where the promoter activity resulting from transfection with empty vector was set at one.

10. Immunofluorescence, immunohistochemistry and TUNEL

For immunofluorescence, cells were seeded in 8-well chamber slides and washed with PBS, fixed in 4% paraformaldehyde, and blocked with 3% BSA for 1 h, and incubated with primary antibodies overnight. After washing, samples were incubated with biotinylated anti-rabbit or anti-mouse secondary antibodies and then incubated with fluorescein isothiocyanate (FITC)-conjugated avidin (Vector Laboratories, Burlingame, CA). Slides were mounted in Vectashield fluorescent mounting medium containing 4, 6-diamidino-2-phenylindole (DAPI) (Vector Laboratories). Cells were then observed using standard UV, rhodamine, or FITC filters under 40X and 63X differential interference contrast oil immersion objectives using a Zeiss LSM 5 PASCAL confocal microscope. Images were obtained with an Axiocam HRc color digital camera and LSM 5 PASCAL software (Zeiss, Jena, Germany).

For immunohistochemistry, tissues were formalin-fixed and paraffin-embedded. Antigen retrieval was performed in 10 mM sodium citrate buffer on heat plate with a temperature above 90 ℃ for 20 minutes. Immunohistochemistry was performed using the VECTASTAIN Elite ABC Kit (rabbit IgG). Reactions were visualized with DAB. Slides were mounted in Vectashield fluorescent mount media containing DAPI (Vector Laboratories).

For TUNEL staining, cells were seeded in 8-well chamber slides and washed with PBS, fixed in 1% paraformaldehyde. Cells were then permeabilized with ethanol:acetic acid 2:1 and washed with PBS. TUNEL staining was performed using the Apoptag Florescein *In Situ* Apoptosis Detection Kit (Millipore S7110). Slides were mounted in Vectashield fluorescent mounting medium containing 4, 6-diamidino-2-phenylindole (DAPI) (Vector Laboratories). Cells were then observed using standard UV and FITC

filters under 40X and 63X differential interference contrast oil immersion objectives using a Zeiss LSM 5 PASCAL confocal microscope. Images were obtained with an Axiocam HRc color digital camera and LSM 5 PASCAL software (Zeiss, Jena, Germany).

11. Wound healing assays and invasion assays

For the wound healing assays, cells were grown to confluence in 6-well plates and serum-starved for 24 hours. Wounds were carefully made across the cell monolayer, and the medium was replaced by fresh complete growth medium. Cell migration was monitored for 24 hours.

BD BioCoat™ Matrigel Invasion Chambers (BD Pharmingen) were used for invasion assays. Cells were serum-starved for another 24 hours. 5×10^4 cells were plated in the top chamber of a Transwell (24-well insert; pore size, 8 μm; Corning) and incubated with 1% FBS containing medium. 20% FBS containing medium was added to the lower chamber as a chemoattractant. After 18 hours, cells that did not migrate through the pores were removed by a cotton swab, and the cells on the lower surface of the membrane were stained by crystal violet. Images were taken under the phase-contrast microscope using 10X magnification.

12. Animals, xenograft/allograft assay and intravenous tail vein injection

The CreERT2 strain (Strain 01XAB) was obtained from Tyler Jacks' laboratory (Massachusetts Institute of Technology, USA). Foxm1b fl/fl strain was previously generated in the lab. The C57Bl/6 p53 +/- strain was obtained from the Jackson Laboratories (Bar Harbor, ME). The triple transgenic CreERT2, Foxm1b fl/fl, p53-/-

mice were generated by mating the three individual strains. NU/NU nude mice were obtained from Charles River Laboratories (Wilmington, MA). ICR SCID mice were obtained from Taconic Farms (Germantown, N.Y.)

Cells were counted and suspended in cold PBS. For allograft model, 1x106 cells were injected subcutaneously into rear flank of the nude mice. After palpable tumor formation, mice were randomized into two groups. Either corn oil or tamoxifen (1mg/per injection) were injected into the nude mice intraperitoneally every other day. Tumor sizes were measured with a caliper and calculated by length*height*width*0.5. For xenograft model, cells were treated with control or FoxM1 siRNA for 24 hours. $1x10^6$ cells were injected subcutaneously into nude mice (Nu/Nu strain, Charles River). Picture of the mice were taken four weeks after injection.

For tail vein injection, cells were stably transduced with pFU-L2G luciferase construct obtained from Sanjiv Sam Gambhir (M.D., Ph.D) of Stanford University and optimized by Dr. Huiping Liu. This construct enables the expression of both the bioluminescence and green fluorescence protein. eGFP positive cells were sorted by Beckman Coulter MoFlo. 3x106 cells were suspended in cold PBS and injected through tail vein. Live animal imaging was done on the IVIS Spectrum optical imaging machine (Caliper Life Sciences, Alameda, CA).

13. Peptide treatment

Both wild type ARF 26-44 (rrrrrrrrrKFVRSRRPRTASCALAFVN) and mutant ARF 37-44 rrrrrrrrrSCALAFVN peptides were synthesized by Genemed Synthesis Inc. (San Antonio ,Texas). The N-terminus of each peptide was modified with nine D-Arg(r)

residues. The peptides were also blocked with amidation at the C terminus and acetylation at the N terminus. For sarcoma cells, mice were treated with 5mg/kg body weight of peptide every other day for 10 times. For lymphoma cells, mice were treated with 2.5mg/kg body weight of peptide every other day for 10 times.

14. Statistical analysis

Statistical significance was calculated by the Student's t test (two tailed) with GraphPad Prism software, Microsoft Excel and R. Statistically significant changes were indicated with asterisks (* $p<0.05$, ** $p<0.01$). Kaplan-Meier survival proportion was plotted and analyzed by SAS 9.2.

III. RESULTS

1. FoxM1 in Tumorigenicity of the Neuroblastoma Cells and in Renewal of the Neural Progenitors

A. Backgrounds

Neuroblastoma, a malignancy derived from neural crest of the sympathetic nervous systems (SNS), is the second most common solid tumor in childhood and the most common tumor of infancy with a incidence of 10.2 cases per million children under age of 15 (56, 57). The origin of neuroblastoma is thought to be incompletely committed precursor cells derived from neural crest tissues (57). Neuroblastoma is unique in terms of its clinical bipolarity. Although tumors found in patients younger than one year are highly curable and undergo regression with minimal treatments, tumors diagnosed in older patients often grow relentlessly despite intensive and multimodal treatments with only 30% to 40% long-term survival rate (56-58). The unfavorable prognosis has been associated with several factors including MYCN and TrkB gene amplification and chromosome 1p losses (59-61). However, the molecular pathways mediating tumorigenicity of aggressive neuroblastoma remain largely unclear.

Consistent with its clinical bipolarity, neuroblastomas are heterogeneous in terms of pathological features, ranging from tumors containing predominantly undifferentiated neuroblast cells to those that are mainly well-differentiated neurons surrounded by Schwann stroma cells (56, 62). This heterogeneous feature is manifested in the cell lines established in vitro. The less malignant S-type cells (substrate-adherent and non-neuronal) are usually flattened and attach strongly to the substrate. The N-type neuroblastoma cells

(neuroblastic), which grow as poorly attached aggregates of small and rounded cells, are tumorigenic and rapidly proliferating. The I-type (intermediate) cells, which are less differentiated than the N type, represent malignant, multipotent neural crust stem cells (63-65). The I-type neuroblastoma cells possess self-renewal ability and have significantly higher tumor-forming capacity, as determined by soft agar colony formation and tumor growth in immunodeficient mice (62, 64, 65).

Studies from both patient samples and in vitro cell culture system suggested that neuroblastoma contains pluripotent tumor initiating cells (TICs) (66-69). The existence of TICs may account for both the heterogeneity nature of neuroblastoma as well as the tumor relapse (66, 68, 69). It is also consistent with the observation that the I-type neuroblastoma cells, the most aggressive type of neuroblastoma cells, are malignant neural crest stem cells that possess the ability to self-renewal (65). High frequency of the I-type cells in tumor is associated with increased recurrence (64). A better understanding of the tumorigenicity mechanism of the neuroblastoma possessing stem-cell properties will be critical to improve therapeutic outcomes.

Sox2 (sex determining region Y box 2) is a transcription factor that is essential for the maintenance of self-renewal and growth of both embryonic and adult stem cells (70). Recent evidence implies that Sox2 is involved in promoting tumorigenicity in malignant tissues. Sox2 functions as a lineage-survival oncogene in lung and esophageal squamous cell carcinoma, where it promotes oncogenic function of tumor cells (71). Consistently, Sox2 silencing in glioma leads to inhibition of proliferation and loss of tumorigenicity (72). Its expression is also detectable in several other types of malignant tumors including neuroblastoma (73-77).

I discovered that depletion of FoxM1 inhibits tumorigenicity of neuroblastoma, which is associated with the induction of differentiation. Furthermore, I found FoxM1 is able to directly activate the expression of pluripotency gene Sox2 in neuroblastoma. Also, deletion of FoxM1 impairs the self-renewal of mouse neural stem/progenitor cells.

B. FoxM1 is critical for the tumorigenicity of neuroblastoma cells

Expression studies with patient samples by several groups have revealed that FoxM1 mRNA is significantly up-regulated in neuroblastoma tissue samples compared with noncancerous ganglioneuroma or less aggressive ganglioneuroblastoma (78-80). A box plot representing two different datasets from publicly available database is shown (Fig. 1A) (78, 79). However, the biological function of FoxM1 in neuroblastoma has not been elucidated. To evaluate the role of FoxM1 in neuroblastoma, I first investigated the effects of FoxM1 on anchorage-independent growth, which is a hallmark of tumorigenicity. I reduced FoxM1 expression by siRNA in two different types of aggressive neuroblastoma cell lines: SK-N-BE (2) and BE(2)-C. SK-N-BE(2) belongs to N-type neuroblastoma cells, whereas BE(2)-C belongs to the most malignant I-type neuroblastoma cells (63-65). After 72 hours siRNA transfection, the protein level of FoxM1 was reduced significantly in these two cell lines, as evidenced by the western blot (Fig. 1B). The anchorage-independent growth capacity of neuroblastoma cells was checked by performing soft agar colony formation assay. Ablation of FoxM1 by siRNA led to a profound decrease in the number of colonies formed in both cell lines (Fig. 1C). The SK-N-BE (2) cells formed about 80% less colonies in FoxM1 siRNA treated cells compared with control siRNA treated cells. For the BE (2)-C line, the reduction was

even more severe. FoxM1 knockdown led to about 90% reduction in the number of colonies by quantification (Fig. 1C).

Similar effect was observed in vivo when BE(2)-C cells (1 X 10^6 cells) were injected subcutaneously in nude mice. The control group, expressing control siRNA, formed tumors within two weeks of injection, whereas the FoxM1 siRNA expressing cells failed to form tumors in four weeks (Fig. 1D). The strong inhibition of tumor growth demonstrated that FoxM1 is critical for the tumorigenicity of the neuroblastoma cells. The loss of tumorigenicity could not be explained sufficiently by the inhibition of cell growth. A growth curve analysis following depletion of FoxM1 indicated only a partial retardation of growth at the initial time-points (Fig. 2A). At later time-points, cell counts from FoxM1 silenced increased, most likely due to re-expression of FoxM1. Moreover, I did not see any significant increase in apoptosis based on changes in the sub-G1 population and caspase-3 activation following depletion of FoxM1 in the BE(2)-C cells (Fig. 2B and C). The differential effect of transient FoxM1 knockdown on growth curve versus anchorage-independent growth or growth in xenografts suggests that a continuous presence of FoxM1 is critical for the tumorigenicity of the neuroblastoma cells.

Figure 1

FoxM1 is critical for the tumorigenicity of neuroblastoma. A, Normalized FoxM1 mRNA level in 2 publically available mRNA expression profile datasets. White box= benign ganglioneuroma or ganglioneuroblastoma. Grey box=neuroblastoma. P values for the two datasets are 2.06E-10 and 3.82E-6. B, Immunoblot showing depletion of FoxM1 by siRNA in BE(2)-C and SK-N-BE (2) cells. Cell lysates were collected at 72 hours after transfection. C, Representative pictures and quantification of anchorage-independent growth on soft-agar plates. 24 hours after FoxM1 or control siRNA silencing, cells were plated at a density of 8x103 cells per well in a six-well plate. Colonies were stained and counted after three weeks. D, Picture of nude mice after 4 weeks subcutaneous injection of BE(2)-C cells treated with control or FoxM1 siRNA.

Figure 1

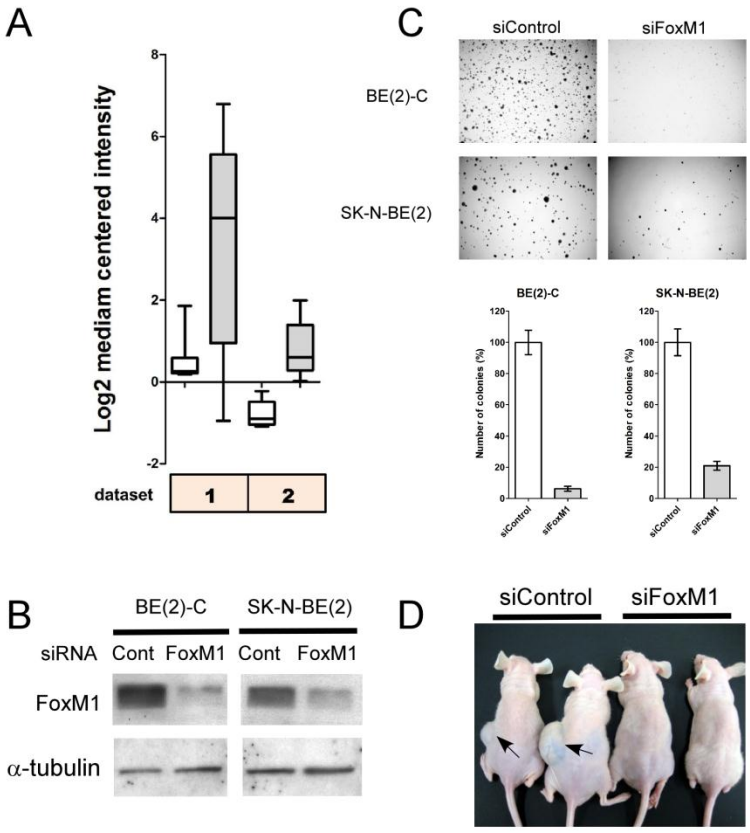
A
Log2 mediam centered intensity
8
6
4
2
0
-2
dataset
1
2
C
siControl
siFoxM1
BE(2)-C
SK-N-BE(2)
BE(2)-C
SK-N-BE(2)
Number of colonies (%)
120
100
80
60
40
20
0
siControl
siFoxM1
B
BE(2)-C
SK-N-BE(2)
siRNA
Cont
FoxM1
Cont
FoxM1
FoxM1
α-tubulin
D
siControl
siFoxM1

Figure 2

FoxM1 moderately affects the growth of neuroblastoma cells. A, 24 hours after FoxM1 or control siRNA transfection, cells were trypsinized and seeded at a density of 2x103 cells per 48-well plate for proliferation assay. Viable cell number was measured by using CellTiter-Glo luminescent cell viability assay kit (Promega) every two days. The fold change in cell count was presented by luminescence unit and was normalized by day zero. B, 72 hours after FoxM1 or control siRNA transfection, cells were fixed and stained with propidium iodide (PI) and analyzed by flow cytometry for sub-G1 population. C, 72 hours after FoxM1 or control siRNA transfection, cell lysates were collected and assayed for cleaved caspase-3 by immunoblot. β-catenin was used as loading control.

Figure 2

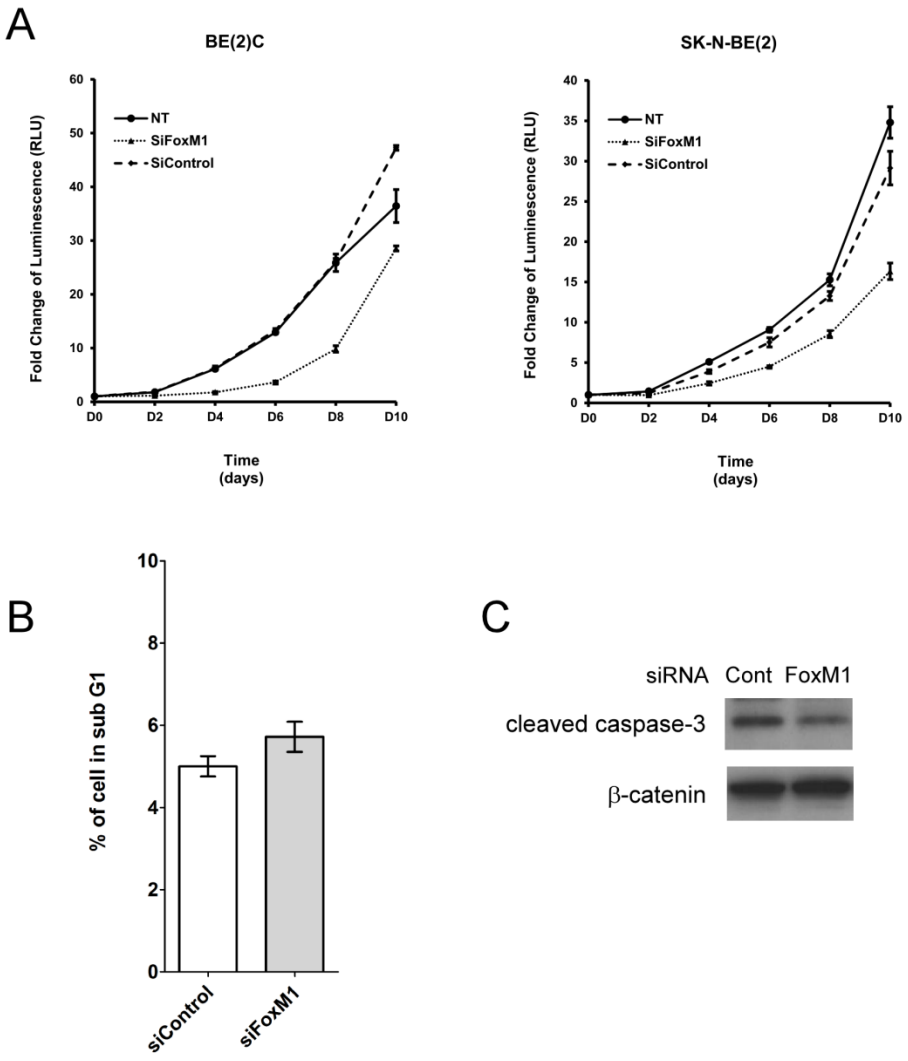
A
BE(2)C
SK-N-BE(2)
NT
SiFoxM1
SiControl
Fold Change of Luminescence (RLU)
Time (days)
D0
D2
D4
D6
D8
D10
B
% of cell in sub G1
siControl
siFoxM1
C
siRNA Cont FoxM1
cleaved caspase-3
β-catenin

C. Transient loss of FoxM1 leads to spontaneous differentiation

Several recent studies, in other tumor models, indicated a link between the state of differentiation of the tumor cells and their tumorigenicity. For example, in human liver cancer it was shown that the tumorigenicity correlated with the presence of stem cell-like cancer cells (81). Moreover, there is a strong association between poor differentiation and aggressiveness of breast cancers (82). Since the neuroblastoma cells used in our tumorigenicity studies contain stem-like progenitor cells, I considered the possibility that the depletion of FoxM1 inhibits tumorigenicity by inducing differentiation. I investigated the effects of FoxM1 depletion on differentiation of the BE (2)-C cells, which belong to I-type neuroblastoma cells representing the neural crust stem cell. Retinoic acid is able to induce differentiation of these cells towards neuronal lineage (65). I observed that following five days after retinoic acid treatment, BE (2)-C cells started to exhibit morphology of differentiated neurons with neurite extension (Fig. 3A). Interestingly, the level of FoxM1 was significantly decreased in the differentiated cells (Fig. 3B). Moreover, I observed that FoxM1 knockdown alone was able to induce a significant increase of the neuronal differentiation phenotype in BE (2)-C cells (Fig. 3A). Furthermore, depletion of FoxM1 alone resulted in a significant increase in the levels of neuronal differentiation markers NF-M and beta-tubulin III (Fig. 3B). Interestingly, the pluripotency gene Sox2 was down-regulated by both retinoic acid and FoxM1 siRNA (Fig. 3B). Together these results clearly indicate that FoxM1 is important for maintaining the undifferentiated state of the I-type neuroblastoma cells.

Figure 3

BE(2)-C cells with reduced FoxM1 undergo differentiation. A, BE(2)-C cells were transfected with control siRNA or FoxM1 siRNA. Retinoic acid (RA) was added to induce differentiation 72 hours after transfection. Representative pictures of these cells were taken 3 days (d3) and 5 days (d5) after retinoic acid (RA) treatment under microscope. Cells without retinoic acid treatment were also pictured at the same time point (CONT). B, Immunoblot of cell lysates collected 5 days after retinoic acid treatment. FoxM1, Sox2, Neurofilament medium (NF-M) and tubulin β III were detected by western blot. β-catenin was used as loading control.

Figure 3

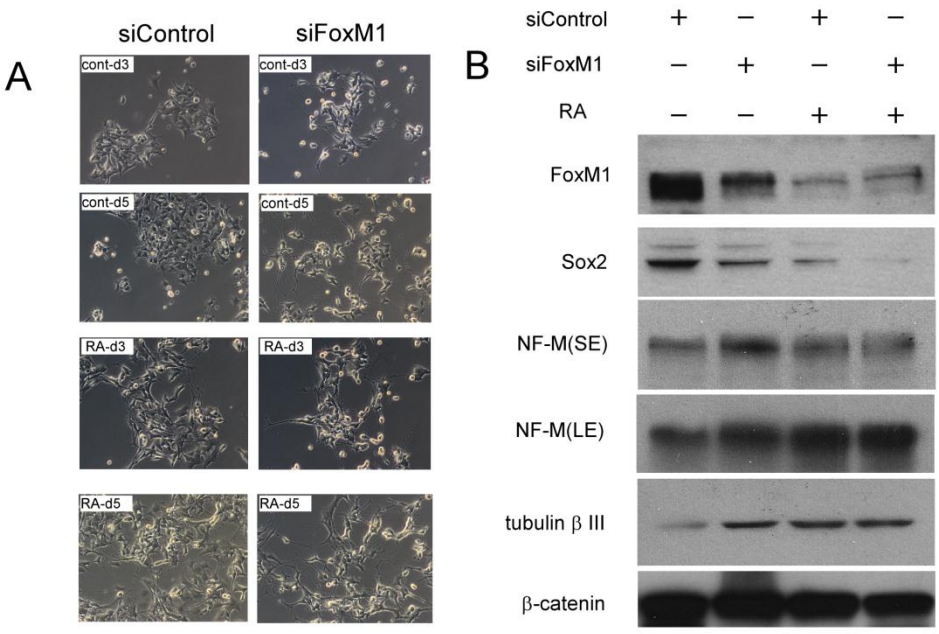
A
siControl
siFoxM1
cont-d3
cont-d3
cont-d5
cont-d5
RA-d3
RA-d3
RA-d5
RA-d5
B
siControl + − + −
siFoxM1 − + − +
RA − − + +
FoxM1
Sox2
NF-M(SE)
NF-M(LE)
tubulin β III
β-catenin

D. FoxM1 directly activates expression of the pluripotency gene Sox2

The pluripotency gene Sox2 has been implicated in the maintenance of neural stem cell pool (70) and it has been found to be involved in mediating tumorigenicity of several types of human malignancies by impacting the anchorage-independent growth (71, 72). Therefore, I tested the hypothesis that FoxM1 is critical for the expression of Sox2 in the neuroblastoma cells. One study reported that over-expression of FoxM1 in P19 teratocarcinoma cells increases expression of Sox2(83). However, it is unclear whether the regulation is direct. In order to elucidate the connection between FoxM1 and Sox2 in neuroblastoma, I checked the expression level of Sox2 after FoxM1 silencing. The mRNA level of Sox2 was remarkably reduced in both SK-N-BE(2) and BE(2)-C cells following FoxM1-silencing (Fig. 4A). Furthermore, the protein level of Sox2 was decreased in FoxM1 siRNA treated samples compared with control siRNA treated or non-treated samples, evidenced by immunoblot (Fig. 4B). These results indicated that FoxM1 might regulate Sox2 at the transcriptional level. I assayed for the expression of polycomb family member Bmi1, which has been implicated in promoting tumorigenicity of neuroblastoma cells (84, 85). Interestingly, it was observed that, similar to Sox2, Bmi1 expression level also tightly correlated with FoxM1 in neuroblastoma, which indicated that it might also be involved in FoxM1 mediated tumorigenicity of neuroblastoma cells (Fig. 4A, B).

Bmi-1 has been previously reported to function downstream of FoxM1 through activation of c-Myc (36). Therefore, I focused on revealing the relationship between FoxM1 and Sox2. To test whether FoxM1 is able to stimulate Sox2 expression in neuroblastoma cells, I transiently transfected FoxM1 expression plasmid into BE(2)-C

cells. Expression of FoxM1 led to an increase in the Sox2 mRNA level (Fig. 4C). In addition, by immunoblot, I observed that the Sox2 protein also responded to FoxM1 up-regulation compared with the control transfection (Fig. 4D). Similar result was observed by stably over-expressing FoxM1 in S-type neuroblastoma SK-N-AS cells (Fig. 5) and the ectopic expression of FoxM1 led to increased colony formation on plate and anchorage-independent growth in soft agar (Fig. 5A and B).

Figure 4

Sox2 expression correlates with FoxM1 in neuroblastoma cells. A, mRNA levels of FoxM1, Sox2 and Bmi1 detected by qRT-PCR. BE(2)-C and SK-N-BE (2) cells were transfected with control siRNA or FoxM1 siRNA for 72 hours. The mRNA levels were normalized to human cyclophilin mRNA, and the control groups were set to one. B, Immunoblot showing the protein level of FoxM1, Sox2 and Bmi1 from the same samples described in A. α-tubulin was used as loading control. C, mRNA levels of FoxM1 and Sox2 detected by qRT-PCR 24 hours after transfecting BE(2)-C cells with empty vector or pCMV-FoxM1 plasmid. The mRNA levels were normalized to human cyclophilin mRNA, and the control groups were set to one fold. D, Immunoblot showing the expression of FoxM1 and Sox2 from the samples described in C. β-catenin and β-actin were used as loading controls.

Figure 4

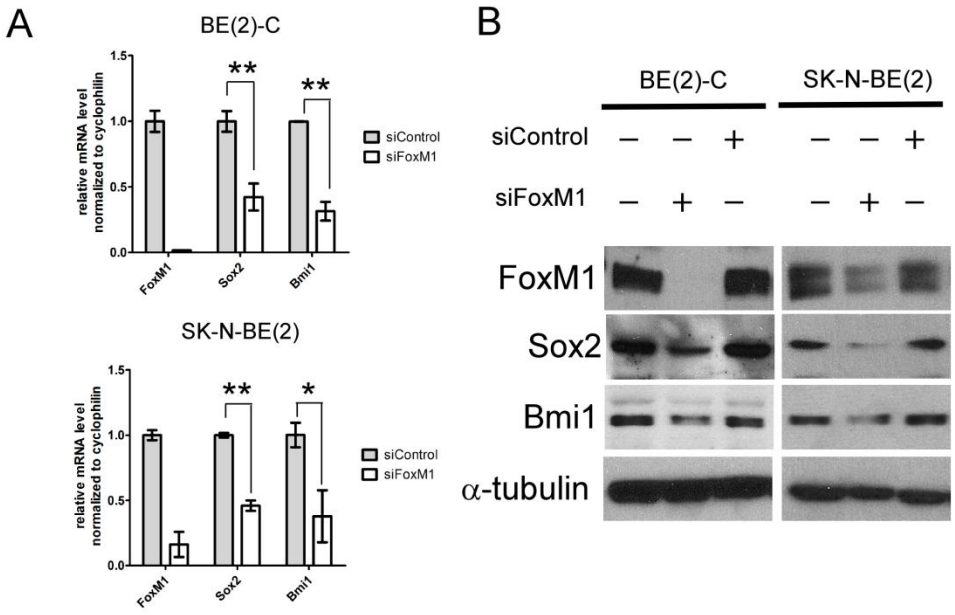
A
BE(2)-C
relative mRNA level normalized to cyclophilin
1.5
1.0
0.5
0.0
**
**
siControl
siFoxM1
FoxM1
Sox2
Bmi1
SK-N-BE(2)
relative mRNA level normalized to cyclophilin
**
*
siControl
siFoxM1
FoxM1
Sox2
Bmi1
B
BE(2)-C
SK-N-BE(2)
siControl – – + – – +
siFoxM1 – + – – + –
FoxM1
Sox2
Bmi1
α-tubulin

Figure 5

FoxM1 promotes tumorigenicity in SK-N-AS cells. A, Colony formation is induced in cells stably expressing FoxM1. $2x10^3$ SK-N-AS cells stabling expressing empty vector or FoxM1 were plated per well in a six-well plate in triplicate. Colonies were stained and quantified after 2 weeks. B, Representative pictures and quantification of anchorage-independent growth of SK-N-AS cells stabling expressing empty vector or FoxM1. Cells were plated a density of $1.6x10^4$ cells per well in a six-well plate. Colonies were stained and counted after three weeks. C, Immunoblot showing expression of FoxM1 and Sox2 of SK-N-AS cells stabling expressing empty vector for FoxM1. α–tubulin was used as the loading control.

Figure 5

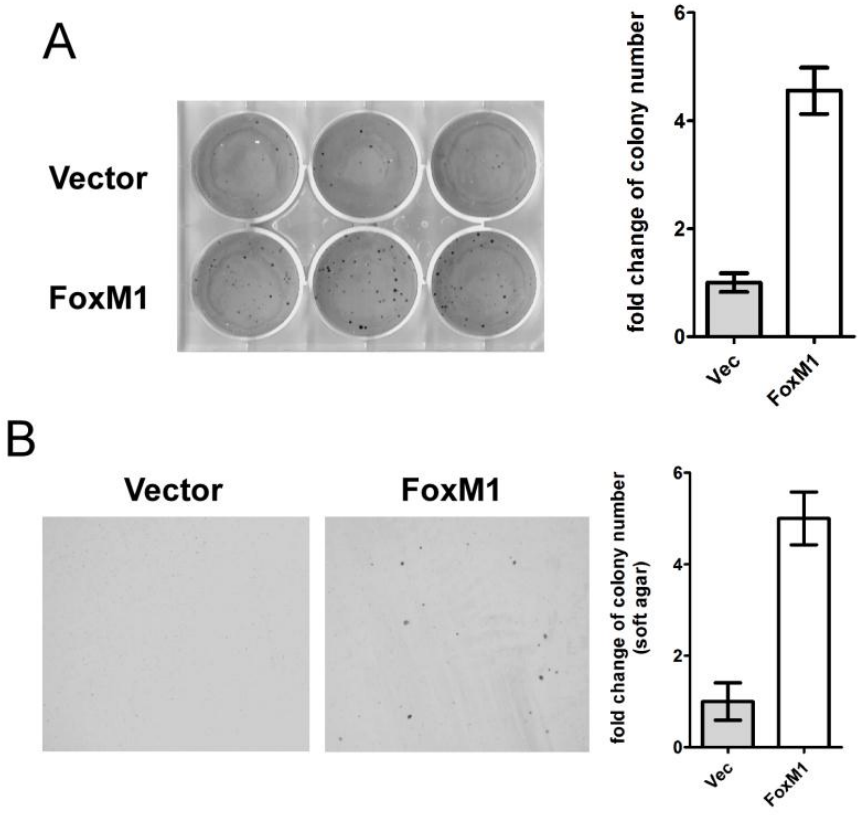
A
Vector
FoxM1
fold change of colony number
6
4
2
0
Vec
FoxM1
B
Vector
FoxM1
fold change of colony number (soft agar)
6
4
2
0
Vec
FoxM1
C
SK-N-AS
Vector FoxM1
FoxM1
Sox2
α-tubulin

Next, I tested the possibility that FoxM1 directly stimulates Sox2 expression by binding to its regulatory region. Analysis of human Sox2 upstream regulatory region by using MacVector software revealed one putative FoxM1 binding motif 15kb upstream of the transcriptional start site (-15023 to -14991) (Fig. 6A). To determine whether FoxM1 binds to this site, I utilized quantitative chromatin immnoprecipitation assay (ChIP). I first tested whether FoxM1 binds to Sox2 regulatory region at endogenous level. BE (2)-C cells were cross-linked and sonicated. The chromatins were immunoprecipitated with either FoxM1 specific antibody (Ab) or rabbit serum (control). The amount of endogenous Sox2 DNA bound by FoxM1 was determined by PCR using two different sets of primers flanking the DNA sequences near the potential binding sites (-14963 to -14801 and -15148 to -15040). Compared with serum control, FoxM1 antibody was able to enrich the DNA fragments upstream 15kb region of the Sox2 gene with both sets of primers and there was no enrichment by using primers flanking non-specific region around -2.5kb upstream (Fig. 6A). To confirm the specificity of the endogenous binding of FoxM1 to the Sox2 regulatory region, I investigated whether knockdown of FoxM1 would disrupt the interaction. Chromatin samples were collected from both FoxM1 siRNA treated BE(2)-C cells and control siRNA treated BE(2)-C cells. The amount of Sox2 regulatory region DNA enriched by FoxM1 antibody in both samples was quantified by RT-PCR with two different sets of primers specific to upstream 15kb region of the Sox2 gene. FoxM1 knockdown led to a half fold reduction in the immunoprecipitation of the -15kb region amplicons (Fig. 6B) which indicated the binding is FoxM1 specific. These results showed that, in the BE(2)-C cells, endogenous FoxM1 binds to the Sox2 upstream region (Fig. 6A) and activates expression of Sox2 (Fig. 5A).

To test the transcriptional activity FoxM1 on human *Sox2* upstream regulatory region, I cloned the human *Sox2* upstream sequence (-15178 to -14836) encompassing the predicted binding motif into pGl3 construct (wt-pGl3-Sox2) as well as the mutated human *Sox2* sequence where four canonical FoxM1 binding motif GTTTs were mutated into CTTTs (mut-pGl3-Sox2) (Fig. 6C). I performed dual luciferase assay by co-transfecting BE (2)-C cells with FoxM1b expression construct and either wild-type *Sox2* reporter plasmid or mutated reporter plasmid. Overexpression of FoxM1b resulted in a 3-fold increase in wild type *Sox2* promoter activation relative to empty vector transfection; whereas it failed to stimulate the mutated *Sox2* luciferase construct (Fig. 6C). Similar results were obtained in U2OS cells (data not shown).

In addition, I found that expression of Sox2 in BE(2)-C cells treated with FoxM1-siRNA caused a partial, but significant, reversal of the anchorage-independent growth (Fig. 6D). An incomplete reversal is consistent with the possibility that FoxM1 activates expression of other genes required for the anchorage-independent growth. It is likely that Bmi1, the expression of which decreased following FoxM1 silencing, is involved (Fig. 5A and B). Also, I assayed for other pluripotency genes in BE(2)-C cells for their dependence on FoxM1. Depletion of FoxM1 resulted in a significant loss of Oct4, Ezh2 and Suz12 expression (Data now shown). To further investigate the role of Sox2 in the anchorage-independent growth of the BE(2)-C cells, I employed Sox2 siRNA, which caused a significant loss of the anchorage-independent growth in soft agar colony formation assay compared with control siRNA treatment, indicating a critical role of Sox2 in neuroblastoma cells (Fig. 7A,B and C). More interestingly, silencing of Sox2 largely compromised the increased number of soft agar colonies caused by over

expressing of FoxM1 in the BE(2)-C cells (Fig. 7C and D), suggesting that Sox2 is one of the key downstream mediators of FoxM1 in inducing anchorage-independent growth of the neuroblastoma cells.

Figure 6

FoxM1 activates Sox2 by binding to its upstream regulatory region. A, Schematic diagram of human Sox2 upstream region. Predicted FoxM1 binding region was shown in the box (-15023 to -14991). Arrows indicated positions for designed chromatin immunoprecipitation (ChIP) primers -15k-a (-14963 to -14801), -15k-b (-15148 to -15040) and -2.5k (-2668 to -2517). Endogenous binding of FoxM1 to Sox2 upstream region as determined by chromatin immunoprecipitation (ChIP) assay. Crosslinked and sonicated chromatin fragments from BE(2)-C cells were precipitated with either FoxM1 antibody or rabbit IgG. Semiquantitative PCR was performed to determine the amount of DNA that was precipitated by FoxM1 antibody or IgG control by using indicated primers targeting predicted binding region (-15k-a and -15k-b) or non-binding region (-2.5k). B, BE(2)-C cells were transfected with control or FoxM1 siRNA for 72 hours. Chromatins were crosslinked, sonicated and precipitated with FoxM1 antibody. The amount of Sox2 upstream region precipitated by FoxM1 antibody was determined by qRT-PCR by using primers targeting predicted binding region (-15k-a and -15k-b). C, Left, Schematic diagram of wild type and mutated human *Sox2* luciferase constructs. Four canonical FoxM1 binding motif GTTTs were mutated into CTTTs. Right, fold induction of human *Sox2* promoter luciferase activity by overexpression of FoxM1 is shown. The amount of wide type *Sox2* promoter luciferase activity by empty vector stimulation was set at one fold. D, Representative pictures and quantification of anchorage-independent growth on soft-agar plates. BE(2)-C cells were co-transfected with different combination of expression vector and siRNA as indicated. Twenty-four hours after transfection, cells were plated at a density of $2x10^3$ cells per well in a six-well plate. Colonies were stained and counted after three weeks.

Figure 6

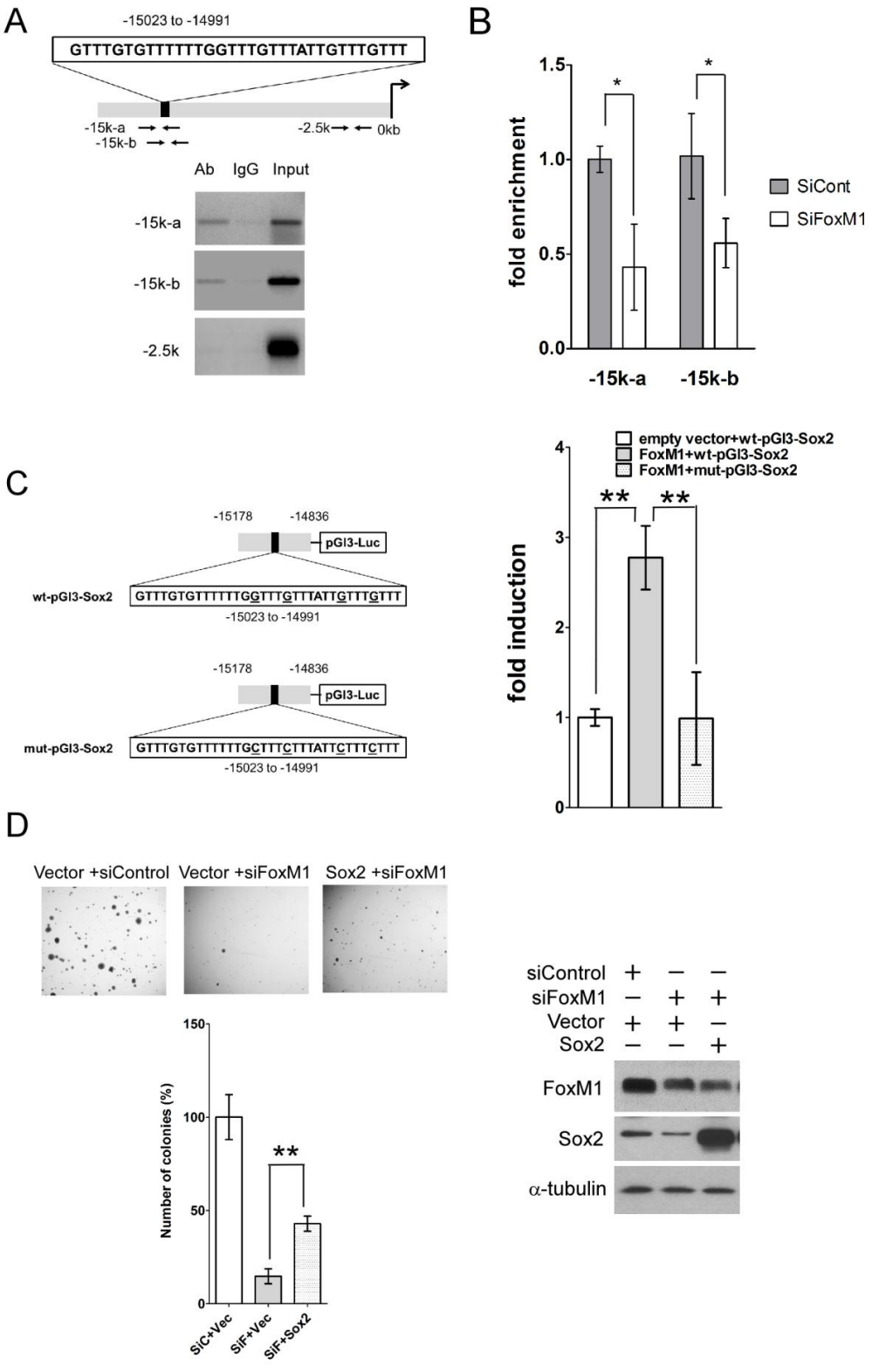
A
-15023 to -14991
GTTTGTGTTTTTTGGTTTGTTTATTGTTTGTTT
-15k-a
-15k-b
-2.5k
0kb
Ab IgG Input
-15k-a
-15k-b
-2.5k
B
fold enrichment
1.5
1.0
0.5
0.0
*
*
SiCont
SiFoxM1
-15k-a
-15k-b
C
-15178
-14836
pGl3-Luc
wt-pGl3-Sox2
GTTTGTGTTTTTTGGTTTGTTTATTGTTTGTTT
-15023 to -14991
-15178
-14836
pGl3-Luc
mut-pGl3-Sox2
GTTTGTGTTTTTTGCTTTCTTTATTCTTTCTTT
-15023 to -14991
empty vector+wt-pGl3-Sox2
FoxM1+wt-pGl3-Sox2
FoxM1+mut-pGl3-Sox2
fold induction
4
3
2
1
0
**
**
D
Vector +siControl
Vector +siFoxM1
Sox2 +siFoxM1
Number of colonies (%)
150
100
50
0
**
SiC+Vec
SiF+Vec
SiF+Sox2
siControl + – –
siFoxM1 – + +
Vector + + –
Sox2 – – +
FoxM1
Sox2
α-tubulin

\

Figure 7

FoxM1 mediated anchorage-independent growth requires expression of Sox2. A, Immunoblot showing depletion of Sox2 by siRNA in BE(2)-C cells. Cell lysates were collected at four days after transfection. B, 24 hours after Sox2 or control siRNA transfection, cells were trypsinized and seeded at a density of $2x10^3$ cells per well in a 48-well plate for proliferation assay. Viable cell number was measured by using CellTiter-Glo luminescent cell viability assay kit (Promega) every two days. The fold change in cell count was presented by luminescence unit and was normalized by day zero. C, BE(2)-C cells were first transfected with empty or pCMV-FoxM1 plasmid for 24 hours, and then transfected with either control siRNA or Sox2 siRNA for another 24 hours. Cells were plated at a density of $8x10^3$ cells per well in a six-well plate in soft agar plate. Colonies were stained and quantified after three weeks. D, Quantification of colonies numbers derived from C. Colony large than 100μm in diameter was defined as large colony and colony which has diameter between 25-100μm was defined as small colony.

Figure 7

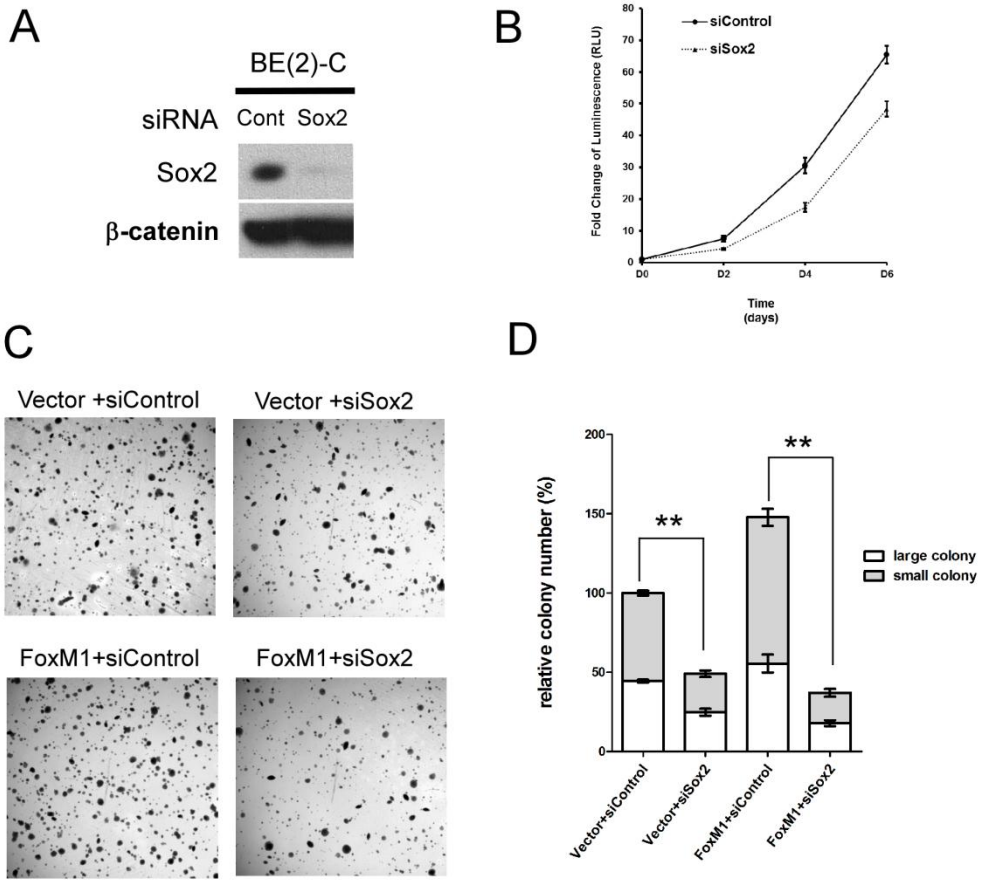
A
BE(2)-C
siRNA
Cont
Sox2
Sox2
β-catenin
B
siControl
siSox2
Fold Change of Luminescence (RLU)
Time (days)
D0
D2
D4
D6
C
Vector +siControl
Vector +siSox2
FoxM1+siControl
FoxM1+siSox2
D
relative colony number (%)
large colony
small colony
**
**
Vector+siControl
Vector+siSox2
FoxM1+siControl
FoxM1+siSox2

E. FoxM1 deletion results in impaired self-renewal of the E14.5 Neural Stem/Progenitor Cells

Both Sox2 and Bmi1 are critical for self-renewal of the neural cortical stem/progenitor cells (70, 86). If FoxM1 is important for expression of these genes in those cell type, I hypothesized that deletion of FoxM1 will inhibit self-renewal of the neural cortical stem/progenitor cells. To test this possibility, I took advantage of the well-established protocol to culture neural cortical stem/progenitor cell in vitro (87) (also see schematic in Fig. 8A). The embryonic cortical tissue from day 14.5 ERT2-Cre FoxM1fl/fl embryo was dissected and digested to generate neurospheres in serum-free medium. The ERT2-Cre FoxM1fl/fl strain was generated by crossing ERT2-Cre strain with FoxM1 fl/fl strain. ERT2-Cre allele allows the activation of Cre-recombinase upon tamoxifen administration, which in turn excises the FoxM1 alleles from the genome. To check whether FoxM1 regulates Sox2 and Bmi1 in neural stem/progenitor cells, same number of dissociated neural stem/progenitor cells was kept in serum-free NSC medium containing either 4-OH tamoxifen or ethanol as vehicle control. After 4 days, FoxM1 mRNA was remarkably decreased along with decreases in Sox2 and Bmi1 expression, as evidenced by RT-PCR and immunoblot (Fig. 8B and C). The level of Nestin, another neural stem cell marker, also went down (Fig. 8C). To exclude the possible side effect from tamoxifen, in parallel, wildtype neurospheres were generated and cultured in the same setting. Tamoxifen treatment did not lead to any significant reduction of Sox2 and Bmi1, which indicated the effect of Sox2 and Bmi1 reduction is due to FoxM1 ablation (Fig. 8B).

Figure 8

Decreased Sox2 expression in neural stem/progenitor cells following FoxM1 depletion. A, Schematic diagram describing the experimental procedure. B, ERT2-Cre FoxM1fl/fl neural stem/progenitor cells were treated with vehicle or 50nM 4OH-tamoxifen treatment for four days after being dissociated into single cells. mRNA levels of FoxM1, Sox2 and Bmi1 were detected by qRT-PCR. Wildtype neural stem/progenitor cells with same treatment were used as control. The mRNA levels were normalized to mouse cyclophilin mRNA, and the vehicle control groups were set to one fold. C, Immunoblot showing the expression of FoxM1, Bmi1, Sox2 and Nestin of ERT2-Cre FoxM1fl/fl neural stem/progenitor cells treated with vehicle or 50nM 4OH-tamoxifen. β-actin was used as loading control.

Figure 8

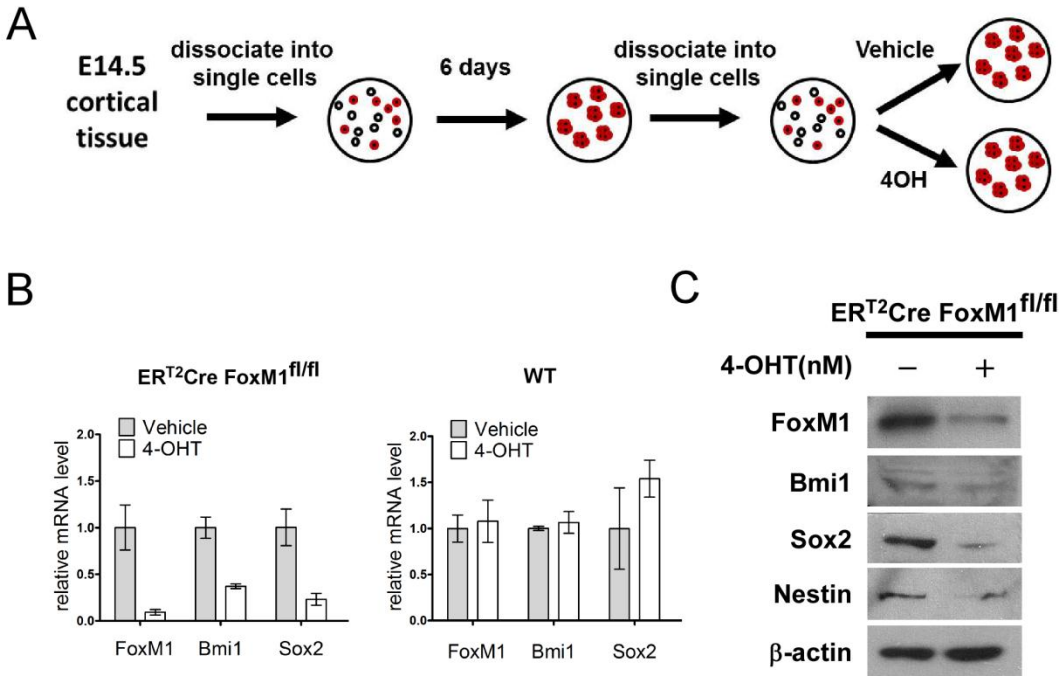
A
E14.5 cortical tissue
dissociate into single cells
6 days
dissociate into single cells
Vehicle
4OH
B
ERT2Cre FoxM1fl/fl
WT
Vehicle
4-OHT
relative mRNA level
2.0
1.5
1.0
0.5
0.0
FoxM1
Bmi1
Sox2
C
ERT2Cre FoxM1fl/fl
4-OHT(nM)
–
+
FoxM1
Bmi1
Sox2
Nestin
β-actin

In addition, I performed the neurosphere assay, which measures the capacity of a primary neurosphere to form new multipotent neurosphere after dissociation, as an indicator of self-renewal capacity (See schematic in Fig. 9A). The ERT2-Cre FoxM1fl/fl neurospheres were dissociated into single cells. Same number of cells was kept in serum-free NSC medium containing either 4-OH tamoxifen or ethanol as vehicle control. After 6 days, number of neurosphere formed was counted. A representative picture of the neurospheres counted was shown (Fig.9B). I found that FoxM1 deletion by tamoxifen treatment led to a significant decrease in the frequency of newly-formed neurosphere compared with vehicle control (Fig. 9C), indicating that loss of FoxM1 impairs the self-renewal of previous neural stem/progenitor cell population. The same procedure was repeated with the newly formed primary neurospheres to obtain secondary neurospheres in either 4-OHT tamoxifen treated and control treated samples (Fig. 9A). After 6 days, I found the difference in neurosphere frequency was even more dramatic (Fig. 9D). I observed no obvious difference in primary neurosphere frequency in the wild type neurospheres. Similar effects on primary neurosphere frequency were observed when the ERT2Cre FoxM1fl/fl neurospheres were treated with adenovirus expressing lacZ gene or Cre recombinase. The primary frequency of neurosphere was decreased by adeno-Cre treatment (Fig. 9C). Together, these data suggested that FoxM1 is necessary to maintain the self-renewal of cortical neural stem/progenitor cells.

Figure 9

Loss of FoxM1 impairs the self-renewal of neural stem/progenitor cells. A, Schematic diagram describing the experimental procedure of neurosphere assay. B, Representative picture of neurospheres. C, Quantification of primary neurosphere frequency. Neural stem/progenitor cells were dissociated into single cells and same amount of cells were plated in triplicate for each treatment. Wildtype neural stem/progenitor cells were treated with vehicle or 50nM 4OH-tamoxifen as controls. ERT2-Cre FoxM1fl/fl neural stem/progenitor cells were treated with vehicle or 50nM 4OH-tamoxifen in one set and AdlacZ or AdCre virus in another set. Six days later, the number of neurospheres was counted under microscope. The frequency of neurosphere was calculated by dividing the number of neurospheres formed by the number of initial single neural stem/progenitor cells plated. The neurosphere frequency was normalized to the vehicle control which was set to 100%. D, ERT2-Cre FoxM1fl/fl neurosphere formed from the set treated with vehicle or 50nM 4OH-tamoxifen described in C were dissociated again and same amount of cells were plated and treated with another round of vehicle or 50nM 4OH-tamoxifen. Six days later, the secondary neurosphere frequency was obtained in the same way.

Figure 9

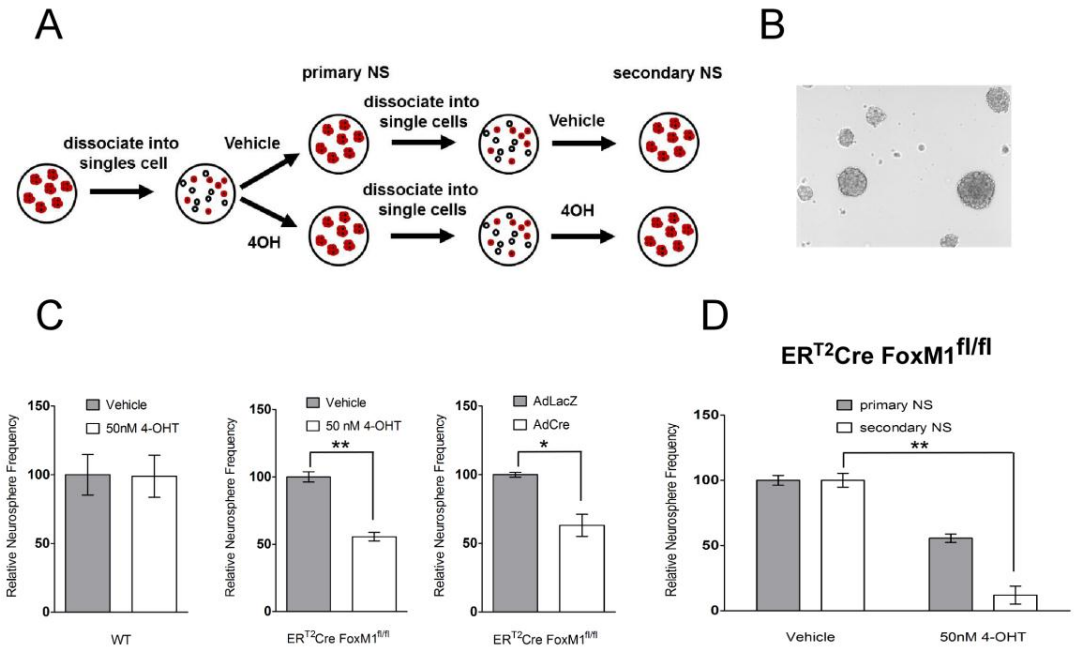
A
primary NS
secondary NS
dissociate into singles cell
Vehicle
dissociate into single cells
Vehicle
4OH
dissociate into single cells
4OH
B
C
Relative Neurosphere Frequency
Vehicle
50nM 4-OHT
WT
Vehicle
50 nM 4-OHT
**
ER^T2Cre FoxM1^fl/fl
AdLacZ
AdCre
*
ER^T2Cre FoxM1^fl/fl
D
ER^T2Cre FoxM1^fl/fl
primary NS
secondary NS
**
Vehicle
50nM 4-OHT

2. Targeting FoxM1 effectively retards p53-null lymphoma and sarcoma

A. Backgrounds

The tumor suppressor p53, encoded by the TP53 gene, is a short-lived transcription factor involved in a wide range of cellular processes that are critical for tumor suppression (88-90). Though p53 is expressed at a low level in normal cells, it serves as a protective barrier against development of many types of cancers mainly through preventing proliferation of the incipient cancer cells, induction of apoptosis, as well as through its role in the maintenance of genome integrity (90). Mice deficient in p53 develop spontaneous tumors including thymic lymphoma and sarcoma (90, 91). The essential role of p53 as a tumor suppressor is further manifested by the fact that the p53 gene is mutated in approximately half of the human cancers (88). Given the high prevalence of p53 inactivation in human cancers, it is important to validate therapeutic strategies targeting cancer cells with loss of p53 function.

Given the multifaceted functions of FOXM1 in tumor progression, targeting FOXM1 represents a rational and promising anti-cancer therapeutic strategy. This is further supported by the fact that FOXM1 is a proliferative-specific transcriptional factor whose expression is unique to the proliferating cells (4, 92). Several strategies have been developed to target FoxM1 in cancer cells. Based on the fact that FoxM1 is an inhibitory target of mouse ARF tumor suppressor, a cell penetrating ARF $_{26\text{-}44}$ peptide which consists of 9 N-terminal D-arginine (D-Arg) residues and amino acid residues 26-44 of the mouse ARF protein was synthesized (30). The ARF $_{26\text{-}44}$ peptide, which inhibits FOXM1 by sequestering it to the nucleolus, is effective in diminishing tumor size in HCC by reducing tumor cell proliferation and inducing apoptosis (51). That ARF peptide

also effectively prevents pulmonary metastasis of HCC cells (42). In addition, thiazole antibiotics have been shown to down-regulate FOXM1 and induce apoptosis in various cancer cells (52, 53).

In this study, I demonstrate that FOXM1 is critical for survival and growth of p53-/- tumor cells both *in vitro* and *in vivo*. The ARF $_{26\text{-}44}$ peptide, which inhibits the activity of FOXM1, induces apoptosis in p53 null tumors. These observations validate the therapeutic strategy of targeting FOXM1 in tumors with p53 loss of function.

B. p53 null thymic lymphoma and sarcoma cells are addicted to FoxM1 for survival

FoxM1 is a p53-regulated gene (34, 35). Our database analyses indicated that FoxM1-mRNA is up regulated in cancers harboring mutations in p53 (Fig. 10) (93-96). In this study, I analyzed the role of FoxM1 in p53 loss-of-function tumors. To investigate that, I generated a strain of triple transgenic mice harboring CreERT2, *Foxm1 fl/fl* and p53 -/- alleles by crossing the three individual strains. Mice developed a spectrum of spontaneous tumors, as expected from the p53 null background (91). The presence of CreERT2 allele in the triple transgenic strain permits Cre recombinase expression upon 4-OH tamoxifen treatment to excise flox flanked *Foxm1* alleles and thus silencing FoxM1 expression. However, our attempts to study the effects of *Foxm1* deletion on endogenous lymphomas/sarcomas were inconclusive mainly because the lymphomas/sarcomas developed at different times in the cohorts of mice used in the study. Also, since the *Foxm1* alleles are deleted in most cell types in this system, it would be difficult to avoid the effects of *Foxm1*-deletion in the other cell types on the lymphoma/sarcoma

development and progression. Therefore, I decided to isolate lymphoma/sarcoma cells from the triple transgenic and analyze them in host mice. Two thymic lymphoma (L1 and L2) and a sarcoma (S) triple transgenic cell lines were generated from the endogenous tumors. In addition, a control thymic lymphoma line (C) isolated from *Foxm1 fl/fl* p53-/- tumor was established in parallel. I tested the deletion efficiency of FoxM1 by immunoblot and confirmed that FoxM1 expression was significantly reduced in triple transgenic lines L1, L2 and S but not in control line C upon treatments with 4-OH tamoxifen (Fig. 11A-D). A sarcoma line stably transduced with exogenous FoxM1 expression was generated. Treatments with 4-OH tamoxifen did not diminish the exogenous FoxM1 expression (Fig. 11D).

To examine the effect of FoxM1 ablation, growth curves were plotted following 4-OH tamoxifen treatment. FoxM1 deletion led to a profound decrease in the cell viability starting from early time point in all of the three triple transgenic lines L1, L2 and S (Fig. 11A, B and D). The control lymphoma cell line C (Fig. 11C) as well as the sarcoma cells stably expressing the exogenous FoxM1 (Fig. 11D) did not exhibit inhibition, demonstrating that the phenotype was caused by FoxM1 ablation. I also tested the tumorigenic properties of the sarcoma cells by performing soft agar assay. FoxM1 deletion significantly reduced the ability of cells to grow under anchorage-independent conditions (Fig. 12A). Cells after FoxM1 deletion formed about 60% less colonies on soft agar plate compared to the control. In addition, cells without FoxM1 also formed about 50% less colonies on adherent plate (Fig. 12B). These results indicate that FoxM1 function is important for the survival and tumorigenicity of tumor cells with p53 loss of function.

Figure 10

FoxM1 mRNA is elevated in p53 mutated tumors. Box plot of FoxM1 mRNA expression level in tumors harboring mutations in p53 or having wild type p53. Datasets were extracted from ONCOMINE database. P values were calculated using Student's t test.

Figure 10

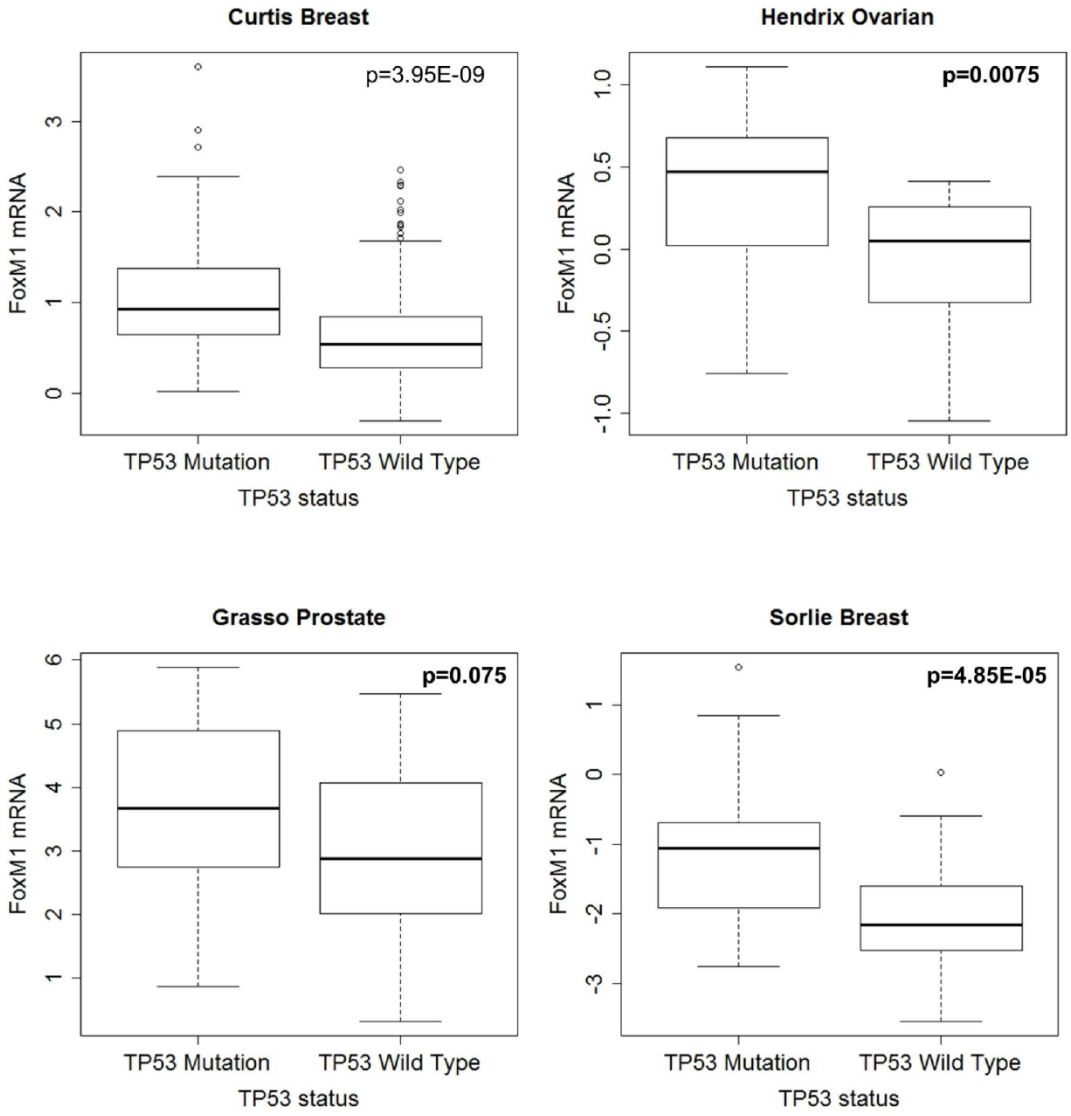
Curtis Breast
p=3.95E-09
FoxM1 mRNA
0
1
2
3
TP53 Mutation
TP53 Wild Type
TP53 status
Hendrix Ovarian
p=0.0075
FoxM1 mRNA
-1.0
-0.5
0.0
0.5
1.0
TP53 Mutation
TP53 Wild Type
TP53 status
Grasso Prostate
p=0.075
FoxM1 mRNA
1
2
3
4
5
6
TP53 Mutation
TP53 Wild Type
TP53 status
Sorlie Breast
p=4.85E-05
FoxM1 mRNA
-3
-2
-1
0
1
TP53 Mutation
TP53 Wild Type
TP53 status

Figure 11

FoxM1 is critical for the survival and tumorigenicity of p53 null thymic lymphoma and sarcoma. A-C, CreERT2, *Foxm1 fl/fl* and p53 -/- thymic lymphoma (represented by "L1" and "L2") and *Foxm1 fl/fl* and p53 -/- thymic lymphoma (represented by "C") were treated with ethanol as vehicle or 800nM of 4OH-tamoxifen (Tam). D, CreERT2, *Foxm1 fl/fl* and p53 -/- sarcoma (represented by "S") was treated with ethanol as vehicle or 800nM of 4OH-tamoxifen (Tam). Sarcoma line stably transduced with FoxM1 expression was constructed (S: FoxM1) and treated with 800nM of 4OH-tamoxifen. Cell viability was measured by proportional luminescence signal generated by celltiter-glo assay.

Figure 11

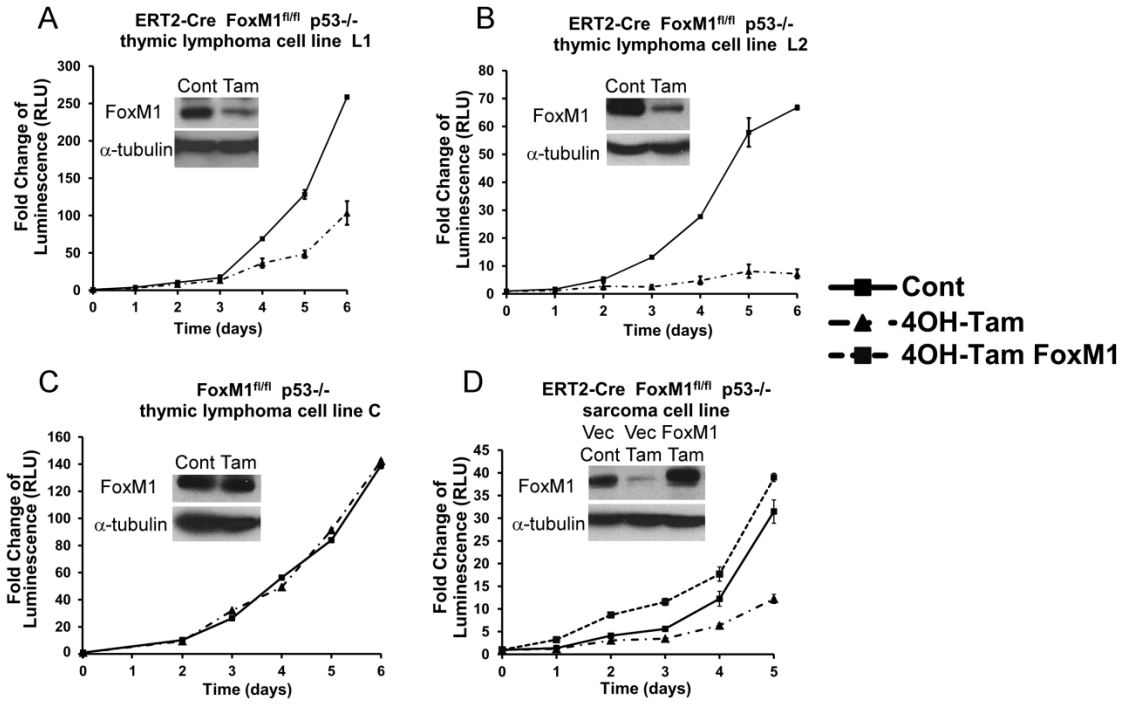
A
ERT2-Cre FoxM1fl/fl p53-/-
thymic lymphoma cell line L1
Cont Tam
FoxM1
α-tubulin
Fold Change of Luminescence (RLU)
Time (days)
B
ERT2-Cre FoxM1fl/fl p53-/-
thymic lymphoma cell line L2
Cont Tam
FoxM1
α-tubulin
Fold Change of Luminescence (RLU)
Time (days)
Cont
4OH-Tam
4OH-Tam FoxM1
C
FoxM1fl/fl p53-/-
thymic lymphoma cell line C
Cont Tam
FoxM1
α-tubulin
Fold Change of Luminescence (RLU)
Time (days)
D
ERT2-Cre FoxM1fl/fl p53-/-
sarcoma cell line
Vec Vec FoxM1
Cont Tam Tam
FoxM1
α-tubulin
Fold Change of Luminescence (RLU)
Time (days)

Figure 12

A, Representative pictures and quantification of soft agar colonies of CreERT2, *Foxm1 fl/fl* and p53 -/- sarcoma cells following control, 400nM and 800nM 4OH-tamoxifen treatment. B, Representative pictures and quantification of foci formation assay of CreERT2, *Foxm1 fl/fl* and p53 -/- sarcoma cells following control, 400nM and 800nM 4OH-tamoxifen treatment.

Figure 12

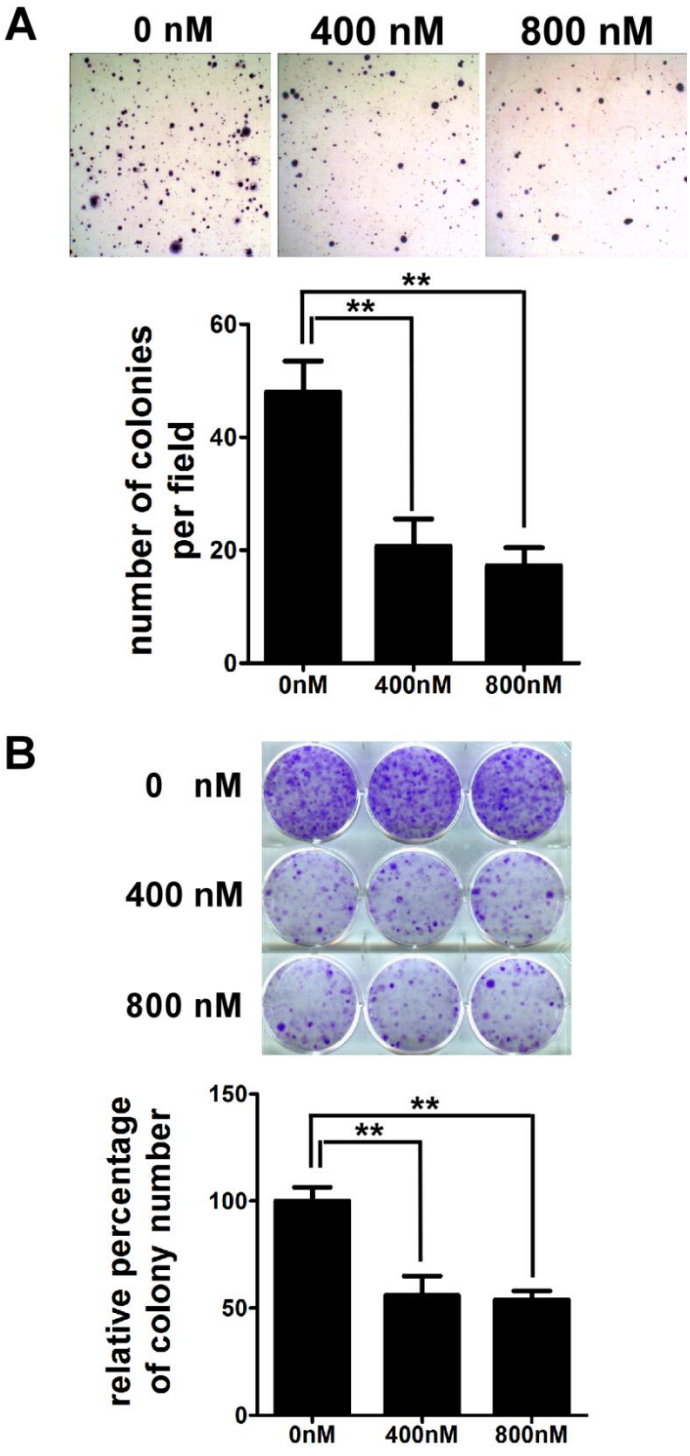
A
0 nM
400 nM
800 nM
number of colonies per field
60
40
20
0
**
**
0nM
400nM
800nM
B
0 nM
400 nM
800 nM
relative percentage of colony number
150
100
50
0
**
**
0nM
400nM
800nM

C. FoxM1 ablation diminishes expression of Survivin and Bmi1 in p53 null tumors accompanied by apoptosis

Several studies have suggested targeting FoxM1 could serve as a therapeutic strategy towards treatment of cancer (3, 51, 97). To validate this strategy in tumors harboring p53 loss of function, I utilized nude mice allograft model. One million thymic lymphoma (L1) or sarcoma (S) triple transgenic cells were injected subcutaneously into nude mice. About one week after injection, when the tumors became palpable, I randomized animals into two treatment groups and started to administer either tamoxifen or vehicle for two weeks. For both p53 null tumor lines, the tumors in the vehicle-treated control group grew significantly faster than of the tumors treated with tamoxifen (Fig. 13A and B). FoxM1 expression was examined by performing immunohistochemical staining. FoxM1 expression was largely reduced following two-weeks of tamoxifen treatment, while in the vehicle treated group abundant FoxM1 staining was detected, consistent with FoxM1 over-expression in tumor cells (Fig. 14A-D).

To investigate the basis for delayed tumor growth, I assayed for apoptosis of the tumor cells using TUNEL staining. In both lymphoma and sarcoma derived tumor sections, I observed an increased number of apoptotic cells following FoxM1 depletion, evidenced by increase number of TUNEL positive cells (Fig. 13C-D, Fig. 14E-L). I also assayed for cleaved caspase-3 and cleaved PARP, two apoptosis markers. Significant increases in the number of cleaved caspase-3 and cleaved PARP positive cells were detected in FoxM1-depleted cells (Fig. 14M-N). These observations suggested that the inhibition of the p53-/- tumors following loss of FoxM1 resulted from enhanced apoptosis of the tumor cells.

The increased apoptosis upon FoxM1-depletion was somewhat surprising because the p53-/- tumor cells are generally resistant to apoptosis (98). Survivin, which belongs to the inhibitor of apoptosis protein (IAP) family, is a known transcriptional target of FoxM1 that plays important roles in both cell cycle regulation and inhibition of apoptosis (59, 99). Previously, it was shown that reduced Survivin levels contributed to apoptosis of HCC cells (51). Consistent with this finding, I observed that expression of Survivin, which is abundant in control groups for both p53 null lymphoma and sarcoma, was down-regulated following depletion of FoxM1 (Fig. 15A-D, I). Bmi1, another FoxM1-induced gene (8, 36), was shown also to protect tumor cells from apoptotic stimuli (100). Therefore, I assayed for expression of Bmi1 in the tumor sections. I observed that the expression of Bmi1 was largely diminished in FoxM1-ablated tumors (Fig. 15E-H, I). These observations suggest important roles of Bmi1 and Survivin in the survival of the p53-/- lymphoma and sarcoma. In Fig. 15I, the doublet for Bmi1 is not obvious in the Sarcoma samples because a higher percentage resolving gel was used. It is noteworthy that although the reduction of Survivin and Bmi1 was evident, it was not complete possibly due to the presence of other signaling pathways that control expression of these two proteins. In that regard, NF-κB/STAT3 and ERK/AMPK/p38MARK signaling pathways were shown to activate the expression of Survivin (101, 102). In addition, the expression of Bmi1 is regulated by microRNAs (103).

Figure 13

FoxM1 ablation retards growth and **induces apoptosis of allografted p53 null lymphoma and sarcoma** A, Tumor volumes of the subcutaneously inoculated CreERT2 *Foxm1 fl/fl* and p53 -/- thymic lymphoma cell L1 following FoxM1 ablation by tamoxifen and control treatment are indicated. B, Tumor volumes of the subcutaneously inoculated CreERT2 *Foxm1 fl/fl* and p53 -/- sarcoma cell S following FoxM1 ablation by tamoxifen and control treatment are shown. C, Quantification of percentage of TUNEL positive cell per field of sarcoma. D, Quantification of percentage of TUNEL positive cell per field of thymic lymphoma.

Figure 13

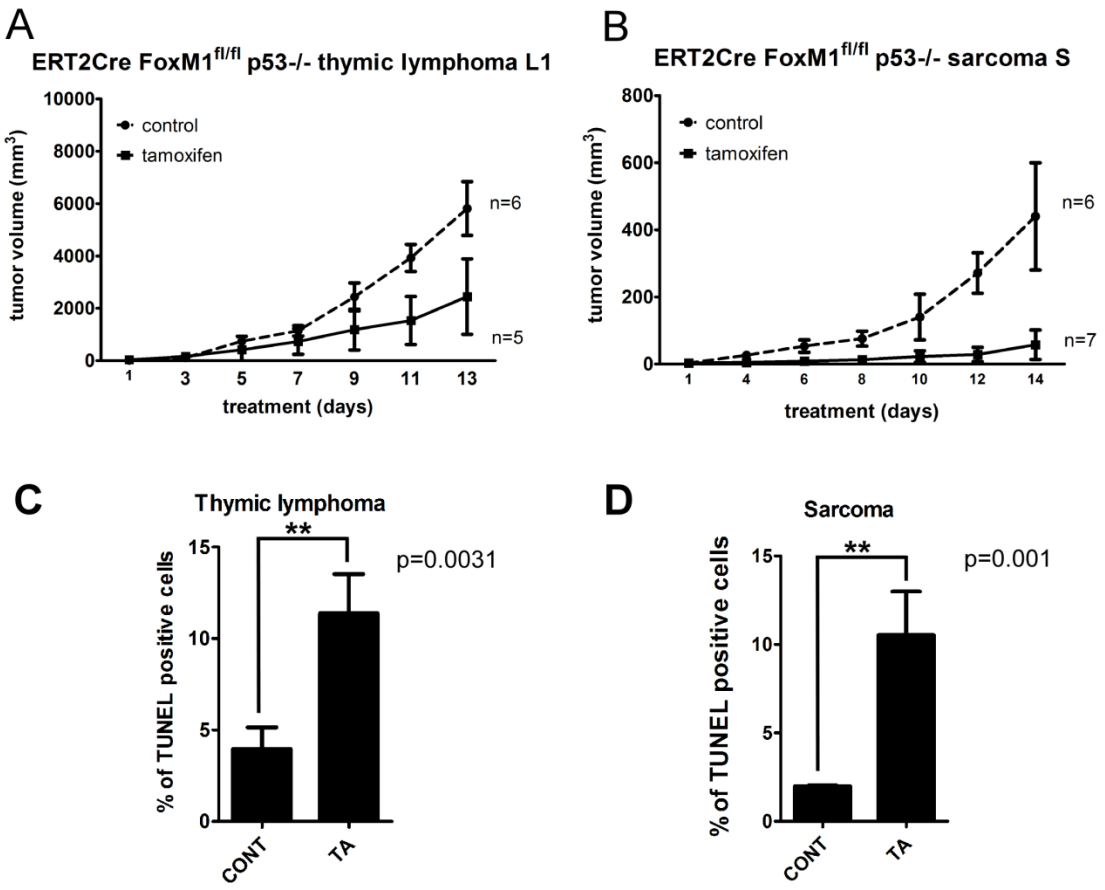
A
ERT2Cre FoxM1fl/fl p53-/- thymic lymphoma L1
tumor volume (mm3)
control
tamoxifen
n=6
n=5
treatment (days)
B
ERT2Cre FoxM1fl/fl p53-/- sarcoma S
tumor volume (mm3)
control
tamoxifen
n=6
n=7
treatment (days)
C
Thymic lymphoma
% of TUNEL positive cells
**
p=0.0031
CONT
TA
D
Sarcoma
% of TUNEL positive cells
**
p=0.001
CONT
TA

Figure 14

A, FoxM1 IHC staining of 5 micron allografted sarcoma tissue of control group. B, tamoxifen treated group. C, thymic lymphoma control group. D, thymic lymphoma tamoxifen group. E-F and I-J, Representative TUNEL and DAPI staining of tumor sections from the subcutaneously inoculated CreERT2 *Foxm1 fl/fl* and p53 -/- sarcoma after tamoxifen or control treatment are shown. G-H and K-L, Representative TUNEL and DAPI staining of tumor sections from the subcutaneously inoculated CreERT2 *Foxm1 fl/fl* and p53 -/- thymic lymphoma after tamoxifen or control treatment are shown. M, quantification of number of positive cleaved-caspase 3 (Asp175) cells per field of thymic lymphoma is shown. N, quantification of number of positive cleaved-PARP (Asp214) cells per field of thymic lymphoma is shown.

Figure 14

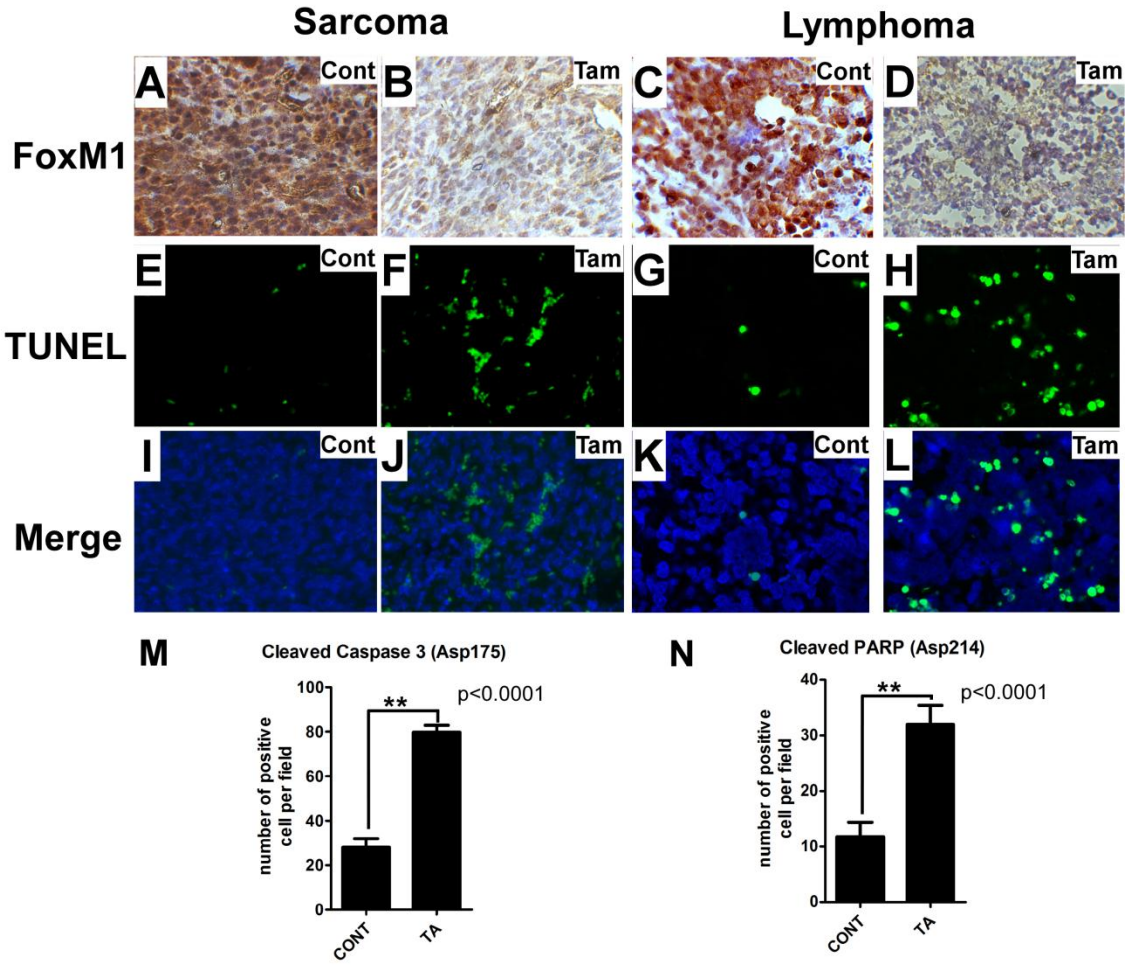
Sarcoma
Lymphoma
FoxM1
TUNEL
Merge
A
B
C
D
E
F
G
H
I
J
K
L
Cont
Tam
M
Cleaved Caspase 3 (Asp175)
number of positive cell per field
p<0.0001
**
CONT
TA
N
Cleaved PARP (Asp214)
number of positive cell per field
p<0.0001
**
CONT
TA

Figure 15

Reduced expression of Survivin and Bmi1 following FoxM1 ablation in p53 null tumors. A-D, Representative Survivin staining of subcutaneously inoculated CreERT2 *Foxm1 fl/fl* and p53 -/- lymphoma and sarcoma cells following tamoxifen and control treatment. E-H, Representative Bmi1 staining of subcutaneously inoculated CreERT2 *Foxm1 fl/fl* and p53 -/- lymphoma and sarcoma cells following tamoxifen and control treatment. I, Western blot of protein lysates extracted from allografted tumors assayed for FoxM1, Bmi1 and Survivin. α–tubulin was used as a loading control. Lysates were collected from both control oil treated mice and tamoxifen treated mice.

Figure 15

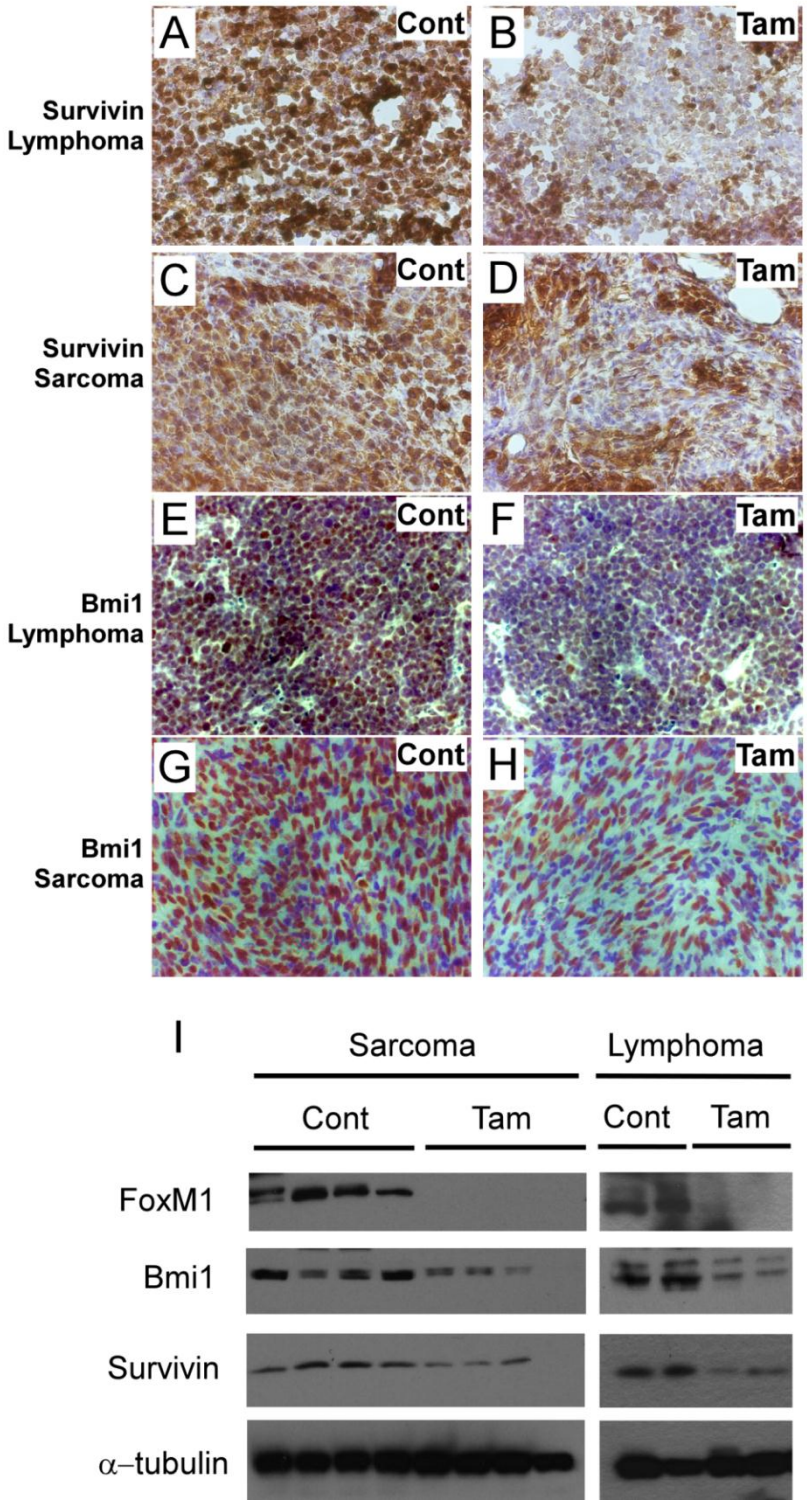
A
Cont
B
Tam
Survivin
Lymphoma
C
Cont
D
Tam
Survivin
Sarcoma
E
Cont
F
Tam
Bmi1
Lymphoma
G
Cont
H
Tam
Bmi1
Sarcoma
I
Sarcoma
Lymphoma
Cont
Tam
Cont
Tam
FoxM1
Bmi1
Survivin
α–tubulin

D. ARF-derived peptide inhibitor of FoxM1 induces apoptosis in p53 null tumor cells

A peptide (ARF 26-44) derived from the mouse tumor suppressor ARF has been described that inhibits the activity of FoxM1 by re-localizing it to the nucleolus (30) (51). A cell-penetrating form of the peptide efficiently targets FoxM1 in liver tumors. In the DEN/PB induced mouse hepatocellular carcinoma model, the ARF-peptide is able to inhibit HCC progression by inducing apoptosis (51). The ARF-peptide induced apoptosis was observed mainly on the FoxM1-expressing cells. In addition, it has been shown to block the metastatic growth of the HCC cells (42). In order to see whether the ARF-peptide is able to inhibit the p53 null tumors, I first examined the effect of the peptide, in vitro. A mutant peptide (ARF 37-44), which lacks the interacting domain with FoxM1, was used as a control. One day after treatment the wild type ARF-peptide treated p53 null thymic lymphoma cell lines L1 and L2 underwent apoptosis. The number of viable cells was much less following treatment with wild type ARF peptide compared with cells treated with the mutant-peptide or PBS (Fig. 16A). The induction of apoptosis by the wild type peptide was demonstrated by TUNEL staining (Fig. 16B). A similar effect was observed in p53 null sarcoma cells (Fig. 16A-B). However, compared to the sarcoma lines, the p53-/- lymphoma cells are more sensitive to the ARF-peptide, where 5μM of peptide was able to cause significant apoptosis (Fig. 16A). Cell growth and foci formation assay, as well as cleaved caspase-3 staining were performed to confirm the finding (Fig. 17). Treatments with the ARF-peptide strongly inhibited expression of several FoxM1-induced genes, including Survivin, Bmi1, EZH2, Stathmin and MMP9

(Fig. 16D). The ARF-peptide had only a marginal effect on expression of Bax and GADD45, which are not direct targets of FoxM1.

Figure 16

ARF $_{26\text{-}44}$ peptide activates apoptotic response in the p53 null tumor cells. A, Phase contrast picture of CreERT2 *Foxm1 fl/fl* and p53 -/- thymic lymphoma and sarcoma cells treated with PBS, ARF $_{37\text{-}44}$ peptide (Mut) or ARF $_{26\text{-}44}$ peptide (WT) at 24 hours. B, TUNEL and DAPI staining of CreERT2 *Foxm1 fl/fl* and p53 -/- thymic lymphoma and sarcoma cells treated with PBS, ARF $_{37\text{-}44}$ peptide (Mut) or ARF $_{26\text{-}44}$ peptide (WT) . C, Quantification of percentage of TUNEL positive cells per field. D, Western blot of protein lysates extracted from thymic lymphoma cells treated with PBS, ARF $_{37\text{-}44}$ peptide (Mut) or ARF $_{26\text{-}44}$ peptide (WT)**.** α-tubulin was used as a loading control. The band intensities were quantified by Image J program, and the relative intensities after adjusting for loading control (intensity of the tubulin bands) are shown below each panel.

Figure 16

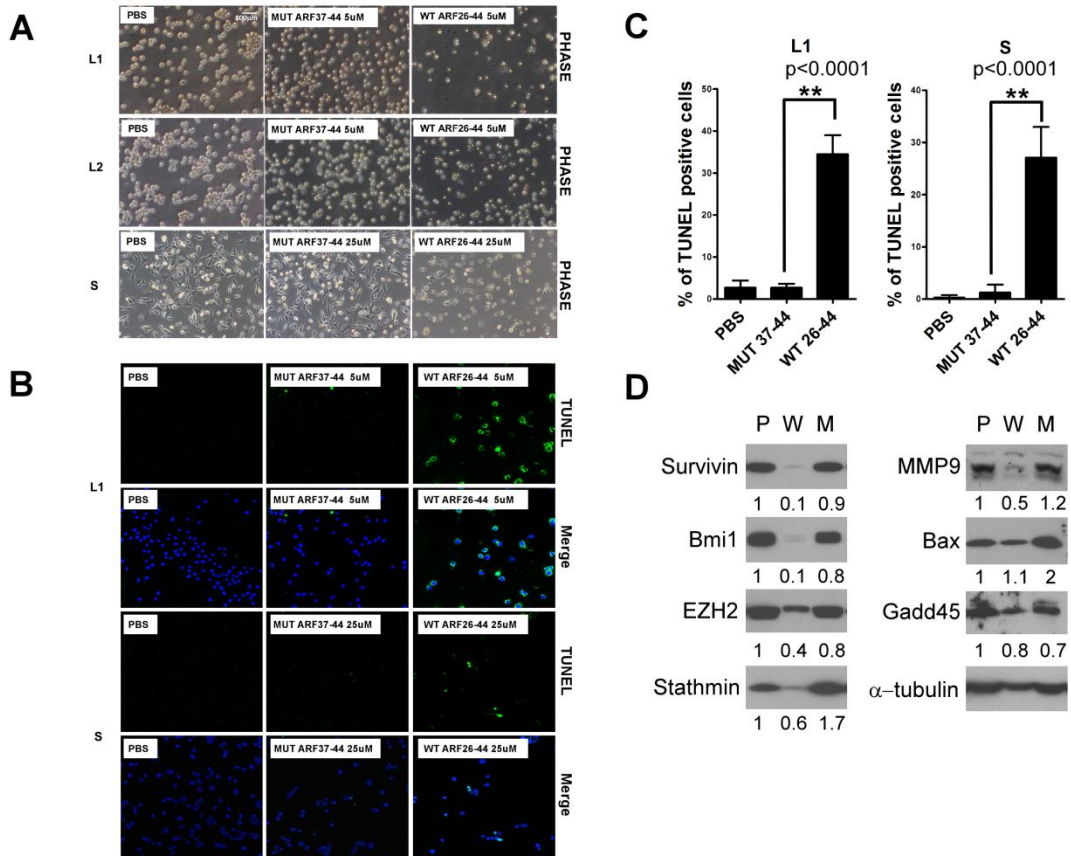
A
PBS
MUT ARF37-44 5uM
WT ARF26-44 5uM
MUT ARF37-44 25uM
WT ARF26-44 25uM
L1
L2
S
PHASE
B
TUNEL
Merge
C
L1
p<0.0001
S
p<0.0001
**
% of TUNEL positive cells
PBS
MUT 37-44
WT 26-44
D
P W M
Survivin
1 0.1 0.9
Bmi1
1 0.1 0.8
EZH2
1 0.4 0.8
Stathmin
1 0.6 1.7
MMP9
1 0.5 1.2
Bax
1 1.1 2
Gadd45
1 0.8 0.7
α–tubulin

Figure 17

Loss of viability of p53 null cells following ARF 26-44 peptide treatment in vitro. A, CreERT2 *Foxm1 fl/fl* and p53 -/- thymic lymphoma cell viability at 0h and 24 hours following non, 5μM of ARF $_{26\text{-}44}$ peptide, 5μM of ARF $_{37\text{-}44}$ peptide or PBS treatment. B, Foci formation of CreERT2 *Foxm1 fl/fl* and p53 -/- sarcoma cells following PBS, 25μM of ARF $_{27\text{-}44}$ peptide, or ARF $_{36\text{-}44}$ peptide treatment. C, Cleaved-caspase 3 staining of CreERT2 *Foxm1 fl/fl* and p53 -/- sarcoma cells 24 hours after 25μM of ARF $_{27\text{-}44}$ peptide treatment.

Figure 17

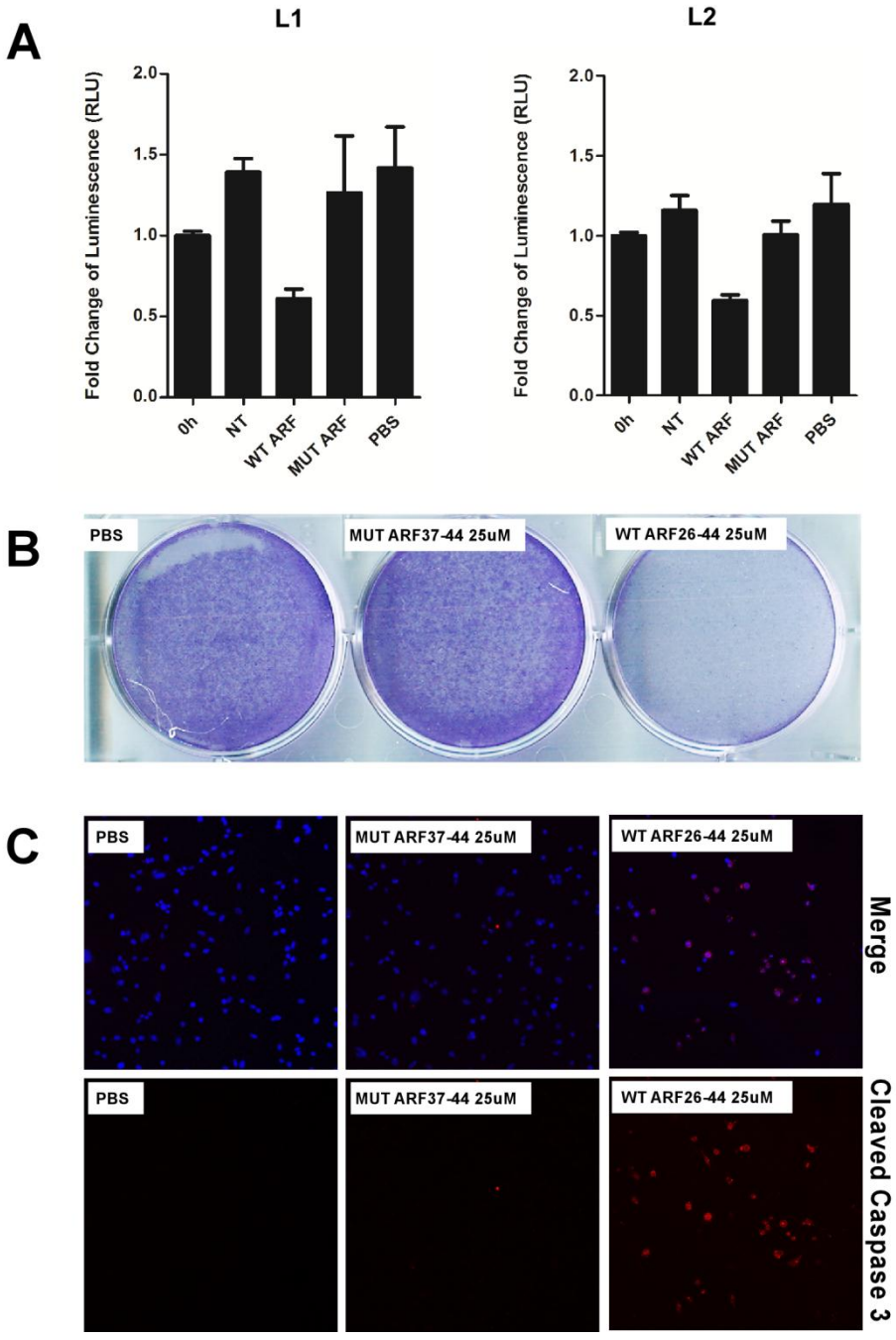
A
L1
L2
Fold Change of Luminescence (RLU)
2.0
1.5
1.0
0.5
0.0
0h
NT
WT ARF
MUT ARF
PBS
B
PBS
MUT ARF37-44 25uM
WT ARF26-44 25uM
C
PBS
MUT ARF37-44 25uM
WT ARF26-44 25uM
Merge
Cleaved Caspase 3

E. ARF-peptide effectively reduces the colonization of p53 null tumor cells in vivo

To test the therapeutic effect of the ARF-peptide on p53 null tumors in vivo, p53 null lymphoma/sarcoma cells were introduced into the circulation of SCID mice through intravenous injection. Both p53 null sarcoma and lymphoma cells were stably transduced with lentivirus carrying luciferase expression before injection. Shortly after injection, comparable fluorescence was detectable in the lung by injecting luciferin using Xenogen IVIS spectrum in vivo imaging machine (Fig. 18 A and C). Mice were randomized into three groups and were treated with PBS, mutant-peptide or the wild type ARF-peptide for 10 injections every other day starting from day 0 by intraperitoneal injection. Ten days after tumor inoculation, p53 null sarcoma cells were found to colonize the lung (Fig. 18A and B). After 20 days following the initial inoculation, compared to the PBS and the mutant peptide treated mice, the amount of luciferase signal from the wild type ARF-peptide treated mice was significantly reduced. The mice were sacrificed and lung sections were analyzed for tumor colonies. A reduced number of tumor colonies that were larger than $100\,\mu m \times 100\,\mu m$ were detected in the lungs of the wild type ARF-peptide treated mice (Fig. 18B). Moreover, Survivin and Bmi1 expression was inhibited in the colonized tumors from mice treated with the wild type ARF-peptide compared to those treated with the mutant peptide (Fig. 18D).

The murine thymic lymphoma cells tended to colonize the kidney, liver and spleen (104). For the p53 null thymic lymphoma cells, I observed metastatic growth in kidney. Around 20 days after inoculation, PBS and the mutant ARF peptide treated mice displayed strong luciferase signals from the colonized lymphoma cells in the lower back

region. On the other hand, the wild type ARF-peptide treated mice emitted very little fluorescence, indicating an inhibition of colonized tumors (Fig. 18C). When the mice were sacrificed, large tumor masses were found in the kidney by microscopic examination in the PBS and in the mutant peptide treated mice. Atypical pale coloration and enlargement of the kidney were observed in the mice, and the mice carried a large tumor mass that encompassed the two kidneys, the connective tissues and the spinal cords. On the other hand, kidneys from the wild type peptide treated mice still retained the original size and structure with only a small white mass started to build up on the surface of the kidney (Fig. 19A and B). These results clearly indicated that the wild type ARF-peptide was able to efficiently block the renal metastasis of the p53 null thymic lymphoma.

Figure 18

ARF $_{26\text{-}44}$ peptide blocks colonization of intravenously inoculated p53 null tumors. A, ICR SCID mice were intravenously inoculated with CreERT2 *Foxm1 fl/fl* and p53 -/- sarcoma cells. Luciferase intensity was monitored with IVIS image machine following peptide treatment at 10 days after initial injection and right after injection at day 0. B, H&E staining of the lung tissue section from MUT or WT peptide treated mice at day 10 and day 20 after initial sarcoma cell injection and quantification of the number of the colonies per field of the corresponding lung tissue section. C, ICR SCID mice were intravenously inoculated with CreERT2 *Foxm1 fl/fl* and p53 -/- thymic lymphoma cells. Luciferase intensity was monitored with IVIS image machine following peptide treatment at 10 days after initial injection and right after injection at day 0. D, Representative pictures of Bmi1 and Survivin IHC staining of colonized sarcoma cells in the lung after either MUT or WT peptide treatment at day 20.

Figure 18

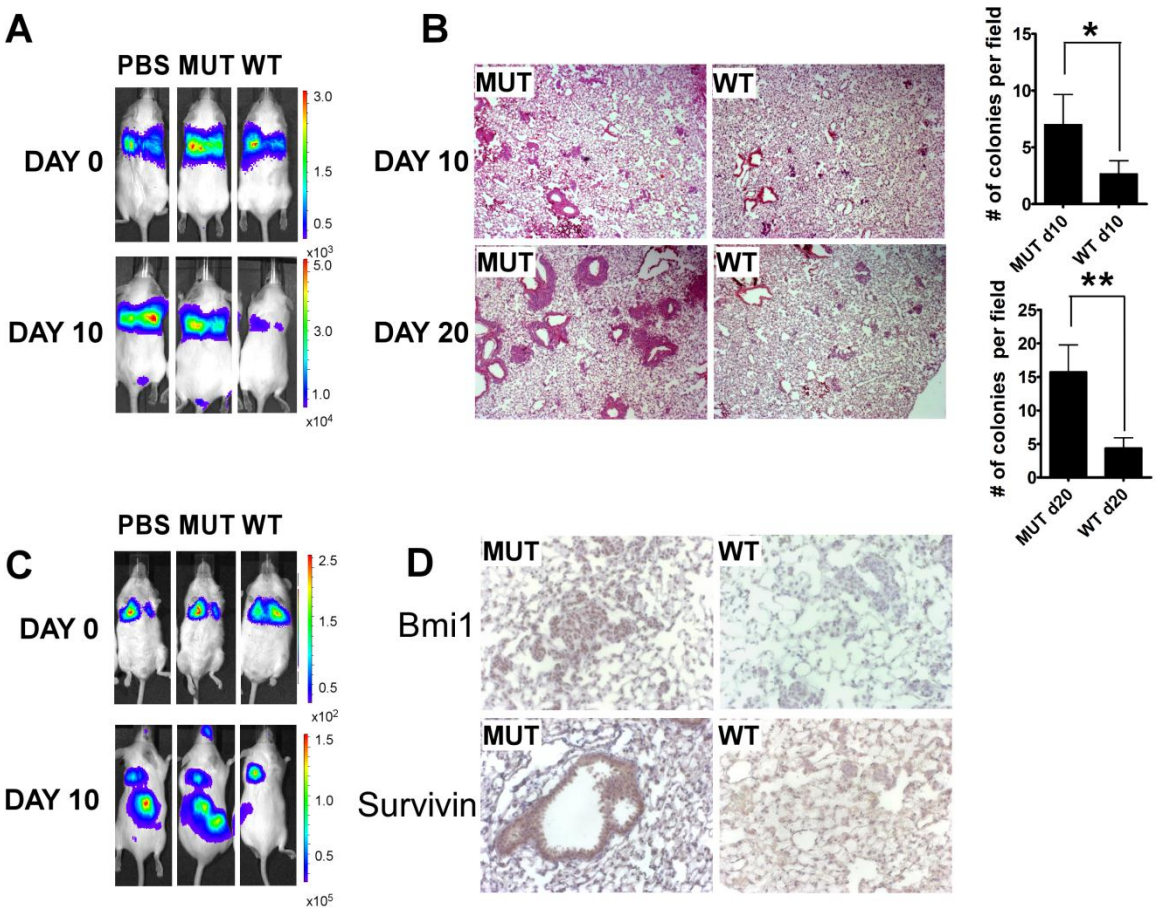
A
PBS MUT WT
DAY 0
DAY 10
3.0
1.5
0.5
x10^3
5.0
3.0
1.0
x10^4
B
MUT
WT
DAY 10
DAY 20
# of colonies per field
MUT d10
WT d10
MUT d20
WT d20
C
PBS MUT WT
DAY 0
DAY 10
2.5
1.5
0.5
x10^2
1.5
1.0
0.5
x10^5
D
Bmi1
Survivin

Figure 19

Colonized p53 null lymphoma cells in the kidney of SCID mice. A, Representative picture of tumor mass in kidney. B, Tumor mass of kidneys dissected from PBS, MUT and WT peptide treated SCID mice. Representative two mice from each group are shown.

Figure 19

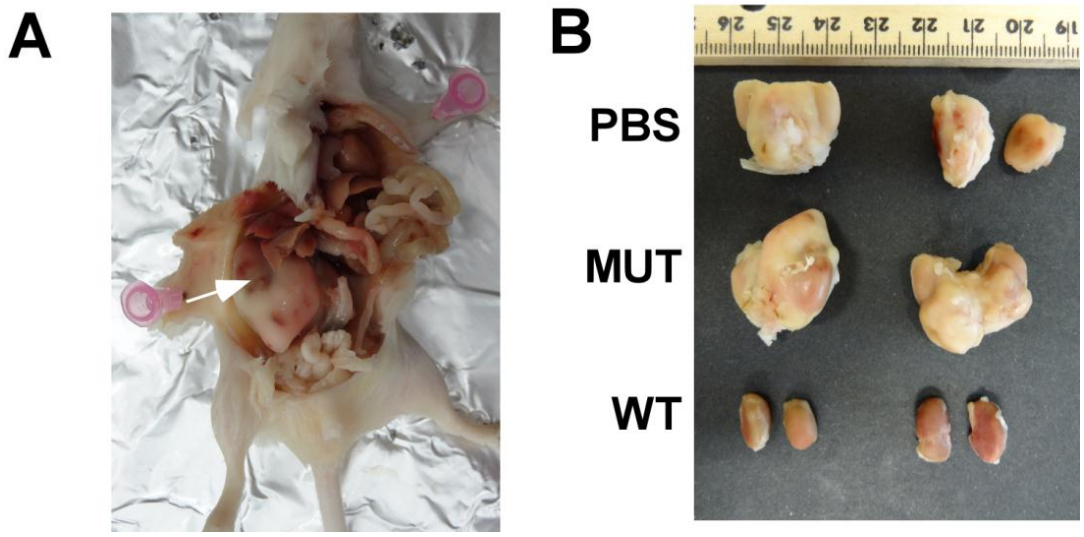

3. FoxM1 regulates EZH2 expression in prostate cancer

A. Backgrounds

The Polycomb group (PcG) proteins are epigenetic chromatin modifiers that are essential for defining cell identity during early embryogenesis and through adulthood (105). PcG proteins function coordinately to establish the stable silencing at the promoter of the target genes via two complexes: PRC1 (Polycomb repressive complex 1) and PRC2 (Polycomb repressive complex 1). Enhancer of zeste homolog 2 (EZH2) is a key component of the PRC2 complex that mediate the initial binding to the target promoters. EZH2 carries histone methyltransferase activity which specifically methylates lysine 27 of histone H3 (H3K7) and thus establishes the silencing mark at the promoter region and thereby facilitates the consequent recognition of the target promoters by the PRC1 complex (105). Deregulation of the PcG proteins are often found in human malignancies, indicating a close connection between epigenetic modification and cancer initiation (106).

Numerous studies provide direct evidence supporting an essential role of EZH2 in prostate cancer development (107). (108) (109). Higher EZH2 expression is evident in metastatic hormone-refractory prostate cancer compared to PCA (clinically localized prostate cancer) or benign prostate (107). Silencing EZH2 results in diminished proliferation in prostate cancer with increased amount of cells arrested in G2-M phase of the cell cycle, as well as reduced invasiveness(107, 110). Several genes have been characterized as direct repression targets of EZH2 in prostate cancer, including ADRB2, DAB2IP, RUNX3 and E-Cadherin(108, 109, 111-113). By repressing the expression of its target genes, which are often tumor suppressors, EZH2 promotes the aggressiveness of

prostate cancers. However, the molecular mechanisms that lead to the overexpression of EZH2 are not well characterized. EZH2 gene amplification was reported in prostate cancer cell lines, xenografts and clinical tumors with fluorescence in situ hybridization which could contributes to its aberrant overexpression in prostate cancer cells (114). EZH2 is negatively regulated by miR-101(microRNA-101), which is often found to undergo somatic loss during prostate cancer progression (115). In addition, E2F1-RB and human papillomavirus E7 are involved in regulating EZH2 expression (116, 117).

B. EZH2 positively correlates the expression of FoxM1 in prostate tumors and over-expression of the two proteins predicts poor survival outcome.

Both FoxM1 and EZH2 have been implicated in prostate cancer progression by promoting the proliferative and invasive feature of the cells. It has been shown that prostate cancer cells depleted of FoxM1 could not progress through mitosis and underwent G2-M arrest (10). Similarly, silencing EZH2 also led to attenuated proliferation and G2-M cell cycle arrest (107), which suggested a potential link between these two genes. To investigate this in the context of prostate cancer, I compiled and analyzed six publicly available microarray datasets from NCBI GEO (Gene Expression Omnibus) and the ONCOMINE depository. Consistent with previous finding, EZH2 mRNA increased gradually as disease progress to more malignant stage, with highest expression in metastatic prostate samples (Fig.20A) (107). Interestingly, FoxM1 mRNA expression resembled the expression pattern of EZH2 in the same dataset (Fig.20A). By fitting a linear regression model, I discovered that expression of the two is highly correlated, and FoxM1 is a significant predictor of EZH2 mRNA expression (Fig.20A). To confirm this discovery, I compiled additional four prostate cancer datasets from

ONCOMINE and investigate the Pearson correlation between FoxM1 and EZH2. Indeed, expression of these two genes are positively correlated at a significant level in all of the dataset analyzed, suggesting the presence of a regulatory link (Fig.20B). High EZH2 expression has been associated with poor clinical outcome in melanoma and prostate cancer and is considered as a biomarker for advanced prostate and breast cancer (118, 119). Interestingly, by stratifying prostate cancer patients based on EZH2 and FoxM1coexpression profile, the high EZH2 and high FoxM1 subgroup which includes patients with both top 25% EZH2 and top 25% FoxM1 expression level have significantly worse survival outcome based on univariate analysis compared with the rest of the patients (Fig.20C). These result suggested that the presence of high FoxM1 and EZH2 expression may contribute to the aggressive nature of the prostate cancer cells. The correlation also exists at the protein level. Strong EZH2 and FoxM1 staining was evident in adenocarcinoma tissue, but not detectable cancer adjacent normal prostatic tissue (Fig.20D).

Figure 20

EZH2 expression is tightly correlated with FoxM1 in prostate patient samples. A. Increased expression of FoxM1 mRNA and EZH2 mRNA in metastatic prostate cancer tissue samples. FoxM1 mRNA is significantly positively correlated with EZH2 from normal to metastatic prostate tissues and FoxM1 is a significant linear predictor of EZH2 mRNA level (NCBI: GDS2545). B. Significant positive correlation between FoxM1 and EZH2 mRNA in prostate cancer datasets extracted from ONCOMINE cancer transcriptome. (Arredouani Prostate N=21 (120), Taylor Prostate N=150 (121), Varambally Prostate N=19 (122), Yu Prostate N=112 (123)) C. Kaplan-Meier survival curve of patients stratified by FoxM1 and EZH2 expression. High FoxM1 and high EZH2 expression predicts poor survival outcome (N=34 for high FoxM1 and high EZH2 group, N=329 for other, Log-rank $p<0.0001$, (124)). D. Immunohistochemistry staining of FoxM1 and EZH2. AN: Cancer adjacent normal prostatic tissue. AC: Adenocarcinoma.

Figure 20

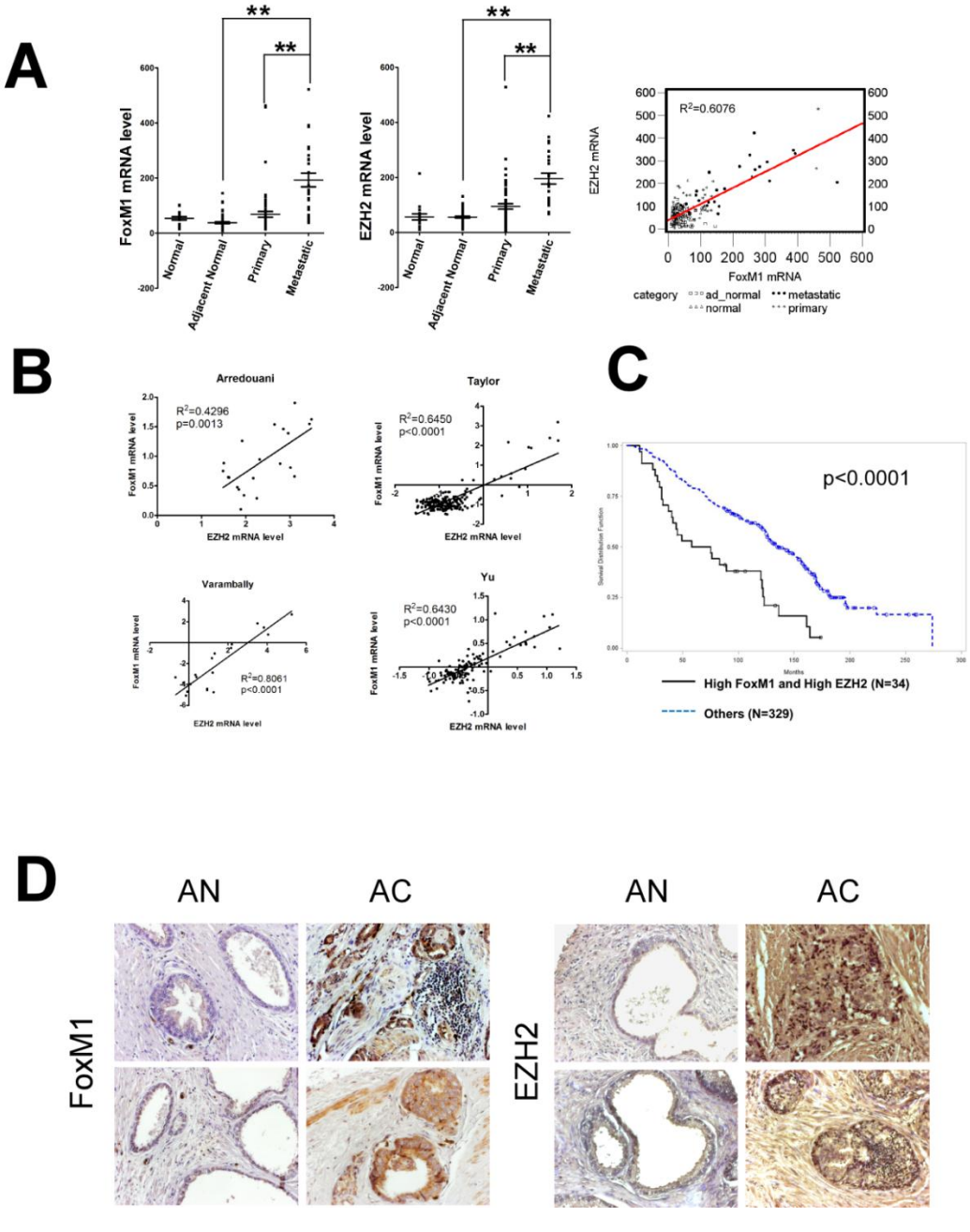
A
FoxM1 mRNA level
EZH2 mRNA level
Normal
Adjacent Normal
Primary
Metastatic
**
EZH2 mRNA
FoxM1 mRNA
R2=0.6076
category
ad_normal
metastatic
normal
primary
B
Arredouani
R2=0.4296
p=0.0013
Taylor
R2=0.6450
p<0.0001
Varambally
R2=0.8061
p<0.0001
Yu
R2=0.6430
p<0.0001
C
p<0.0001
High FoxM1 and High EZH2 (N=34)
Others (N=329)
D
AN
AC
FoxM1
EZH2

C. FoxM1 is critical for the expression of EZH2 in prostate cancer cells.

To elucidate the mechanism that accounts for the tight connection between EZH2 and FoxM1. I tested the hypothesis that FoxM1 is necessary for the expression of EZH2. In order to address this, FoxM1 siRNA was utilized to diminish the expression of FoxM1 in two metastatic prostate cancer cell lines: LnCAP (AR positive) and DU145 (AR negative). The mRNA level of EZH2 was significantly attenuated, evidenced by semi-quantitative PCR in both cell lines upon depletion of FoxM1 (Fig.21A). On the other hand, ectopic expression of FoxM1 in benign prostate hyperplasia cell line BPH led to an increase in EZH2 mRNA level. GTPase-activating protein DAB2IP was reported to be repressed by EZH2(109). Moreover, ADRB2 (adrenergic receptor, beta-2) and E-Cadherin which contribute to the disease progression in prostate cancers are repressed by EZH2 (108, 112). Coupled with EZH2 reduction, the mRNA expression of *DABR2P*, *ADRB2 and E-Cadherin* were reduced in FoxM1 overexpressing cells, as they were in EZH2 overexpressing cells (Fig.21B). However, the ectopic expression of EZH2 did not simulate the expression of FoxM1 in BPH1 cells. Therefore, I conclude that the presence of FoxM1 is critical for the expression of EZH2 in prostate cancer cells.

Figure 21

The presence of FoxM1 is necessary for EZH2 expression in prostate cancer cells. A. Semi-quantitative PCR of FoxM1, EZH2 in LnCAP and DU145 cells treated with control siRNA (CONT) or FoxM1 siRNA (FoxM1). The intensity of the band is quantified and normalized by cyclophilin. B. Semi-quantitative PCR of FoxM1, EZH2, DAB2IP, ADRB2 and E-Cadherin in BPH cells transfected with control (CONT), pCMV-FoxM1(FoxM1) or pCMV-EZH2 (EZH2) plasmid. Cyclophilin was used as internal control. The intensity of the band is quantified and normalized by cyclophilin. C. Western blots of FoxM1, EZH2, E-Cadherin in DU145 and LnCAP treated with control siRNA (CONT), FoxM1 siRNA (FoxM1) or without treatment (NT). α-tubulin was used as loading control. D. Western blots of FoxM1 and EZH2 in BPH1 cells stably transduced with control (VEC) or FoxM1 (FoxM1) retrovirus. α-tubulin was used as loading control.

Figure 21

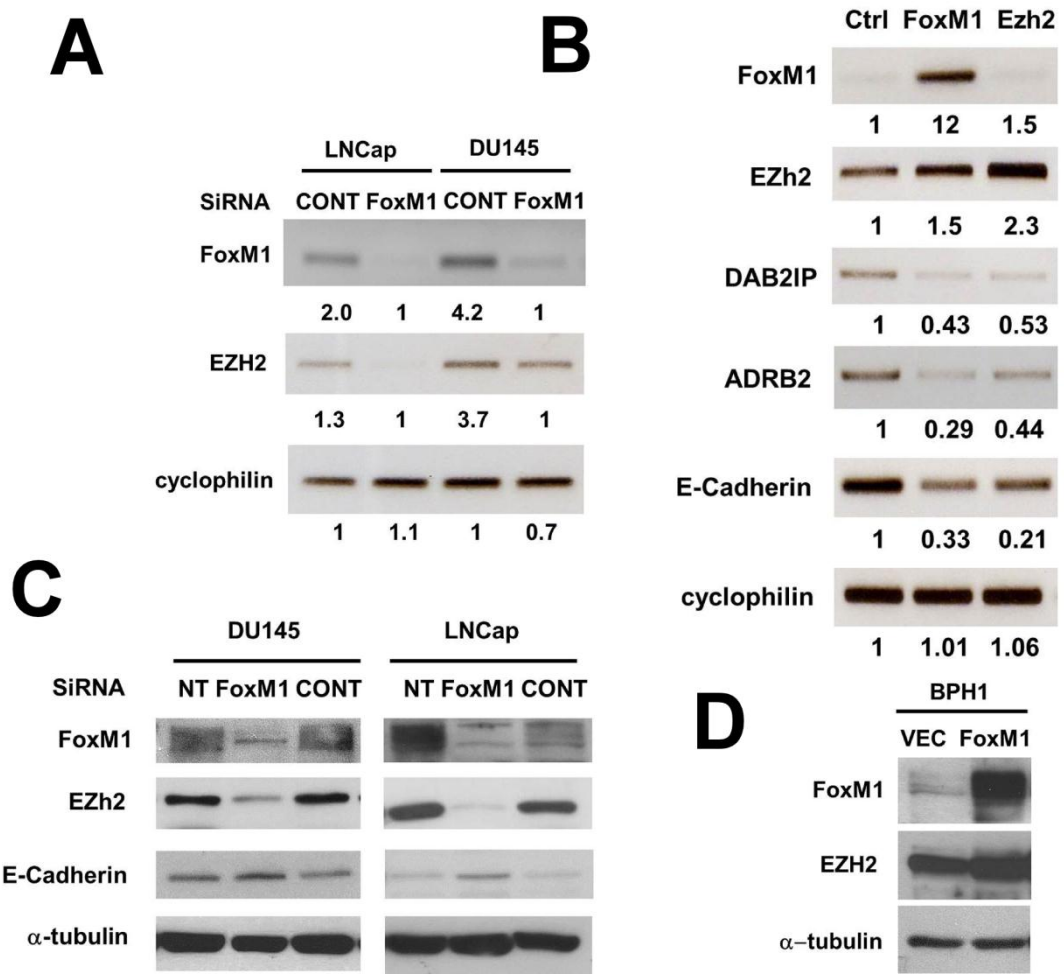
A
LNCap
DU145
SiRNA
CONT FoxM1 CONT FoxM1
FoxM1
2.0 1 4.2 1
EZH2
1.3 1 3.7 1
cyclophilin
1 1.1 1 0.7
B
Ctrl FoxM1 Ezh2
FoxM1
1 12 1.5
EZh2
1 1.5 2.3
DAB2IP
1 0.43 0.53
ADRB2
1 0.29 0.44
E-Cadherin
1 0.33 0.21
cyclophilin
1 1.01 1.06
C
DU145
LNCap
SiRNA
NT FoxM1 CONT
NT FoxM1 CONT
FoxM1
EZh2
E-Cadherin
α-tubulin
D
BPH1
VEC FoxM1
FoxM1
EZH2
α–tubulin

D. FoxM1 promotes invasive properties of prostate cancer cells by activating expression of EZH2.

Prostate metastasis is highly incurable and accounts for the most prostate cancer related death mostly due to the lack of understanding in molecular mechanism that drives the progression to the advanced metastatic diseases. In liver HCC, FoxM1 function an essential mediator of metastatic phenotype by regulating a number of cellular processes that favors the survival and dissemination of the metastatic cells (42, 125). However, the involvement of FoxM1 in mediating prostate metastasis has not been investigated. To study whether FoxM1-EZH2 axis contributes to the metastatic nature of the prostate cancer cells, I first study the effect of FoxM1 overexpression on directional cell migration by performing in vitro wound healing assay in DU145 cells. Compared with control cells, FoxM1 stably expressing DU145 cells migrated at a faster rate evidenced at 20 hours following initial scratch (Fig.23A). In addition, the invasive phenotype of DU145 cells was significantly enhanced through stable expression of FoxM1 evidence by matrigel chamber assay (Fig.23B and 23C). More cells were able to invade through extracellular matrix layer to the bottom membrane when FoxM1 is overexpressed. Cells depleted of EZH2 by siRNA displayed reduced ability of invasion. Interestingly, the enhancement of invasive capacity of the FoxM1 expressing cells were largely diminished following EZH2 silencing as well, suggesting EZH2 function as a critical downstream factor of FoxM1 in mediating the invasiveness of the prostate cancer cells (Fig.23B and 23C). Loss of E-Cadherin has been associated with high grade prostate cancer (126). E-Cadherin promoter was epigenetically silenced by Polycomb proteins in prostate cancers and in ES cells(108, 127). Consistent with these findings, the E-Cadherin expression was

activated in DU145 cells treated with siRNA against EZH2. FoxM1 overexpression drove the reduction of E-Cadherin expression. However, silencing EZH2 in FoxM1 overexpressing cells caused the re-expression of E-Cadherin in spite of the abundant presence of FoxM1 (Fig.23D)

Figure 22

FoxM1 promotes invasiveness and migration of prostate cancer cells via EZH2. A. Wound healing of DU145 cells stably expressing empty vector (VEC) or FoxM1 (FoxM1) at 0 hour and 20 hour. B. Matrigel invasion chamber assay of DU145 cells stably expressing empty vector (VEC) or FoxM1 (FoxM1) treated with control siRNA (SiCONT) or EZH2 siRNA (SiEZH2). C. Quantification of invasion assay. D. Immunofluorescence staining of E-Cadherin in the above cells.

Figure 22

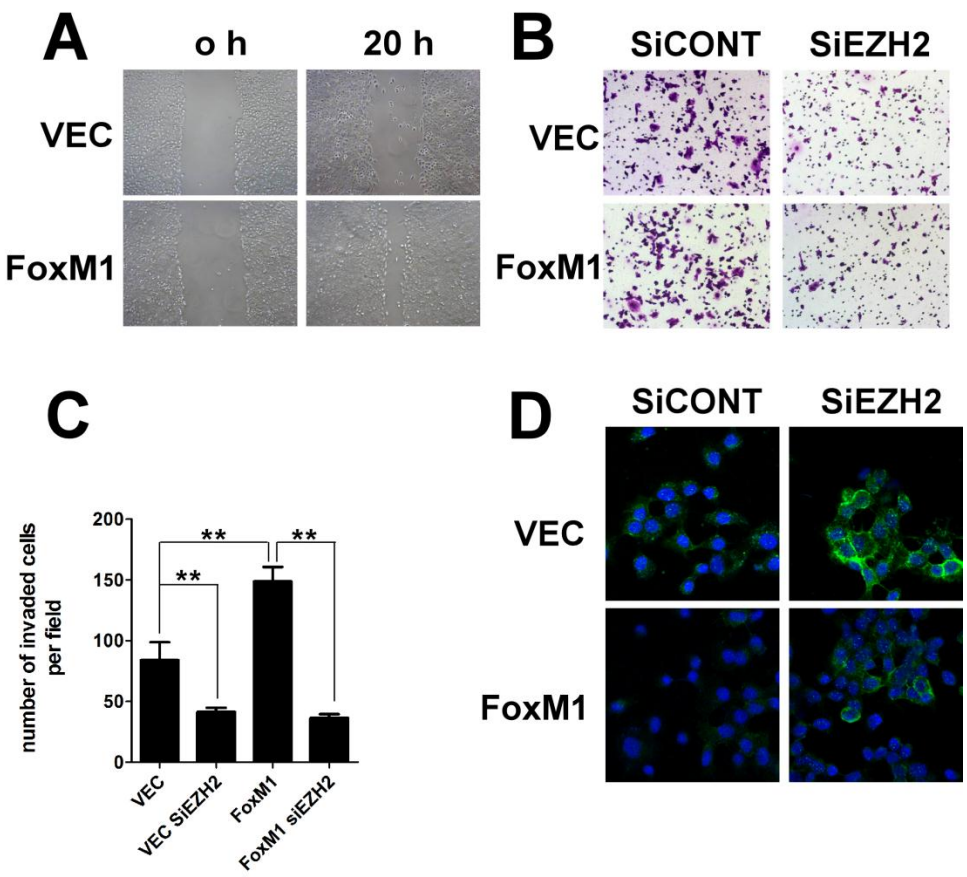
A
o h
20 h
VEC
FoxM1
B
SiCONT
SiEZH2
VEC
FoxM1
C
number of invaded cells per field
200
150
100
50
0
**
**
**
VEC
VEC SiEZH2
FoxM1
FoxM1 siEZH2
D
SiCONT
SiEZH2
VEC
FoxM1

IV. DISCUSSION

1. FoxM1 and neuroblastoma

The aggressive forms of neuroblastoma still remain a challenge in the clinic, largely due to limited knowledge of biologic and prognostic characteristic of this childhood disease. My study revealed that FoxM1 is crucial for the tumorigenicity of aggressive neuroblastoma cells, which is often related to the metastatic potential of the tumors. These observations make FoxM1 an attractive therapeutic target for treating neuroblastoma patients. That is particularly significant because several groups are actively involved in characterizing inhibitors of FoxM1 that also inhibits tumor progression (30, 52).

Studies described here on neuroblastoma are significant as they provide new molecular insights into the aggressive nature of this disease. Although FoxM1 is over-expressed in the aggressive forms of neuroblastoma, its involvement in neuroblastoma has not been investigated. I demonstrated a dual role of FoxM1 in positively regulating tumorigenicity and in maintenance of the progenitor population in neuroblastoma. First, I showed that FoxM1 serves as a critical activator of tumorigenic properties of the aggressive forms of the neuroblastoma cells. In addition, I discovered a direct connection between FoxM1 and pluripotency-associated gene Sox2 in mediating the anchorage-independent growth of the neuroblastoma cells. Moreover, I observed that neuroblastoma cells with reduced FoxM1 expression undergo spontaneous differentiation with diminished levels of Sox2. Furthermore, in mouse cortical neural stem/progenitor cells, loss of FoxM1 largely impaired the self-renewal ability.

Mounting evidences suggested the existence of tumor initiating cells within neuroblastoma might be responsible for its clinical relapse (66, 68). The striking clinical bipolarity of its pathological feature also indicated that neuroblastoma may be a disease of stem cells (57, 58). Expression of the pluripotency genes, which are critical for normal stem cell maintenance, have been detected in neuroblastoma cells (67, 68). However, very little is known about the molecular basis of how the pluripotency genes get activated. In my work, I discovered that one of the core pluripotent genes Sox2 is directly activated by FoxM1. My observation suggests that the pluripotency gene Sox2 is critical for the tumorigenic activity of FoxM1. Thus, FoxM1 might be involved in altering the cellular characteristic favoring oncogenic growth of tumor cells by potentially up-regulating pluripotency-associated genes.

2. FoxM1 regulates core pluripotency-associated genes in cancer

The link between FoxM1 and the expression of pluripotency genes in cancers has been recently investigated. In P19 mouse embryonic carcinoma cell lines, ectopic expression of FoxM1 prevents the decrease of Oct4 and Nanog during P19 cell differentiation and promotes the expression of Oct4, Nanog and Sox2 in human fibroblasts(83). I observed that in neuroblastoma the ectopic expression of FoxM1 stimulated Sox2, but not Oct4 and Nanog (data not shown). However, when I depleted FoxM1 by siRNA, expressions of Sox2, Oct4 and Nanog were reduced, indicating that endogenous FoxM1is required for the expression of pluripotency genes in neuroblastoma cells. These observations were made with cell types that still retain the potential to be

further differentiated in culture. The neuroblastoma cell lines used in my study contains cells that represent the progenitor population of the neural crust. Therefore, it would be interesting to investigate whether FoxM1 behaves differentially in terms of stimulating expression of the pluripotency genes in various sub-populations of the neuroblastoma cells categorized by differentiation state.

The regulation on Sox2 by FoxM1 is observed in neuroblastoma, a type of tumor where Sox2 is known to be required for the maintenance of the progenitor identity. The oncogenic function of Sox2 has been observed in other types of human malignancies. In breast cancer, Sox2 facilitates the G1/S transition via transcriptional activation of *CCND1*, which in turn promotes proliferation of the cells (128). Loss of tumorigenicity is found to be associated with Sox2 silencing in glioblastoma(72). Genetic evidence directly demonstrates that Sox2 is an amplified lineage-survival oncogene in lung and esophageal squamous cell carcinomas (71). However, it remains unclear what leads to the aberrant expression of Sox2 in malignant tissues. It is possible that Sox2 has already been expressed in the benign tissues preceding the onset of neoplasia. Or it is stimulated later during oncogenesis. Nevertheless, the over-expression of FoxM1 in human malignancies can serve as one mechanism that leads to the expression of Sox2.

Also, in my study, I discovered that the self-renewal capacity of neural progenitor/stem cells is diminished following FoxM1 silencing. Sox2 reduction is associated with the loss of self-renewal, but it remains unclear what is the major downstream effector pathway that is responsible for the phenotype. Based on preliminary bioinformatics analysis, a group of cell cycle genes appear to be common targets for both FoxM1 and Sox2. But the exact effectors await validation in the context

of neural progenitor/stem cells. In addition, the cellular fate of neural progenitor/stem cell following FoxM1 silencing has not been fully investigated. The neural progenitor/stem cells can be further differentiated into neurons, astrocytes and oligodendrocytes in culture. Whether neural progenitor/stem cells upon FoxM1 depletion preferentially differentiate into certain type of cells would reveal critical information on role of FoxM1 in differentiation.

2. FoxM1, polycomb group (PcG) proteins and epigenetic regulation

The polycomb group (PcG) proteins are essential epigenetic regulators during embryogenesis and for the maintenance of the adult stem cells (106). Deregulated developmental pathways resulting from the aberrant expression of polycomb proteins often lead to cancer development (129). Bmi1 and EZH2, two of the polycomb proteins, are the found to be overexpressed in cancers (129).

Interestingly, the phenotypes associated with loss of Bmi1 resemble those associated with loss of FoxM1. For example, in mouse embryonic fibroblasts (MEFs), the absence of Bmi1 leads to premature senescence at passage three with elevated expression of $p16^{Ink4a}$ and $p19^{Arf}$ (130). Similar phenotype is observed in FoxM1-/- mouse embryonic fibroblasts (MEFs), where most of the cells fail to exit mitosis and are positive for β-galactosidase (25). Both Bmi1 and FoxM1 in cancer cells increase tumorigenicity *in vitro* and *in vivo*, enhanced mobility and more invasive phenotype (131). In breast cancer, expression of Bmi1 increases as the tumor advanced to late and more malignant stage (131). It is also true for FoxM1. In breast cancer FoxM1 displays higher expression

in high grade, poorly differentiated tumors (17). All these observations suggested a possible connection between FoxM1 and Bmi1, which is confirmed by my study in neuroblastoma cells. I found the expression of Bmi1 tightly correlated with change of FoxM1 at both mRNA and protein level.

In prostate cancer, I found that FoxM1 expression correlates tightly with EZH2, the enzymatic component of the PRC2 complex. I also provide evidence that EZH2 expression requires the presence of FoxM1 in prostate cancer cells. The reduction of E-Cadherin expression in FoxM1 over-expressing cells is found to be diminished following EZH2 silencing which suggested the involvement of EZH2 in mediating the E-Cadherin repression promoted by FoxM1. E-Cadherin loss is related to more invasive phenotype of the prostate cancer cells, but whether E-Cadherin is the major effector in this pathway is not clear. Other EZH2 target genes *DAB2IP, ADRB2* have been also associated to promote invasiveness of the cancer cells (112, 132).

The EZH2 silenced cells are arrested at G2-M transition, similar to FoxM1 silenced cells (115). It is unclear what genes are responsible for the G2-M arrest observed in EZH2 ablated cells. In case of FoxM1, aurora kinase B (AurB), polo-like kinase 1 (PLK1), Cyclin B and CENP-F have been proposed as the major target genes that are down-regulated by FoxM1 during G2-M transition. However, the re-expression of these genes individually could only partially rescue the phenotype seen in FoxM1 ablated cells. It is possible that more than one gene are required to execute G2-M transition mediated by FoxM1. Since EZH2 function downstream of FoxM1, it will be interesting to see whether ectopic expression of EZH2 can rescue the G2-M arrest observed in FoxM1 silenced cells. In addition, it will be also interesting to investigate

which aspects of mitotic defects are associated with EZH2 loss of function. As epigenetic silencers, whether PcG proteins can potentially participate in repressing key regulators of cell cycle genes is of great interest. Similar to PLK1, a key cell cycle gene that is important for the mitosis execution, EZH2 is phosphorylated by CDK1 in a cell-cycle dependent manner (133). Though total EZH2 level remains constant throughout the cell cycle, the phosphorylated forms of EZH2 peak at G2/M phase (133), suggesting a potential role of EZH2 phosphorylation in regulating the G2/M transition.

The Polycomb proteins play important roles in maintaining the progenitor cell identity in various organs (106). FoxM1 positively regulates both Bmi1 and EZH2, which indicates an involvement of FoxM1 in regulating the progenitor cells. In neural stem/progenitor cells, the loss of FoxM1 is accompanied by the reduction of both Sox2 and Bmi1. It remains unclear whether ectopic expression of either of the two could rescue the loss of self-renewal in FoxM1 ablated cells.

3. Targeting FoxM1 in tumors harboring *TP53* mutations

My observations that p53-null lymphoma and sarcoma cells depend upon FOXM1 and are highly sensitive to inhibition of FOXM1 suggest that the p53-null tumors are also candidates for therapeutic strategies that target FOXM1. Based on my study, this is at least partially caused by the induction of apoptosis due to the reduction of FoxM1 target genes Survivin and Bmi1 (Fig. 23).

By analyzing publicly available microarray datasets, I found that FoxM1 is up-regulated in tumors harboring p53 mutations compared to tumors with wild type p53.

This observation is consistent with the finding that p53 negatively regulates the expression of FoxM1 (35). In my study, the sensitivity of cells to FoxM1 deletion in p53 null background was investigated. However, the results could be different in the case of p53 mutated background that also includes p53 gain-of-function mutations. In addition, although the p53-null cancer cells are sensitive to FoxM1 depletion, it remains unclear whether p53-null or p53 mutated cells are more sensitive to FoxM1 silencing compared with the wild type counterparts.

Loss-of-function of p53 confers resistance to apoptosis, because p53 stimulates expression of several pro-apoptotic genes, including Puma, Noxa, Bax, Bad, DR4, DR5, Apaf1, Caspase 6 and others(134). P53 also represses expression of anti-apoptotic genes, such as Survivin (135). The pro-apoptotic function of p53 is critical for elimination of cells harboring irreparable levels of DNA damage. It is noteworthy that p53 also stimulates several DNA repair genes (136). In the absence of p53, reduced DNA repair and apoptosis lead to the accumulation of mutant cells, which contribute to tumor development. For example, p53-null mice, used in this study, spontaneously develop lymphomas and sarcomas (91). P53 also stimulates expression of the cell cycle inhibitor p21 (137) and represses FoxM1 (34, 35), contributing to cell cycle arrest following DNA damage. Therefore it is not surprising that p53 mutation also leads to aggressive progression of already developed tumor cells because of increased survival and proliferation. Increased expression of FoxM1 in the p53 mutant tumors is expected to drive aggressive progression because of its role in cell proliferation and inhibition of apoptosis. FoxM1 has been shown to inhibit apoptosis by activating expression of Survivin, which is inhibited by p53.

FoxM1 is an important target for cancer therapy. It is expressed mainly in the proliferating cells and in tumors (4). Based on available evidence, it appears that FoxM1 is dispensable for survival or function of the normal cells in a tissue. For example, deletion of FoxM1 in the adult mouse liver has not visible effect for at least one year (30). But, it blocks development of hepatocellular carcinoma (HCC). Moreover, conditional deletion of FoxM1 after HCC development causes inhibition of tumor progression (51). Moreover, a peptide inhibitor derived from the tumor suppressor ARF, the ARF-peptide used in this study, was shown to inhibit liver tumors, through increased apoptosis, without affecting the neighboring normal cells in the tumor bearing liver (51). Therefore, selective inhibition of FoxM1 would be effective in cancer treatment. Our observations with p53-null lymphoma and sarcoma are significant in that regard because over 50% of tumors harbor p53 mutations.

The observations that p53-null lymphoma and sarcoma cells depend upon FoxM1 and are highly sensitive to inhibition of FoxM1 suggest that the p53-null tumors are also candidates for therapeutic strategies that target FoxM1. Cre-recombinase mediated deletion of FoxM1 inhibited tumor growth at least partly by inducing apoptosis. Deletion of FoxM1 caused a reduction in the expression of Survivin, an anti-apoptotic protein. Moreover, there was a strong reduction of Bmi1, which was shown to support survival of tumor cells (138). It is therefore likely that these FoxM1 target genes are involved in the survival of the p53-null lymphoma and sarcoma. Moreover, a cell-penetrating form of the ARF-peptide, which inhibits FoxM1, also induced apoptosis and inhibited colonization of the p53-null lymphoma and sarcoma cells. The lymphoma cells were more sensitive to the peptide. It is possible that the entry of the peptide is more efficient in the less

adherent lymphoma cells, raising the possibility that the ARF-peptide would be highly effective against the tumor cells in circulation. Consistent with that, there was a drastic inhibition of the lymphoma colonization to the kidney, a major site of colonization for the T-lymphoma cells (104). These observations indicate the possibility of a new application of the ARF-peptide in targeting the tumor cells in the circulation.

Figure 23

A Model summarizing the effect of targeting FoxM1 in p53-null tumors

Figure 23

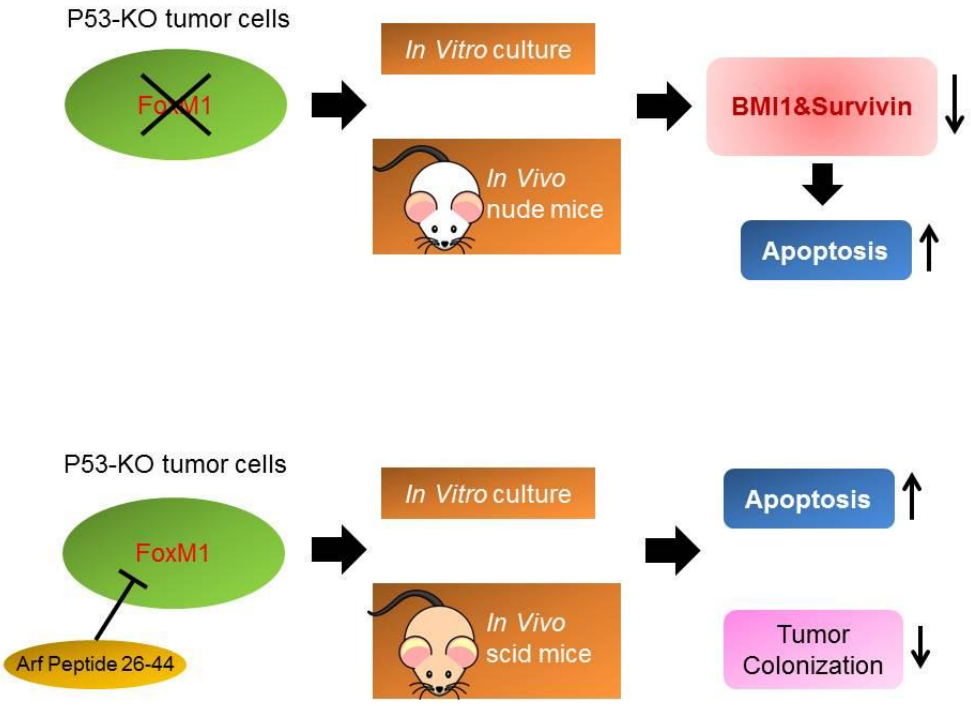
P53-KO tumor cells
FoxM1
In Vitro culture
In Vivo
nude mice
BMI1&Survivin
Apoptosis
P53-KO tumor cells
FoxM1
Arf Peptide 26-44
In Vitro culture
In Vivo
scid mice
Apoptosis
Tumor
Colonization

V. CITED LITERATURE

1. Jackson, B. C., Carpenter, C., Nebert, D. W., and Vasiliou, V. Update of human and mouse forkhead box (FOX) gene families. Hum Genomics, *4:* 345-352.

2. Carlsson, P. and Mahlapuu, M. Forkhead transcription factors: key players in development and metabolism. Dev Biol, *250:* 1-23, 2002.

3. Myatt, S. S. and Lam, E. W. The emerging roles of forkhead box (Fox) proteins in cancer. Nat Rev Cancer, *7:* 847-859, 2007.

4. Korver, W., Roose, J., and Clevers, H. The winged-helix transcription factor Trident is expressed in cycling cells. Nucleic Acids Res, *25:* 1715-1719, 1997.

5. Ye, H., Kelly, T. F., Samadani, U., Lim, L., Rubio, S., Overdier, D. G., Roebuck, K. A., and Costa, R. H. Hepatocyte nuclear factor 3/fork head homolog 11 is expressed in proliferating epithelial and mesenchymal cells of embryonic and adult tissues. Mol Cell Biol, *17:* 1626-1641, 1997.

6. Laoukili, J., Stahl, M., and Medema, R. H. FoxM1: at the crossroads of ageing and cancer. Biochim Biophys Acta, *1775:* 92-102, 2007.

7. Liu, M., Dai, B., Kang, S. H., Ban, K., Huang, F. J., Lang, F. F., Aldape, K. D., Xie, T. X., Pelloski, C. E., Xie, K., Sawaya, R., and Huang, S. FoxM1B is overexpressed in human glioblastomas and critically regulates the tumorigenicity of glioma cells. Cancer Res, *66:* 3593-3602, 2006.

8. Wang, Z., Park, H. J., Carr, J. R., Chen, Y. J., Zheng, Y., Li, J., Tyner, A. L., Costa, R. H., Bagchi, S., and Raychaudhuri, P. FoxM1 in tumorigenicity of the neuroblastoma cells and renewal of the neural progenitors. Cancer Res, *71:* 4292-4302.

9. Yoshida, Y., Wang, I. C., Yoder, H. M., Davidson, N. O., and Costa, R. H. The forkhead box M1 transcription factor contributes to the development and growth of mouse colorectal cancer. Gastroenterology, *132:* 1420-1431, 2007.

10. Kalin, T. V., Wang, I. C., Ackerson, T. J., Major, M. L., Detrisac, C. J., Kalinichenko, V. V., Lyubimov, A., and Costa, R. H. Increased levels of the FoxM1 transcription factor accelerate development and progression of prostate carcinomas in both TRAMP and LADY transgenic mice. Cancer Res, *66:* 1712-1720, 2006.

11. Sun, H., Teng, M., Liu, J., Jin, D., Wu, J., Yan, D., Fan, J., Qin, X., Tang, H., and Peng, Z. FOXM1 expression predicts the prognosis in hepatocellular carcinoma patients after orthotopic liver transplantation combined with the Milan criteria. Cancer Lett, *306:* 214-222.

12. Wang, Z., Banerjee, S., Kong, D., Li, Y., and Sarkar, F. H. Down-regulation of Forkhead Box M1 transcription factor leads to the inhibition of invasion and angiogenesis of pancreatic cancer cells. Cancer Res, *67:* 8293-8300, 2007.

13. Korver, W., Schilham, M. W., Moerer, P., van den Hoff, M. J., Dam, K., Lamers, W. H., Medema, R. H., and Clevers, H. Uncoupling of S phase and mitosis in cardiomyocytes and hepatocytes lacking the winged-helix transcription factor Trident. Curr Biol, *8:* 1327-1330, 1998.

14. Krupczak-Hollis, K., Wang, X., Kalinichenko, V. V., Gusarova, G. A., Wang, I. C., Dennewitz, M. B., Yoder, H. M., Kiyokawa, H., Kaestner, K. H., and Costa, R. H. The mouse Forkhead Box m1 transcription factor is essential for hepatoblast mitosis and development of intrahepatic bile ducts and vessels during liver morphogenesis. Dev Biol, *276:* 74-88, 2004.

15. Ueno, H., Nakajo, N., Watanabe, M., Isoda, M., and Sagata, N. FoxM1-driven cell division is required for neuronal differentiation in early Xenopus embryos. Development, *135:* 2023-2030, 2008.

16. Bolte, C., Zhang, Y., Wang, I. C., Kalin, T. V., Molkentin, J. D., and Kalinichenko, V. V. Expression of Foxm1 transcription factor in cardiomyocytes is required for myocardial development. PLoS One, *6:* e22217.

17. Carr, J. R., Kiefer, M. M., Park, H. J., Li, J., Wang, Z., Fontanarosa, J., DeWaal, D., Kopanja, D., Benevolenskaya, E. V., Guzman, G., and Raychaudhuri, P. FoxM1 regulates mammary luminal cell fate. Cell Rep, *1:* 715-729.

18. Schuller, U., Zhao, Q., Godinho, S. A., Heine, V. M., Medema, R. H., Pellman, D., and Rowitch, D. H. Forkhead transcription factor FoxM1 regulates mitotic entry and prevents spindle defects in cerebellar granule neuron precursors. Mol Cell Biol, *27:* 8259-8270, 2007.

19. Xue, L., Chiang, L., He, B., Zhao, Y. Y., and Winoto, A. FoxM1, a forkhead transcription factor is a master cell cycle regulator for mouse mature T cells but not double positive thymocytes. PLoS One, *5:* e9229.

20. Xia, L., Huang, W., Tian, D., Zhu, H., Zhang, Y., Hu, H., Fan, D., Nie, Y., and Wu, K. Upregulated FoxM1 expression induced by hepatitis B virus X protein promotes tumor metastasis and indicates poor prognosis in hepatitis B virus-related hepatocellular carcinoma. J Hepatol, *57:* 600-612.

21. Major, M. L., Lepe, R., and Costa, R. H. Forkhead box M1B transcriptional activity requires binding of Cdk-cyclin complexes for phosphorylation-dependent recruitment of p300/CBP coactivators. Mol Cell Biol, *24:* 2649-2661, 2004.

22. Chen, Y. J., Dominguez-Brauer, C., Wang, Z., Asara, J. M., Costa, R. H., Tyner, A. L., Lau, L. F., and Raychaudhuri, P. A conserved phosphorylation site within

the forkhead domain of FoxM1B is required for its activation by cyclin-CDK1. J Biol Chem, *284:* 30695-30707, 2009.

23. Park, H. J., Carr, J. R., Wang, Z., Nogueira, V., Hay, N., Tyner, A. L., Lau, L. F., Costa, R. H., and Raychaudhuri, P. FoxM1, a critical regulator of oxidative stress during oncogenesis. Embo J, *28:* 2908-2918, 2009.

24. Yu, J., Deshmukh, H., Payton, J. E., Dunham, C., Scheithauer, B. W., Tihan, T., Prayson, R. A., Guha, A., Bridge, J. A., Ferner, R. E., Lindberg, G. M., Gutmann, R. J., Emnett, R. J., Salavaggione, L., Gutmann, D. H., Nagarajan, R., Watson, M. A., and Perry, A. Array-based comparative genomic hybridization identifies CDK4 and FOXM1 alterations as independent predictors of survival in malignant peripheral nerve sheath tumor. Clin Cancer Res, *17:* 1924-1934.

25. Wang, I. C., Chen, Y. J., Hughes, D., Petrovic, V., Major, M. L., Park, H. J., Tan, Y., Ackerson, T., and Costa, R. H. Forkhead box M1 regulates the transcriptional network of genes essential for mitotic progression and genes encoding the SCF (Skp2-Cks1) ubiquitin ligase. Mol Cell Biol, *25:* 10875-10894, 2005.

26. Laoukili, J., Kooistra, M. R., Bras, A., Kauw, J., Kerkhoven, R. M., Morrison, A., Clevers, H., and Medema, R. H. FoxM1 is required for execution of the mitotic programme and chromosome stability. Nat Cell Biol, *7:* 126-136, 2005.

27. Wonsey, D. R. and Follettie, M. T. Loss of the forkhead transcription factor FoxM1 causes centrosome amplification and mitotic catastrophe. Cancer Res, *65:* 5181-5189, 2005.

28. Wang, I. C., Chen, Y. J., Hughes, D. E., Ackerson, T., Major, M. L., Kalinichenko, V. V., Costa, R. H., Raychaudhuri, P., Tyner, A. L., and Lau, L. F. FoxM1 regulates transcription of JNK1 to promote the G1/S transition and tumor cell invasiveness. J Biol Chem, *283:* 20770-20778, 2008.

29. Petrovic, V., Costa, R. H., Lau, L. F., Raychaudhuri, P., and Tyner, A. L. FoxM1 regulates growth factor-induced expression of kinase-interacting stathmin (KIS) to promote cell cycle progression. J Biol Chem, *283:* 453-460, 2008.

30. Kalinichenko, V. V., Major, M. L., Wang, X., Petrovic, V., Kuechle, J., Yoder, H. M., Dennewitz, M. B., Shin, B., Datta, A., Raychaudhuri, P., and Costa, R. H. Foxm1b transcription factor is essential for development of hepatocellular carcinomas and is negatively regulated by the p19ARF tumor suppressor. Genes Dev, *18:* 830-850, 2004.

31. Wang, I. C., Meliton, L., Ren, X., Zhang, Y., Balli, D., Snyder, J., Whitsett, J. A., Kalinichenko, V. V., and Kalin, T. V. Deletion of Forkhead Box M1 transcription factor from respiratory epithelial cells inhibits pulmonary tumorigenesis. PLoS One, *4:* e6609, 2009.

32. Hanahan, D. and Weinberg, R. A. Hallmarks of cancer: the next generation. Cell, *144:* 646-674.

33. Teh, M. T., Gemenetzidis, E., Chaplin, T., Young, B. D., and Philpott, M. P. Upregulation of FOXM1 induces genomic instability in human epidermal keratinocytes. Mol Cancer, *9:* 45.

34. Barsotti, A. M. and Prives, C. Pro-proliferative FoxM1 is a target of p53-mediated repression. Oncogene, *28:* 4295-4305, 2009.

35. Pandit, B., Halasi, M., and Gartel, A. L. p53 negatively regulates expression of FoxM1. Cell Cycle, *8:* 3425-3427, 2009.

36. Li, S. K., Smith, D. K., Leung, W. Y., Cheung, A. M., Lam, E. W., Dimri, G. P., and Yao, K. M. FoxM1c counteracts oxidative stress-induced senescence and stimulates Bmi-1 expression. J Biol Chem, *283:* 16545-16553, 2008.

37. Halasi, M. and Gartel, A. L. Suppression of FOXM1 sensitizes human cancer cells to cell death induced by DNA-damage. PLoS One, *7:* e31761.

38. Nguyen, D. X., Bos, P. D., and Massague, J. Metastasis: from dissemination to organ-specific colonization. Nat Rev Cancer, *9:* 274-284, 2009.

39. Zhang, Y., Zhang, N., Dai, B., Liu, M., Sawaya, R., Xie, K., and Huang, S. FoxM1B transcriptionally regulates vascular endothelial growth factor expression and promotes the angiogenesis and growth of glioma cells. Cancer Res, *68:* 8733-8742, 2008.

40. Li, Q., Zhang, N., Jia, Z., Le, X., Dai, B., Wei, D., Huang, S., Tan, D., and Xie, K. Critical role and regulation of transcription factor FoxM1 in human gastric cancer angiogenesis and progression. Cancer Res, *69:* 3501-3509, 2009.

41. Ahmad, A., Wang, Z., Kong, D., Ali, S., Li, Y., Banerjee, S., Ali, R., and Sarkar, F. H. FoxM1 down-regulation leads to inhibition of proliferation, migration and invasion of breast cancer cells through the modulation of extra-cellular matrix degrading factors. Breast Cancer Res Treat, *122:* 337-346.

42. Park, H. J., Gusarova, G., Wang, Z., Carr, J. R., Li, J., Kim, K. H., Qiu, J., Park, Y. D., Williamson, P. R., Hay, N., Tyner, A. L., Lau, L. F., Costa, R. H., and Raychaudhuri, P. Deregulation of FoxM1b leads to tumour metastasis. EMBO Mol Med, *3:* 21-34.

43. Carr, J. R., Park, H. J., Wang, Z., Kiefer, M. M., and Raychaudhuri, P. FoxM1 mediates resistance to herceptin and paclitaxel. Cancer Res, *70:* 5054-5063.

44. Bao, B., Wang, Z., Ali, S., Kong, D., Banerjee, S., Ahmad, A., Li, Y., Azmi, A. S., Miele, L., and Sarkar, F. H. Over-expression of FoxM1 leads to epithelial-

mesenchymal transition and cancer stem cell phenotype in pancreatic cancer cells. J Cell Biochem, *112:* 2296-2306.

45. Huang, C., Qiu, Z., Wang, L., Peng, Z., Jia, Z., Logsdon, C. D., Le, X., Wei, D., Huang, S., and Xie, K. A novel FoxM1-caveolin signaling pathway promotes pancreatic cancer invasion and metastasis. Cancer Res, *72:* 655-665.

46. Bektas, N., Haaf, A., Veeck, J., Wild, P. J., Luscher-Firzlaff, J., Hartmann, A., Knuchel, R., and Dahl, E. Tight correlation between expression of the Forkhead transcription factor FOXM1 and HER2 in human breast cancer. BMC Cancer, *8:* 42, 2008.

47. Kwok, J. M., Peck, B., Monteiro, L. J., Schwenen, H. D., Millour, J., Coombes, R. C., Myatt, S. S., and Lam, E. W. FOXM1 confers acquired cisplatin resistance in breast cancer cells. Mol Cancer Res, *8:* 24-34.

48. Millour, J., Constantinidou, D., Stavropoulou, A. V., Wilson, M. S., Myatt, S. S., Kwok, J. M., Sivanandan, K., Coombes, R. C., Medema, R. H., Hartman, J., Lykkesfeldt, A. E., and Lam, E. W. FOXM1 is a transcriptional target of ERalpha and has a critical role in breast cancer endocrine sensitivity and resistance. Oncogene, *29:* 2983-2995.

49. Xu, N., Zhang, X., Wang, X., Ge, H. Y., Wang, X. Y., Garfield, D., Yang, P., Song, Y. L., and Bai, C. X. FoxM1 mediated resistance to gefitinib in non-small-cell lung cancer cells. Acta Pharmacol Sin, *33:* 675-681.

50. Okada, K., Fujiwara, Y., Takahashi, T., Nakamura, Y., Takiguchi, S., Nakajima, K., Miyata, H., Yamasaki, M., Kurokawa, Y., Mori, M., and Doki, Y. Overexpression of Forkhead Box M1 Transcription Factor (FOXM1) is a Potential Prognostic Marker and Enhances Chemoresistance for Docetaxel in Gastric Cancer. Ann Surg Oncol.

51. Gusarova, G. A., Wang, I. C., Major, M. L., Kalinichenko, V. V., Ackerson, T., Petrovic, V., and Costa, R. H. A cell-penetrating ARF peptide inhibitor of FoxM1 in mouse hepatocellular carcinoma treatment. J Clin Invest, *117:* 99-111, 2007.

52. Radhakrishnan, S. K., Bhat, U. G., Hughes, D. E., Wang, I. C., Costa, R. H., and Gartel, A. L. Identification of a chemical inhibitor of the oncogenic transcription factor forkhead box M1. Cancer Res, *66:* 9731-9735, 2006.

53. Bhat, U. G., Halasi, M., and Gartel, A. L. Thiazole antibiotics target FoxM1 and induce apoptosis in human cancer cells. PLoS One, *4:* e5592, 2009.

54. Bhat, U. G., Halasi, M., and Gartel, A. L. FoxM1 is a general target for proteasome inhibitors. PLoS One, *4:* e6593, 2009.

55. Aasen, T., Raya, A., Barrero, M. J., Garreta, E., Consiglio, A., Gonzalez, F., Vassena, R., Bilic, J., Pekarik, V., Tiscornia, G., Edel, M., Boue, S., and Izpisua

Belmonte, J. C. Efficient and rapid generation of induced pluripotent stem cells from human keratinocytes. Nat Biotechnol, *26:* 1276-1284, 2008.

56. Brodeur, G. M. Neuroblastoma: biological insights into a clinical enigma. Nat Rev Cancer, *3:* 203-216, 2003.

57. Maris, J. M., Hogarty, M. D., Bagatell, R., and Cohn, S. L. Neuroblastoma. Lancet, *369:* 2106-2120, 2007.

58. Maris, J. M. Recent advances in neuroblastoma. N Engl J Med, *362:* 2202-2211.

59. Attiyeh, E. F., London, W. B., Mosse, Y. P., Wang, Q., Winter, C., Khazi, D., McGrady, P. W., Seeger, R. C., Look, A. T., Shimada, H., Brodeur, G. M., Cohn, S. L., Matthay, K. K., and Maris, J. M. Chromosome 1p and 11q deletions and outcome in neuroblastoma. N Engl J Med, *353:* 2243-2253, 2005.

60. Brodeur, G. M., Seeger, R. C., Schwab, M., Varmus, H. E., and Bishop, J. M. Amplification of N-myc in untreated human neuroblastomas correlates with advanced disease stage. Science, *224:* 1121-1124, 1984.

61. Jaboin, J., Kim, C. J., Kaplan, D. R., and Thiele, C. J. Brain-derived neurotrophic factor activation of TrkB protects neuroblastoma cells from chemotherapy-induced apoptosis via phosphatidylinositol 3'-kinase pathway. Cancer Res, *62:* 6756-6763, 2002.

62. Ross, R. A., Biedler, J. L., and Spengler, B. A. A role for distinct cell types in determining malignancy in human neuroblastoma cell lines and tumors. Cancer Lett, *197:* 35-39, 2003.

63. Ciccarone, V., Spengler, B. A., Meyers, M. B., Biedler, J. L., and Ross, R. A. Phenotypic diversification in human neuroblastoma cells: expression of distinct neural crest lineages. Cancer Res, *49:* 219-225, 1989.

64. Walton, J. D., Kattan, D. R., Thomas, S. K., Spengler, B. A., Guo, H. F., Biedler, J. L., Cheung, N. K., and Ross, R. A. Characteristics of stem cells from human neuroblastoma cell lines and in tumors. Neoplasia, *6:* 838-845, 2004.

65. Ross, R. A., Spengler, B. A., Domenech, C., Porubcin, M., Rettig, W. J., and Biedler, J. L. Human neuroblastoma I-type cells are malignant neural crest stem cells. Cell Growth Differ, *6:* 449-456, 1995.

66. Hansford, L. M., McKee, A. E., Zhang, L., George, R. E., Gerstle, J. T., Thorner, P. S., Smith, K. M., Look, A. T., Yeger, H., Miller, F. D., Irwin, M. S., Thiele, C. J., and Kaplan, D. R. Neuroblastoma cells isolated from bone marrow metastases contain a naturally enriched tumor-initiating cell. Cancer Res, *67:* 11234-11243, 2007.

67. Mahller, Y. Y., Williams, J. P., Baird, W. H., Mitton, B., Grossheim, J., Saeki, Y., Cancelas, J. A., Ratner, N., and Cripe, T. P. Neuroblastoma cell lines contain pluripotent tumor initiating cells that are susceptible to a targeted oncolytic virus. PLoS One, *4:* e4235, 2009.

68. Hirschmann-Jax, C., Foster, A. E., Wulf, G. G., Nuchtern, J. G., Jax, T. W., Gobel, U., Goodell, M. A., and Brenner, M. K. A distinct "side population" of cells with high drug efflux capacity in human tumor cells. Proc Natl Acad Sci U S A, *101:* 14228-14233, 2004.

69. Smith, K. M., Datti, A., Fujitani, M., Grinshtein, N., Zhang, L., Morozova, O., Blakely, K. M., Rotenberg, S. A., Hansford, L. M., Miller, F. D., Yeger, H., Irwin, M. S., Moffat, J., Marra, M. A., Baruchel, S., Wrana, J. L., and Kaplan, D. R. Selective targeting of neuroblastoma tumour-initiating cells by compounds identified in stem cell-based small molecule screens. EMBO Mol Med.

70. Graham, V., Khudyakov, J., Ellis, P., and Pevny, L. SOX2 functions to maintain neural progenitor identity. Neuron, *39:* 749-765, 2003.

71. Bass, A. J., Watanabe, H., Mermel, C. H., Yu, S., Perner, S., Verhaak, R. G., Kim, S. Y., Wardwell, L., Tamayo, P., Gat-Viks, I., Ramos, A. H., Woo, M. S., Weir, B. A., Getz, G., Beroukhim, R., O'Kelly, M., Dutt, A., Rozenblatt-Rosen, O., Dziunycz, P., Komisarof, J., Chirieac, L. R., Lafargue, C. J., Scheble, V., Wilbertz, T., Ma, C., Rao, S., Nakagawa, H., Stairs, D. B., Lin, L., Giordano, T. J., Wagner, P., Minna, J. D., Gazdar, A. F., Zhu, C. Q., Brose, M. S., Cecconello, I., Jr, U. R., Marie, S. K., Dahl, O., Shivdasani, R. A., Tsao, M. S., Rubin, M. A., Wong, K. K., Regev, A., Hahn, W. C., Beer, D. G., Rustgi, A. K., and Meyerson, M. SOX2 is an amplified lineage-survival oncogene in lung and esophageal squamous cell carcinomas. Nat Genet, *41:* 1238-1242, 2009.

72. Gangemi, R. M., Griffero, F., Marubbi, D., Perera, M., Capra, M. C., Malatesta, P., Ravetti, G. L., Zona, G. L., Daga, A., and Corte, G. SOX2 silencing in glioblastoma tumor-initiating cells causes stop of proliferation and loss of tumorigenicity. Stem Cells, *27:* 40-48, 2009.

73. Rodriguez-Pinilla, S. M., Sarrio, D., Moreno-Bueno, G., Rodriguez-Gil, Y., Martinez, M. A., Hernandez, L., Hardisson, D., Reis-Filho, J. S., and Palacios, J. Sox2: a possible driver of the basal-like phenotype in sporadic breast cancer. Mod Pathol, *20:* 474-481, 2007.

74. Phi, J. H., Park, S. H., Kim, S. K., Paek, S. H., Kim, J. H., Lee, Y. J., Cho, B. K., Park, C. K., Lee, D. H., and Wang, K. C. Sox2 expression in brain tumors: a reflection of the neuroglial differentiation pathway. Am J Surg Pathol, *32:* 103-112, 2008.

75. Riggi, N., Suva, M. L., De Vito, C., Provero, P., Stehle, J. C., Baumer, K., Cironi, L., Janiszewska, M., Petricevic, T., Suva, D., Tercier, S., Joseph, J. M., Guillou,

L., and Stamenkovic, I. EWS-FLI-1 modulates miRNA145 and SOX2 expression to initiate mesenchymal stem cell reprogramming toward Ewing sarcoma cancer stem cells. Genes Dev, *24:* 916-932.

76. Kim, Y., Lin, Q., Zelterman, D., and Yun, Z. Hypoxia-regulated delta-like 1 homologue enhances cancer cell stemness and tumorigenicity. Cancer Res, *69:* 9271-9280, 2009.

77. Melone, M. A., Giuliano, M., Squillaro, T., Alessio, N., Casale, F., Mattioli, E., Cipollaro, M., Giordano, A., and Galderisi, U. Genes involved in regulation of stem cell properties: studies on their expression in a small cohort of neuroblastoma patients. Cancer Biol Ther, *8:* 1300-1306, 2009.

78. Albino, D., Scaruffi, P., Moretti, S., Coco, S., Truini, M., Di Cristofano, C., Cavazzana, A., Stigliani, S., Bonassi, S., and Tonini, G. P. Identification of low intratumoral gene expression heterogeneity in neuroblastic tumors by genome-wide expression analysis and game theory. Cancer, *113:* 1412-1422, 2008.

79. Janoueix-Lerosey, I., Lequin, D., Brugieres, L., Ribeiro, A., de Pontual, L., Combaret, V., Raynal, V., Puisieux, A., Schleiermacher, G., Pierron, G., Valteau-Couanet, D., Frebourg, T., Michon, J., Lyonnet, S., Amiel, J., and Delattre, O. Somatic and germline activating mutations of the ALK kinase receptor in neuroblastoma. Nature, *455:* 967-970, 2008.

80. Wang, Q., Diskin, S., Rappaport, E., Attiyeh, E., Mosse, Y., Shue, D., Seiser, E., Jagannathan, J., Shusterman, S., Bansal, M., Khazi, D., Winter, C., Okawa, E., Grant, G., Cnaan, A., Zhao, H., Cheung, N. K., Gerald, W., London, W., Matthay, K. K., Brodeur, G. M., and Maris, J. M. Integrative genomics identifies distinct molecular classes of neuroblastoma and shows that multiple genes are targeted by regional alterations in DNA copy number. Cancer Res, *66:* 6050-6062, 2006.

81. Yang, Z. F., Ho, D. W., Ng, M. N., Lau, C. K., Yu, W. C., Ngai, P., Chu, P. W., Lam, C. T., Poon, R. T., and Fan, S. T. Significance of CD90+ cancer stem cells in human liver cancer. Cancer Cell, *13:* 153-166, 2008.

82. Ben-Porath, I., Thomson, M. W., Carey, V. J., Ge, R., Bell, G. W., Regev, A., and Weinberg, R. A. An embryonic stem cell-like gene expression signature in poorly differentiated aggressive human tumors. Nat Genet, *40:* 499-507, 2008.

83. Xie, Z., Tan, G., Ding, M., Dong, D., Chen, T., Meng, X., Huang, X., and Tan, Y. Foxm1 transcription factor is required for maintenance of pluripotency of P19 embryonal carcinoma cells. Nucleic Acids Res, *38:* 8027-8038.

84. Cui, H., Hu, B., Li, T., Ma, J., Alam, G., Gunning, W. T., and Ding, H. F. Bmi-1 is essential for the tumorigenicity of neuroblastoma cells. Am J Pathol, *170:* 1370-1378, 2007.

85. Cui, H., Ma, J., Ding, J., Li, T., Alam, G., and Ding, H. F. Bmi-1 regulates the differentiation and clonogenic self-renewal of I-type neuroblastoma cells in a concentration-dependent manner. J Biol Chem, *281:* 34696-34704, 2006.

86. Molofsky, A. V., Pardal, R., Iwashita, T., Park, I. K., Clarke, M. F., and Morrison, S. J. Bmi-1 dependence distinguishes neural stem cell self-renewal from progenitor proliferation. Nature, *425:* 962-967, 2003.

87. Reynolds, B. A., Tetzlaff, W., and Weiss, S. A multipotent EGF-responsive striatal embryonic progenitor cell produces neurons and astrocytes. J Neurosci, *12:* 4565-4574, 1992.

88. Vogelstein, B., Lane, D., and Levine, A. J. Surfing the p53 network. Nature, *408:* 307-310, 2000.

89. Vousden, K. H. and Lane, D. P. p53 in health and disease. Nat Rev Mol Cell Biol, *8:* 275-283, 2007.

90. Meek, D. W. Tumour suppression by p53: a role for the DNA damage response? Nat Rev Cancer, *9:* 714-723, 2009.

91. Donehower, L. A., Harvey, M., Slagle, B. L., McArthur, M. J., Montgomery, C. A., Jr., Butel, J. S., and Bradley, A. Mice deficient for p53 are developmentally normal but susceptible to spontaneous tumours. Nature, *356:* 215-221, 1992.

92. Ye, H., Holterman, A. X., Yoo, K. W., Franks, R. R., and Costa, R. H. Premature expression of the winged helix transcription factor HFH-11B in regenerating mouse liver accelerates hepatocyte entry into S phase. Mol Cell Biol, *19:* 8570-8580, 1999.

93. Curtis, C., Shah, S. P., Chin, S. F., Turashvili, G., Rueda, O. M., Dunning, M. J., Speed, D., Lynch, A. G., Samarajiwa, S., Yuan, Y., Graf, S., Ha, G., Haffari, G., Bashashati, A., Russell, R., McKinney, S., Langerod, A., Green, A., Provenzano, E., Wishart, G., Pinder, S., Watson, P., Markowetz, F., Murphy, L., Ellis, I., Purushotham, A., Borresen-Dale, A. L., Brenton, J. D., Tavare, S., Caldas, C., and Aparicio, S. The genomic and transcriptomic architecture of 2,000 breast tumours reveals novel subgroups. Nature, *486:* 346-352.

94. Hendrix, N. D., Wu, R., Kuick, R., Schwartz, D. R., Fearon, E. R., and Cho, K. R. Fibroblast growth factor 9 has oncogenic activity and is a downstream target of Wnt signaling in ovarian endometrioid adenocarcinomas. Cancer Res, *66:* 1354-1362, 2006.

95. Grasso, C. S., Wu, Y. M., Robinson, D. R., Cao, X., Dhanasekaran, S. M., Khan, A. P., Quist, M. J., Jing, X., Lonigro, R. J., Brenner, J. C., Asangani, I. A., Ateeq, B., Chun, S. Y., Siddiqui, J., Sam, L., Anstett, M., Mehra, R., Prensner, J. R., Palanisamy, N., Ryslik, G. A., Vandin, F., Raphael, B. J., Kunju, L. P., Rhodes, D.

R., Pienta, K. J., Chinnaiyan, A. M., and Tomlins, S. A. The mutational landscape of lethal castration-resistant prostate cancer. Nature, *487:* 239-243.

96. Sorlie, T., Perou, C. M., Tibshirani, R., Aas, T., Geisler, S., Johnsen, H., Hastie, T., Eisen, M. B., van de Rijn, M., Jeffrey, S. S., Thorsen, T., Quist, H., Matese, J. C., Brown, P. O., Botstein, D., Lonning, P. E., and Borresen-Dale, A. L. Gene expression patterns of breast carcinomas distinguish tumor subclasses with clinical implications. Proc Natl Acad Sci U S A, *98:* 10869-10874, 2001.

97. Gartel, A. L. FoxM1 inhibitors as potential anticancer drugs. Expert Opin Ther Targets, *12:* 663-665, 2008.

98. Lopes, U. G., Erhardt, P., Yao, R., and Cooper, G. M. p53-dependent induction of apoptosis by proteasome inhibitors. J Biol Chem, *272:* 12893-12896, 1997.

99. Altieri, D. C. Survivin, versatile modulation of cell division and apoptosis in cancer. Oncogene, *22:* 8581-8589, 2003.

100. Jacobs, J. J., Scheijen, B., Voncken, J. W., Kieboom, K., Berns, A., and van Lohuizen, M. Bmi-1 collaborates with c-Myc in tumorigenesis by inhibiting c-Myc-induced apoptosis via INK4a/ARF. Genes Dev, *13:* 2678-2690, 1999.

101. Tracey, L., Perez-Rosado, A., Artiga, M. J., Camacho, F. I., Rodriguez, A., Martinez, N., Ruiz-Ballesteros, E., Mollejo, M., Martinez, B., Cuadros, M., Garcia, J. F., Lawler, M., and Piris, M. A. Expression of the NF-kappaB targets BCL2 and BIRC5/Survivin characterizes small B-cell and aggressive B-cell lymphomas, respectively. J Pathol, *206:* 123-134, 2005.

102. Gritsko, T., Williams, A., Turkson, J., Kaneko, S., Bowman, T., Huang, M., Nam, S., Eweis, I., Diaz, N., Sullivan, D., Yoder, S., Enkemann, S., Eschrich, S., Lee, J. H., Beam, C. A., Cheng, J., Minton, S., Muro-Cacho, C. A., and Jove, R. Persistent activation of stat3 signaling induces survivin gene expression and confers resistance to apoptosis in human breast cancer cells. Clin Cancer Res, *12:* 11-19, 2006.

103. Bhattacharya, R., Nicoloso, M., Arvizo, R., Wang, E., Cortez, A., Rossi, S., Calin, G. A., and Mukherjee, P. MiR-15a and MiR-16 control Bmi-1 expression in ovarian cancer. Cancer Res, *69:* 9090-9095, 2009.

104. Aoudjit, F., Potworowski, E. F., and St-Pierre, Y. The metastatic characteristics of murine lymphoma cell lines in vivo are manifested after target organ invasion. Blood, *91:* 623-629, 1998.

105. Valk-Lingbeek, M. E., Bruggeman, S. W., and van Lohuizen, M. Stem cells and cancer; the polycomb connection. Cell, *118:* 409-418, 2004.

106. Sparmann, A. and van Lohuizen, M. Polycomb silencers control cell fate, development and cancer. Nat Rev Cancer, *6:* 846-856, 2006.

107. Varambally, S., Dhanasekaran, S. M., Zhou, M., Barrette, T. R., Kumar-Sinha, C., Sanda, M. G., Ghosh, D., Pienta, K. J., Sewalt, R. G., Otte, A. P., Rubin, M. A., and Chinnaiyan, A. M. The polycomb group protein EZH2 is involved in progression of prostate cancer. Nature, *419:* 624-629, 2002.

108. Cao, Q., Yu, J., Dhanasekaran, S. M., Kim, J. H., Mani, R. S., Tomlins, S. A., Mehra, R., Laxman, B., Cao, X., Yu, J., Kleer, C. G., Varambally, S., and Chinnaiyan, A. M. Repression of E-cadherin by the polycomb group protein EZH2 in cancer. Oncogene, *27:* 7274-7284, 2008.

109. Chen, H., Tu, S. W., and Hsieh, J. T. Down-regulation of human DAB2IP gene expression mediated by polycomb Ezh2 complex and histone deacetylase in prostate cancer. J Biol Chem, *280:* 22437-22444, 2005.

110. Bryant, R. J., Cross, N. A., Eaton, C. L., Hamdy, F. C., and Cunliffe, V. T. EZH2 promotes proliferation and invasiveness of prostate cancer cells. Prostate, *67:* 547-556, 2007.

111. Fujii, S., Ito, K., Ito, Y., and Ochiai, A. Enhancer of zeste homologue 2 (EZH2) down-regulates RUNX3 by increasing histone H3 methylation. J Biol Chem, *283:* 17324-17332, 2008.

112. Yu, J., Cao, Q., Mehra, R., Laxman, B., Yu, J., Tomlins, S. A., Creighton, C. J., Dhanasekaran, S. M., Shen, R., Chen, G., Morris, D. S., Marquez, V. E., Shah, R. B., Ghosh, D., Varambally, S., and Chinnaiyan, A. M. Integrative genomics analysis reveals silencing of beta-adrenergic signaling by polycomb in prostate cancer. Cancer Cell, *12:* 419-431, 2007.

113. Ren, G., Baritaki, S., Marathe, H., Feng, J., Park, S., Beach, S., Bazeley, P. S., Beshir, A. B., Fenteany, G., Mehra, R., Daignault, S., Al-Mulla, F., Keller, E., Bonavida, B., de la Serna, I., and Yeung, K. C. Polycomb protein EZH2 regulates tumor invasion via the transcriptional repression of the metastasis suppressor RKIP in breast and prostate cancer. Cancer Res, *72:* 3091-3104.

114. Saramaki, O. R., Tammela, T. L., Martikainen, P. M., Vessella, R. L., and Visakorpi, T. The gene for polycomb group protein enhancer of zeste homolog 2 (EZH2) is amplified in late-stage prostate cancer. Genes Chromosomes Cancer, *45:* 639-645, 2006.

115. Varambally, S., Cao, Q., Mani, R. S., Shankar, S., Wang, X., Ateeq, B., Laxman, B., Cao, X., Jing, X., Ramnarayanan, K., Brenner, J. C., Yu, J., Kim, J. H., Han, B., Tan, P., Kumar-Sinha, C., Lonigro, R. J., Palanisamy, N., Maher, C. A., and Chinnaiyan, A. M. Genomic loss of microRNA-101 leads to overexpression of histone methyltransferase EZH2 in cancer. Science, *322:* 1695-1699, 2008.

116. Holland, D., Hoppe-Seyler, K., Schuller, B., Lohrey, C., Maroldt, J., Durst, M., and Hoppe-Seyler, F. Activation of the enhancer of zeste homologue 2 gene by the human papillomavirus E7 oncoprotein. Cancer Res, *68:* 9964-9972, 2008.

117. Bracken, A. P., Pasini, D., Capra, M., Prosperini, E., Colli, E., and Helin, K. EZH2 is downstream of the pRB-E2F pathway, essential for proliferation and amplified in cancer. Embo J, *22:* 5323-5335, 2003.

118. Bachmann, I. M., Halvorsen, O. J., Collett, K., Stefansson, I. M., Straume, O., Haukaas, S. A., Salvesen, H. B., Otte, A. P., and Akslen, L. A. EZH2 expression is associated with high proliferation rate and aggressive tumor subgroups in cutaneous melanoma and cancers of the endometrium, prostate, and breast. J Clin Oncol, *24:* 268-273, 2006.

119. Kleer, C. G., Cao, Q., Varambally, S., Shen, R., Ota, I., Tomlins, S. A., Ghosh, D., Sewalt, R. G., Otte, A. P., Hayes, D. F., Sabel, M. S., Livant, D., Weiss, S. J., Rubin, M. A., and Chinnaiyan, A. M. EZH2 is a marker of aggressive breast cancer and promotes neoplastic transformation of breast epithelial cells. Proc Natl Acad Sci U S A, *100:* 11606-11611, 2003.

120. Arredouani, M. S., Lu, B., Bhasin, M., Eljanne, M., Yue, W., Mosquera, J. M., Bubley, G. J., Li, V., Rubin, M. A., Libermann, T. A., and Sanda, M. G. Identification of the transcription factor single-minded homologue 2 as a potential biomarker and immunotherapy target in prostate cancer. Clin Cancer Res, *15:* 5794-5802, 2009.

121. Taylor, B. S., Schultz, N., Hieronymus, H., Gopalan, A., Xiao, Y., Carver, B. S., Arora, V. K., Kaushik, P., Cerami, E., Reva, B., Antipin, Y., Mitsiades, N., Landers, T., Dolgalev, I., Major, J. E., Wilson, M., Socci, N. D., Lash, A. E., Heguy, A., Eastham, J. A., Scher, H. I., Reuter, V. E., Scardino, P. T., Sander, C., Sawyers, C. L., and Gerald, W. L. Integrative genomic profiling of human prostate cancer. Cancer Cell, *18:* 11-22.

122. Varambally, S., Yu, J., Laxman, B., Rhodes, D. R., Mehra, R., Tomlins, S. A., Shah, R. B., Chandran, U., Monzon, F. A., Becich, M. J., Wei, J. T., Pienta, K. J., Ghosh, D., Rubin, M. A., and Chinnaiyan, A. M. Integrative genomic and proteomic analysis of prostate cancer reveals signatures of metastatic progression. Cancer Cell, *8:* 393-406, 2005.

123. Yu, Y. P., Landsittel, D., Jing, L., Nelson, J., Ren, B., Liu, L., McDonald, C., Thomas, R., Dhir, R., Finkelstein, S., Michalopoulos, G., Becich, M., and Luo, J. H. Gene expression alterations in prostate cancer predicting tumor aggression and preceding development of malignancy. J Clin Oncol, *22:* 2790-2799, 2004.

124. Setlur, S. R., Mertz, K. D., Hoshida, Y., Demichelis, F., Lupien, M., Perner, S., Sboner, A., Pawitan, Y., Andren, O., Johnson, L. A., Tang, J., Adami, H. O., Calza, S., Chinnaiyan, A. M., Rhodes, D., Tomlins, S., Fall, K., Mucci, L. A.,

Kantoff, P. W., Stampfer, M. J., Andersson, S. O., Varenhorst, E., Johansson, J. E., Brown, M., Golub, T. R., and Rubin, M. A. Estrogen-dependent signaling in a molecularly distinct subclass of aggressive prostate cancer. J Natl Cancer Inst, *100:* 815-825, 2008.

125. Raychaudhuri, P. and Park, H. J. FoxM1: a master regulator of tumor metastasis. Cancer Res, *71:* 4329-4333.

126. Umbas, R., Schalken, J. A., Aalders, T. W., Carter, B. S., Karthaus, H. F., Schaafsma, H. E., Debruyne, F. M., and Isaacs, W. B. Expression of the cellular adhesion molecule E-cadherin is reduced or absent in high-grade prostate cancer. Cancer Res, *52:* 5104-5109, 1992.

127. Herranz, N., Pasini, D., Diaz, V. M., Franci, C., Gutierrez, A., Dave, N., Escriva, M., Hernandez-Munoz, I., Di Croce, L., Helin, K., Garcia de Herreros, A., and Peiro, S. Polycomb complex 2 is required for E-cadherin repression by the Snail1 transcription factor. Mol Cell Biol, *28:* 4772-4781, 2008.

128. Chen, Y., Shi, L., Zhang, L., Li, R., Liang, J., Yu, W., Sun, L., Yang, X., Wang, Y., Zhang, Y., and Shang, Y. The molecular mechanism governing the oncogenic potential of SOX2 in breast cancer. J Biol Chem, *283:* 17969-17978, 2008.

129. Richly, H., Aloia, L., and Di Croce, L. Roles of the Polycomb group proteins in stem cells and cancer. Cell Death Dis, *2:* e204.

130. Jacobs, J. J., Kieboom, K., Marino, S., DePinho, R. A., and van Lohuizen, M. The oncogene and Polycomb-group gene bmi-1 regulates cell proliferation and senescence through the ink4a locus. Nature, *397:* 164-168, 1999.

131. Guo, B. H., Feng, Y., Zhang, R., Xu, L. H., Li, M. Z., Kung, H. F., Song, L. B., and Zeng, M. S. Bmi-1 promotes invasion and metastasis, and its elevated expression is correlated with an advanced stage of breast cancer. Mol Cancer, *10:* 10.

132. Xie, D., Gore, C., Liu, J., Pong, R. C., Mason, R., Hao, G., Long, M., Kabbani, W., Yu, L., Zhang, H., Chen, H., Sun, X., Boothman, D. A., Min, W., and Hsieh, J. T. Role of DAB2IP in modulating epithelial-to-mesenchymal transition and prostate cancer metastasis. Proc Natl Acad Sci U S A, *107:* 2485-2490.

133. Kaneko, S., Li, G., Son, J., Xu, C. F., Margueron, R., Neubert, T. A., and Reinberg, D. Phosphorylation of the PRC2 component Ezh2 is cell cycle-regulated and up-regulates its binding to ncRNA. Genes Dev, *24:* 2615-2620.

134. Kuribayashi, K., Finnberg, N., Jeffers, J. R., Zambetti, G. P., and El-Deiry, W. S. The relative contribution of pro-apoptotic p53-target genes in the triggering of apoptosis following DNA damage in vitro and in vivo. Cell Cycle, *10:* 2380-2389.

135. Mirza, A., McGuirk, M., Hockenberry, T. N., Wu, Q., Ashar, H., Black, S., Wen, S. F., Wang, L., Kirschmeier, P., Bishop, W. R., Nielsen, L. L., Pickett, C. B., and Liu, S. Human survivin is negatively regulated by wild-type p53 and participates in p53-dependent apoptotic pathway. Oncogene, *21:* 2613-2622, 2002.

136. Sengupta, S. and Harris, C. C. p53: traffic cop at the crossroads of DNA repair and recombination. Nat Rev Mol Cell Biol, *6:* 44-55, 2005.

137. Agarwal, M. L., Agarwal, A., Taylor, W. R., and Stark, G. R. p53 controls both the G2/M and the G1 cell cycle checkpoints and mediates reversible growth arrest in human fibroblasts. Proc Natl Acad Sci U S A, *92:* 8493-8497, 1995.

138. Liu, L., Andrews, L. G., and Tollefsbol, T. O. Loss of the human polycomb group protein BMI1 promotes cancer-specific cell death. Oncogene, *25:* 4370-4375, 2006.

VI. VITA

NAME: Zebin Wang

EDUCATION: Bachelor of Science in Biological Sciences
Fudan University, Shanghai, China, 2005

PUBLICATIONS: Wang Z, Zheng Y, Park HJ, Li J, Carr JR, Chen YJ, Kiefer MM, Kopanja D, Srilata Bagchi S, Tyner AL, Raychaudhuri P. Targeting FoxM1 effectively retards p53-null lymphoma and sarcoma. 2012 (Under Revision)

Wang Z, Park HJ, Carr JR, Chen YJ, Zheng Y, Li J, Tyner AL, Costa RH, Bagchi S, Raychaudhuri P. FoxM1 in Tumorigenicity of the Neuroblastoma Cells and Renewal of the Neural Progenitors. Cancer Res. 2011 Jun 15;71(12):4292-302.

Zheng Y,Gierut JJ, Wang Z, and Tyner AL. 2012. Protein tyrosine kinase 6 protects cell from anoikis by phosphorylating and activation focal adhesion kinase. Oncogene. 2012 Oct 1.

Carr JR, Kiefer MM, Park HJ, Li J, Wang Z, Fontanarosa J, DeWaal D, Kopanja D, Benevolenskaya VE, Guzman G, Raychaudhuri. P. 2012. FoxM1 Regulates Mammary Luminal Cell Fate. Cell Reports. 2012 Jun ;1(6): 715-729

Park HJ, Gusarova G, Wang Z, Carr JR, Li J, Kim KH, Qiu J, Park YD, Williamson PR, Hay N, Tyner AL, Lau LF, Costa RH, Raychaudhuri P.Deregulation of FoxM1b leads to tumour metastasis. EMBO Mol Med. 2011 Jan;3(1):21-34.

Zheng Y, Peng M, Wang Z, Asara JM, Tyner AL. Protein tyrosine kinase 6 directly phosphorylates AKT and promotes AKT activation in response to epidermal growth factor. Mol Cell Biol. 2010 Sep;30(17):4280-92.

Carr JR, Park HJ, Wang Z, Kiefer MM, Raychaudhuri P. FoxM1 mediates resistance to herceptin and paclitaxel. Cancer Res. 2010 Jun 15;70(12):5054-63.

Chen YJ, Dominguez-Brauer C, Wang Z, Asara JM, Costa RH, Tyner AL, Lau LF, Raychaudhuri P. A conserved phosphorylation site within the forkhead domain of FoxM1B is required for its

activation by cyclin-CDK1. J Biol Chem. 2009 Oct 30;284(44):30695-707.

Park HJ, Carr JR, Wang Z, Nogueira V, Hay N, Tyner AL, Lau LF, Costa RH, Raychaudhuri P. FoxM1, a critical regulator of oxidative stress during oncogenesis. EMBO J. 2009 Oct 7;28(19):2908-18.

Park HJ, Wang Z, Costa RH, Tyner A, Lau LF, Raychaudhuri P. An N-terminal inhibitory domain modulates activity of FoxM1 during cell cycle. Oncogene. 2008 Mar 13;27(12):1696-704.

Yin G, Ji C, Zeng L, Wang Z, Wang J, Shen Z, Wu T, Gu S, Xie Y, Mao Y.Cloning and characterization of a novel KRAB-domain-containing zinc finger gene (ZNF284L). Mol Biol Rep. 2006 Jun;33(2):137-44.

ABSTRACTS:

Wang Z and Raychaudhuri P. FoxM1 in Tumorigenicity of the Neuroblastoma Cells and Renewal of the Neural Progenitors. Stem cells, Cancer and Metastasis, Keystone Symposia, Keystone, Colorado, March, 2011

Wang Z and Raychaudhuri P. Targeting FoxM1 in p53 null cancers. American Association of Cancer Research, Chicago, Illinois, April, 2012